HHS Public Access

Author manuscript

Chem Rev. Author manuscript; available in PMC 2020 November 30.

Published in final edited form as:

Chem Rev. 2020 June 24; 120(12): 5082–5106. doi:10.1021/acs.chemrev.9b00556.

Reduction of Substrates by Nitrogenases

Lance C. Seefeldt, **Zhi-Yong Yang**

Department of Chemistry and Biochemistry, Utah State University, Logan, Utah 84322, United States

Dmitriy A. Lukoyanov,

Department of Chemistry, Northwestern University, Evanston, Illinois 60208, United States

Derek F. Harris,

Department of Chemistry and Biochemistry, Utah State University, Logan, Utah 84322, United States

Dennis R. Dean,

Biochemistry Department, Virginia Tech, Blacksburg, Virginia 24061, United States

Simone Raugei,

Physical and Computational Sciences Directorate, Pacific Northwest National Laboratory, Richland, Washington 99352, United States

Brian M. Hoffman

Department of Chemistry, Northwestern University, Evanston, Illinois 60208, United States

Abstract

Nitrogenase is the enzyme that catalyzes biological N_2 reduction to NH_3. This enzyme achieves an impressive rate enhancement over the uncatalyzed reaction. Given the high demand for N_2 fixation to support food and chemical production and the heavy reliance of the industrial Haber–Bosch nitrogen fixation reaction on fossil fuels, there is a strong need to elucidate how nitrogenase achieves this difficult reaction under benign conditions as a means of informing the design of next generation synthetic catalysts. This Review summarizes recent progress in addressing how nitrogenase catalyzes the reduction of an array of substrates. New insights into the mechanism of N_2 and proton reduction are first considered. This is followed by a summary of recent gains in understanding the reduction of a number of other nitrogenous compounds not considered to be physiological substrates. Progress in understanding the reduction of a wide range of C-based substrates, including CO and CO_2, is also discussed, and remaining challenges in understanding nitrogenase substrate reduction are considered.

Graphical Abstract

Corresponding Authors: **Lance C. Seefeldt** – Department of Chemistry and Biochemistry, Utah State University, Logan, Utah 84322, United States; Phone: +1.435.797.3964; lance.seefeldt@usu.edu.

Complete contact information is available at: https://pubs.acs.org/10.1021/acs.chemrev.9b00556

The authors declare no competing financial interest.

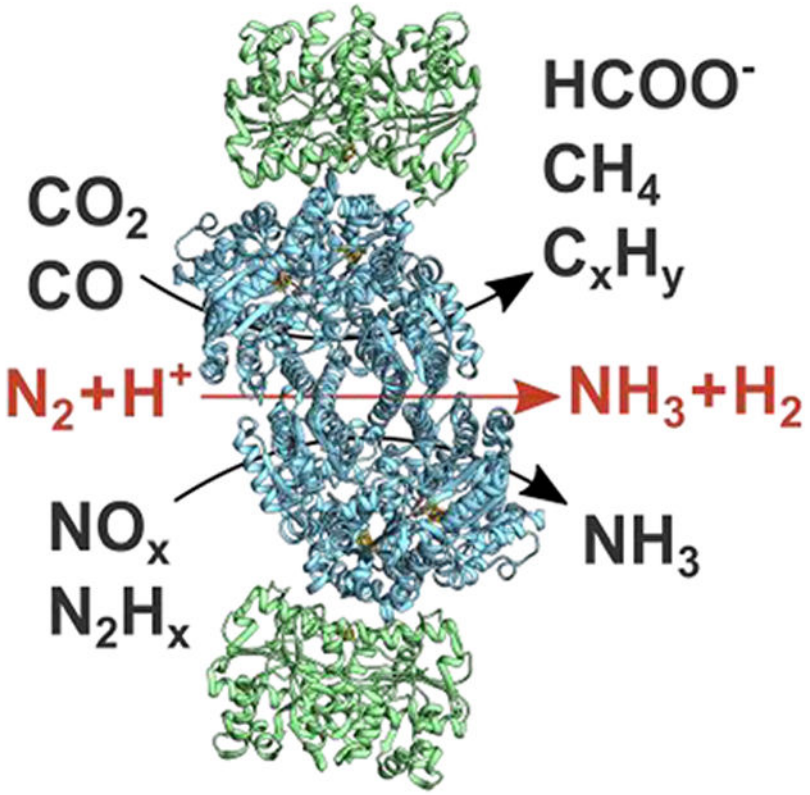

1. INTRODUCTION

The element nitrogen (N) is a constituent of many industrially and biologically important molecules, and thus there is a high worldwide demand for usable forms of N.[1–4] The major simple molecular states of N constitute the global biogeochemical nitrogen cycle, with dinitrogen (N_2) being the most abundant form constituting 78% of the Earth's atmosphere.[5–10] While abundant, N_2 is not generally useable directly but instead must first be "fixed" into a form that is useful for industrial or biological processes.[1,2,11,12] The reduction of N_2 to NH_3, called nitrogen fixation, is the largest contributor of fixed nitrogen into the global N cycle. This reduction reaction occurs at scale in comparable amounts through two processes, the Haber–Bosch industrial reaction[13–15] and by the action of the enzyme nitrogenase operating inside specialized microorganisms, called diazotrophs, found throughout the biosphere.[11,16–18] Nitrogenase catalyzes the N_2 reduction reaction having the following optimal (limiting) stoichiometry:[19–23]

$$N_2 + 8H^+ + 16MgATP + 8e^- \rightarrow 2NH_3 + H_2 + 16MgADP + 16P_i \quad (1)$$

As indicated by eq 1, N_2 reduction by nitrogenase is fundamentally an electrochemical process, employing electrons and protons. In that sense, it differs qualitatively from the chemical industrial Haber–Bosch process, which employs H_2 as the source of reducing equivalents and H (eq 2):[3]

$$3H_2 + N_2 \rightarrow 2NH_3 \quad (2)$$

The nitrogenase catalyzed reaction requires energy input in the form of hydrolysis of ATP, whereas 90% of the energy input for the Haber–Bosch process is used to make the H_2 reactant from methane[24] (eq 3)

$$CH_4 + 2H_2O \rightarrow CO_2 + 4H_2 \quad (3)$$

Finally, the nitrogenase stoichiometry (eq 1) incorporates the obligatory production of one H_2 per N_2 reduced, a long-debated idea that has been established only recently.[21,23]

Enzyme-catalyzed reactions, like all catalyzed reactions, are often measured by the rate enhancement achieved over the uncatalyzed reaction.[25–27] Although nitrogenase catalyzes the reduction of N_2 to 2 NH_3 with a seemingly low rate constant of ~1 s^{-1},[19,20,28,29] this corresponds to a large enhancement over the uncatalyzed reaction that places it as one of the most impressive known catalysts.

Research on nitrogenase over decades has endeavored to understand this complex enzyme and elucidate the mechanism by which this remarkable catalyst achieves its rate enhancement.[20,21,23,30–37] Other reviews in this volume detail diverse aspects of how nitrogenase works, including how electron transfer occurs and the roles of ATP hydrolysis, how spectroscopy provides insights into the properties of the active site metal clusters, and how metal site cofactors are biosynthesized. In this Review, we detail how the field has advanced over the last ~6 years, with an emphasis on the recent breakthroughs in our understanding of how the active site metal cluster achieves substrate reduction.

Although the physiological substrates are protons and N_2, nitrogenases can also reduce a number of other substrates, such as acetylene (C_2H_2), carbon dioxide (CO_2), diazene (HN=NH), and hydrazine (H_2N-NH_2).[20,39,40] We also review the current understanding of the mechanism of reduction of these alternative substrates, which not only is providing new insights into the mechanism of nitrogenase, but also provides insights into possible ways nitrogenase might be used to carry out useful reductions other than N_2 fixation.

2. NITROGENASES

2.1. Enzymes

There are three known isozymes of nitrogenase: the molybdenum-dependent Mo-nitrogenase, vanadium-dependent V-nitrogenase, and iron-only Fe-nitrogenase.[20,41–49] The nitrogenases are broadly distributed throughout nature with corresponding genes necessary to produce nitrogenases predicted in 13 phyla of bacteria and one phylum of archaea.[18,50] Mo-nitrogenase is the predominant isozyme,[51] but many diazotrophs carry genes for at least one, if not both, of the other isozymes.[44] Because of this distribution, the V-nitrogenase and Fe-nitrogenase are often called “alternative” nitrogenases.[41,44,52] Expression of the isozymes

appears to be primarily regulated by metal availability, wherein the absence of Mo or the inability to transport Mo efficiently, one of the alternative systems is expressed.[43,44,46,49,53]

Structures of the Mo- and V-nitrogenase, reviewed elsewhere in this issue, show them to have similar quaternary structures.[54–60] The structure of Fe-nitrogenase has not been solved, but available genetic and spectroscopic evidence indicates it is similar to the other two,[43,45] as depicted in Figure 1. All three isozymes are two-component protein systems[61,62] with the catalytic components for each being encoded by unique gene clusters. Mo-nitrogenase is encoded by *nif* genes,[50,63] V-nitrogenase by *vnf* genes,[64–66] and Fe-nitrogenase by *anf* genes.[66,67] The two component proteins are a catalytic component, or MFe protein (M = Mo, V, Fe) (NifDK, VnfDGK, AnfDGK), which receives electrons from the electron delivery component, or Fe protein (NifH, VnfH, AnfH).[20,31,41,43,44] The MFe proteins form as two identical catalytic halves; MoFe protein is an $\alpha_2\beta_2$ heterotetramer and VFe and FeFe proteins are $\alpha_2\beta_2\gamma_2$ heterohexamers.[41,43,68] Each catalytic half houses an [8Fe-7S] P-cluster and an active site cofactor called FeMo-co,[55–57,69–71] FeV-co,[58,72,73] or FeFe-co[38] as the site of substrate binding and reduction. Fe protein for all three isozymes is a homodimer, which houses a single [4Fe-4S] cluster and two nucleotide-binding sites for ATP (Figure 1).[54,60]

In all three isozymes, electron flow originates from the [4Fe-4S] cluster of the Fe protein, and proceeds through the P-cluster, eventually ending on the active site cofactor FeM-co (Figure 2).[74–77] The process of electron flow is complex and is covered in detail in other chapters of this Review.

2.2. Cofactors

Electrons and protons are accumulated, and substrates are reduced on the active site cofactor (FeMo-co, FeV-co, and FeFe-co, Figure 2). FeMo-co has the chemical composition [7Fe-9S-Mo-C-(*R*)-homocitrate] and is often referred to as the M-cluster.[56,57,69,70,78,79] FeV-co has a chemical composition of [7Fe-8S-V-C-(*R*)-homocitrate], with a carbonate ligand bound in place of the ninth sulfur and is sometimes referred to as V-cluster.[58,59,72] The FeFe-co is less well studied, but from spectroscopic studies is inferred to have a chemical composition of [8Fe-9S-C-(*R*)-homocitrate].[80]

3. MECHANISM OF NITROGENASE REDUCTION OF PROTONS AND N_2

Extensive studies in the 1970s and 1980s[20,31,81] led to the development of the Lowe–Thorneley kinetic scheme for catalysis by the Mo-dependent nitrogenase, Figure 3.[20,31,81] This describes the transformations among catalytic intermediates, denoted E_n where n is the number of steps of electron/proton delivery from the nitrogenase Fe protein to the active-site iron–molybdenum cofactor ([7Fe-9S-Mo-C-*R*-homocitrate]; FeMo-co) Figure 2.[23,82] This scheme's central feature was the mysterious proposal of obligatory formation of one mole of H_2 per mole of N_2 reduced, with the attendant limiting stoichiometric requirement of $8[e^-/H^+]$ per reduction of one N_2 to $2NH_3$, as given by eq 1, in agreement with stoichiometric measurements by Simpson and Burris,[19] but in contrast to the six reducing equivalents from $3H_2$ used in the Haber–Bosch reaction.[14]

Some early reports presented possible explanations for the proposed connection between H_2 evolution and N_2 reduction, including models that involve metal-bound hydrides.[20,31,83–92] These speculations invoked multiple forms of hydride intermediates,[31,88,90] as they sought to explain three important observations of nitrogenase catalysis: (i) obligatory H_2 evolution during N_2 reduction by Mo-nitrogenase (eq 1),[19,93] (ii) H_2 (D_2) as competitive inhibitors of N_2 reduction,[88,90,94,95] and (iii) N_2-dependent HD formation by Mo-nitrogenase during N_2 reduction in the presence of D_2.[85,88–90,96–100] One report suggested a dihydride intermediate after accumulation of three or four reducing equivalents (E_3 or E_4 in Figure 3) on the active site, and even suggested that N_2 somehow binds by displacing one H_2.[31,87] Metal-hydride intermediates were also proposed to be involved in the reduction of C-based substrates (e.g., C_2H_2 and cyclopropene).[101–103] In parallel, progress in understanding binding and activation of small molecules, such as N_2 and NO_3^-, by metal-hydride and metal-dihydrogen inorganic compounds suggested possible N_2 reduction mechanisms that involved hydrides.[83,84,104–108] Such mechanistic speculations included that N_2 binds to Mo-nitrogenase by displacing H_2 through a Mo-dihydride or trihydride intermediate,[83,104] that an H_2 complex bound to Mo might play an important role for N_2 binding,[105] and that nitrogenase evolves H_2 through the reductive elimination of a dihydride species bound to either Mo or Fe, favoring the binding and reduction of N_2.[106] Such multiple contradictory models, although insightful and provocative, were neither experimentally established nor excluded at the time they were suggested.

Despite the connection between N_2 reduction and H_2 release implied by the kinetic scheme of Figure 3, and the speculations it generated, in fact it had been neither confirmed nor universally accepted[20,84] that there is an obligatory, *mechanistic* requirement for formation of one H_2 per N_2 reduced to two NH_3, with the apparent "waste" of 2[e^-/H^+] delivered at the cost of 4 ATP hydrolyzed. Beyond that, *none* of the intermediate states proposed in LT scheme (Figure 3) had been trapped for characterization: the "boxes" connected by the kinetic scheme were empty. Key breakthroughs came after the determination of the structure of the active site FeMo-cofactor[55,56] and the application of a combined strategy using genetic, biochemical, and biophysical methods characterize nitrogenase intermediates trapped during turnover with different substrates as previously reviewed[21,23,33,36,82,110] and further detailed in the following sections. As a result of these recent studies, seven of the ten states in the kinetic cycle have now been trapped for study (boxed in red in Figure 3).[21,23,33,82]

An important step in characterizing catalytic intermediates was the trapping and characterization of an organometallic intermediate allyl alcohol bound as a ferracycle to a single Fe of FeMo-co during turnover with the substrate propargyl alcohol (Figure 4).[109] This was followed by characterization of an electron-accumulation intermediate (FeMo-co spin $S = 1/2$) trapped during turnover of MoFe protein having the α−$70^{Val\rightarrow Ile}$ substitution,[111] which apparently prevents access by all substrates to the active site, other than protons.[112] Because electron delivery cannot be experimentally synchronized during turnover, the number of electrons accumulated by this intermediate (n) was not evident. To determine this, the system was frozen to 77 K to prevent further electron delivery by reduced Fe protein, and then, it was warmed while frozen (cryoannealing) until relaxation toward E_0 is enabled through a process involving 2-electron steps in which an H_2 is released (see Figure 3). This

cryoannealing electron-counting protocol showed this state relaxes in two steps with loss of H_2 in each step, first to $E_2(2H)$ and thence to E_0.[113] As shown in Figure 3, this identifies the intermediate as the key $E_4(4H)$ "Janus" state (defined below),[21] which has accumulated four of the eight reducing equivalents required by eq 1. $^{1,2}H/^{95}$ Mo ENDOR spectroscopy further showed that these equivalents are stored as two [Fe-H-Fe] bridging hydrides,[111,114] not as a previously imagined Mo-H species.[83,104] The $E_4(4H)$ state of the native/wild-type (WT) enzyme itself[115] exhibits identical EPR/ENDOR and photophysical characteristics to this state when trapped in the α-$70^{Val\rightarrow Ile}/\alpha$-$195^{His\rightarrow Gln}$ altered protein.[116] As the WT intermediate accumulates in lower abundance, it has proven to be convenient to have these faithfully equivalent versions of the WT state.[115,116]

3.1. Reductive Elimination/Oxidative Addition (*re/oa*) Mechanism: As Proposed

The $E_4(4H)$ intermediate represents a critical transition point in the N_2 reduction pathway, Figure 3; as both the culmination of the catalytic phase of electron/proton accumulation by the enzyme and the initial step in the N_2 reduction phase, it is poised to "fall back" to the E_0 resting state by successive release of two H_2,[113] but equally poised to eliminate H_2 and proceed to reduce N_2 to two NH_3 through the accumulation of four more equivalents, hence the name, Janus, for the Roman god of transitions.[21] The trapping of this intermediate for study opened, for the first time, the possibility of directly testing for/characterizing the proposed equilibrium between two E_4-level states that interconvert through N_2 binding/release coupled to H_2 release/binding without additional [e^-/H^+] input, as visualized in Figure 3.

The experimental determination that $E_4(4H)$ stored four reducing equivalents as bridging hydrides[111,114] offered explanations of numerous features of nitrogenase mechanism that had defied explanation for decades,[20,106] while forging a connection between nitrogenase catalysis and the organometallic chemistry of metal hydrides.[106,108,117–119] See the earlier reviews for an account of early speculations about a possible role for hydrides in nitrogen fixation.[20,84]

The connection thus established to the chemistry of metal hydrides offered a potential explanation for and justification of the previously mysterious stoichiometry incorporated in eq 1. This explanation was proposed in a pair of "white papers" that showed how the obligatory H_2 formation during nitrogenase N_2 reduction might explain key experimental observations related to mechanism.[21,23] Once it was recognized that $E_4(4H)$ contains two bridging hydrides, then the chemistry of metal-dihydride complexes[117–119] identifies the proposed [$E_4(4H) + N_2$] ↔ [$E_4(2N2H) + H_2$] equilibrium (Figure 3) as representing the reductive elimination (*re*) of H_2 and its reverse, the oxidative addition (*oa*) of H_2: a mechanistically coupled *re/oa* equilibrium Figure 5. The *re* and release of H_2 drives the most difficult (first) step of N_2 cleavage: reduction of the N_2 triple bond to a diazene level (2N2H) intermediate through delivery to the substrate of the remaining two reducing equivalents.[21] As mentioned above and discussed in detail below, this proposal also offered an explanation of the key constraints on a mechanism for nitrogen fixation that had been developed over decades of study.[20]

3.2. Demonstration that Nitrogenase Functions Through the *re/oa* Equilibrium

The process of defining the mechanistic core of N_2 activation, the *re/oa* equilibrium, as visualized in Figure 5, involved multiple steps over a number of years. It included the demonstration that high-spin ($S = 3/2$) intermediates previously trapped during turnover under argon of wild type enzyme are $E_2(2H)$ isomers,[120–123] and was completed by a capstone study of native nitrogenase that trapped and monitored both $E_4(4H)$ and $E_4(2N2H)$ as a function of turnover conditions.[22,115,116,124,125] In so doing, it completed the process of establishing that native nitrogenase is activated by the *re/oa* equilibrium, which mechanistically requires the loss of one H_2 per N_2 and results in the attendant $8e^-$ stoichiometry shown in eq 1.[19,23]

Having identified the EPR spectra of all of the states involved in the relaxation of the $E_4(4H)$ and $E_4(2N2H)$ (Scheme 1), it was possible to monitor the kinetics of the relaxation of WT $E_4(2N2H)$ to the resting-state E_0.[115,124] The progress curves for the relaxation of $E_4(2N2H)$ and kinetically linked intermediates during cryoannealing of WT enzyme at −50 °C presented in Figure 6 are well described by the curves calculated from fits to the sequential kinetic scheme involving the *re/oa* equilibrium of Scheme 1.[115,124] Not only does $E_4(2N2H)$ relax to $E_4(4H)$, but the amount of trapped $E_4(2N2H)$ increases with increasing $[N_2]$, while the amount of $E_4(4H)$ decreases (Figure 7).[115,124]

Correspondingly, the rate of relaxation increases with increasing $[H_2]$, and decreases with increasing $[N_2]$.[115,124] This kinetic coupling of the loss of $E_4(2N2H)$ to the formation of $E_4(4H)$ through *oa* of H_2, directly establishes the operation of the *re/oa* equilibrium and its kinetic reversibility.

The observation of both $E_4(4H)$ and $E_4(2N2H)$ in samples freeze-quenched during N_2 fixation allowed measurement of the equilibrium constant for *re/oa*, $K_{re} = k_f/k_b$ (Figure 5; Scheme 1).[115] This was done by estimating the relative amounts of $E_4(4H)$ and $E_4(2N2H)$ freeze-trapped under experimentally varied partial pressures of N_2 and H_2, yielding the *re/oa* equilibrium constant, K_{re} and the free energy for the equilibrium, eqs 4 and 5

$$K_{re} = \frac{E_4(2N2H)}{E_4(4H)} \cdot \frac{P(H_2)}{P(N_2)} \tag{4}$$

$$\Delta_{re}G^{\circ} = -RT\ln(K_{re}) \sim -2\,\text{kcal/mol} \tag{5}$$

Thus, this first step in the reduction of N_2 by nitrogenase is essentially thermoneutral, $\Delta_{re}G^0 \sim -2$ kcal/mol, whereas direct hydrogenation of gas-phase N_2 is endergonic by more than 50 kcal/mol.[115]

3.2.1. *re/oa* Mechanism Generates the Key Constraints Revealed by Experiment.—

Decades of study had revealed several puzzling features of nitrogen fixation by nitrogenase whose mechanistic origins were not understood, but ultimately served as *key constraints* on any proposed mechanism, Chart 1.[20,21,23] A series of experiments has shown that all of these constraints are generated by the functioning of the *re/oa* mechanism.

These constraints arise from previously confusing results from turnover in the presence of D_2 or T_2. It was found that D_2 and T_2 only react with nitrogenase during turnover under an N_2/D_2 or N_2/T_2 atmosphere[90,98] at the E_4(2N2H) reduction level (c); in this reaction D_2 is stoichiometrically reduced to two HD (with H_2O buffer) (a);[88,89,98] corresponding turnover with T_2 does not lead to exchange of T^+ into H_2O solvent (b).[90] It has now been shown that all these D_2/T_2 constraints arise through the reverse of the *re* process, Figure 5, namely, the oxidative addition (*oa*) of H_2 with loss of N_2.[21,23] According to the mechanism, during turnover under D_2/N_2, reaction of the E_4(2N2H) intermediate with D_2 generates dideutero-E_4 with two [Fe-D-Fe] bridging deuterides that do not exchange with solvent,[22] and the same is true for T_2. These E_4(4H) isotopologues, which are denoted E_4 ($2L^-;2H^+$), L = D or T, would relax through $E_2(L^-;H^+)$ to E_0 with successive loss of two HL.[21,113]

The proposed formation of the $E_4(2D^-;2H^+)$ and $E_2(D^-;H^+)$ states through the thermodynamically allowed reverse of *re*, the *oa* of D_2 with accompanying release of N_2, in fact was the first successful test of the *re/oa* mechanism. When these states were formed during turnover under N_2/D_2, the nonphysiological substrate acetylene (C_2H_2) intercepted them to generate deuterated ethylenes (C_2H_3D and $C_2H_2D_2$).[22] More recently the $E_4(2D^-;2H^+)$ and $E_4(2H^-;2D^+)$ states were observed and characterized by EPR spectroscopy and by studies of isotope effects on the photophysical properties of these isotopologues.[115]

3.2.2. There Are No Reductive Activation Steps Prior to Catalysis.—In recent years, mechanistic proposals have posited that multiple $[e^-/H^+]$ must be delivered to the true resting-state FeMo-co to activate it to a state that acts as the E_0 in an $8[e^-/H^+]$ catalytic cycle equivalent to the scheme of Figure 3.[126] First, of course, no such preactivation process was observed in the many presteady state measurements carried out on as-isolated nitrogenase over decades.[20,31] But most importantly the measurements of the relaxation of the odd-electron $S = 1/2$ E_4(4H) with release of $2H_2$ (Figure 6)[113] unambiguously show that it relaxes directly to the same EPR-active odd-electron E_0 ($S = 3/2$) resting state that has been isolated and characterized crystallographically, not to a different state, which at least in one model, would not even be odd-electron.[126] And there is no doubt that E_4(4H) indeed relaxes to the crystallographically characterized E_0 state. The identity of the crystalline E_0 and the putative E_0 formed by E_4(4H) relaxation is established by the identity of the EPR spectra of the solution E_0 formed by relaxation and that of the crystalline E_0,[57,127] both of which precisely match the long-established EPR spectrum of as-isolated Mo-nitrogenase in solution.

3.3. Exploring the *re/oa* Mechanism

Upon establishing that nitrogen fixation by nitrogenase operates through the *re/oa* mechanism with its $8[e^-/H^+]$ stoichiometry, further experiments and computation have been used to explore the microscopic details.

3.3.1. Reductive Elimination Involves an H_2-Bound Intermediate.—The demonstration that the E_4(4H) Janus intermediate has accumulated four reducing equivalents as two [Fe-H-Fe] bridging hydrides, and the resulting link thus forged between nitrogenase catalysis and the organometallic chemistry of metal hydrides, inspired examination of the

behavior of E_4(4H) under photolysis as a test of this linkage and as a means of obtaining atomic-level details of the *re* activation process. The photolysis of transition metal dihydride complexes typically results in the release of H_2,[108,128–135] and it was found that H_2 release in fact occurred during in situ 450 nm photolysis of E_4(4H) in an EPR cavity at temperatures below 20 K.[116,125] These studies, as supported by density functional theory (DFT) calculations,[136] showed that an H_2 complex on the ground adiabatic potential energy surface $E_4(H_2;2H)$ becomes populated during catalysis, but this state cannot lose H_2 because the resultant, denoted [E_4(2H)* + H_2], is at inaccessibly high energy.[125] However, N_2 can bind and displace the H_2 of $E_4(H_2;2H)$ to complete the conversion of [E_4(4H) + N_2] into [E_4(2N2H) + H_2], as represented in Figure 8.[136]

3.3.2. E_2(2H) States 1b and 1c Are Hydride Isomers.—

As a further use of hydride photolysis to explore nitrogenase function, it was shown that E_2(2H)/1b stores the two reducing equivalents as a hydride, almost surely with the [Fe-H-Fe] bridging mode of binding, and that 1c is a *hydride isomer* of E_2(2H)/1b, either with the hydride bridging a different pair of Fe or having converted to a terminal hydride, as visualized in Figure 9.[123] Relatively modest differences in the occupancy ratio of the two E_2(2H) hydride conformers during turnover, 1b/1c ~ (2–3)/1, suggested that the two are able to readily interconvert during fluid-solution turnover.[123]

3.3.3. Density Functional Studies of the *re/oa* Equilibrium.—

The structure and energetics of possible nitrogenase intermediates were recently explored by DFT calculations on a broad range of structural models for the active site and a variety of DFT exchange and correlation functionals.[136–139] These computations[136] showed that it is necessary to include all residues (and water molecules) interacting directly with FeMo-co via specific H-bonds interactions, nonspecific local electrostatic interactions, and steric confinement to prevent spurious disruption of FeMo-co[126,140–142] upon accumulation of 4[e^-/H^+]. These calculations indicated an important role of sulfide hemilability in the overall conversion of E_0 to a diazene-level intermediate, as suggested by X-ray crystallographic studies.[58,59,143,144] Perhaps most importantly, they explained *how* the enzyme *mechanistically* couples exothermic H_2 formation to endothermic cleavage of the N≡N triple bond in the nearly thermoneutral *re/oa* equilibrium discovered experimentally (Figure 10), while preventing the futile generation of two H_2 without N_2 reduction: hydride *re* generates an H_2 complex, again in agreement with experiment, and H_2 is only lost when displaced by N_2, to form an end-on N_2 complex, which then proceeds to a diazene-level intermediate.[136]

3.3.4. High-Resolution ENDOR Spectroscopy Coupled with Quantum Chemical Calculations Reveals the Structure of Janus Intermediate E_4(4H).—

Because of the central role of E_4(4H) in the *re/oa* mechanism, it was essential to characterize its structure. The original ^{1}H ENDOR study of E_4(4H),[111] and subsequent ^{95}Mo and ^{57}Fe ENDOR study[114,145] demonstrated that FeMo-co in E_4(4H) contains two [Fe-H-Fe] bridging hydrides but were unable to provide a satisfactory picture of the relative spatial relationships of the two hydrides. The nature of E_4(4H) has been the subject of numerous recent computational studies based on DFT.[136–139] The lowest-free-energy E_4 isomers obtained from the DFT studies reported so far have two of the four hydrogens located on μ_2-

S atoms, while the other two hydrogens are either present as hydrides in bridging positions between two Fe atoms, or in mixed bridging/terminal position on the $Fe_{2,3,6,7}$ face of FeMo-co,[136,137,146,147] or as a dihydrogen (η^2-H_2) adduct bound to either Fe_2[136,137,147] or Fe_6.[147]

As we pointed out, limitations in DFT-based schemes—the only ones computationally feasible for a systematic study of complex systems, such as FeMo-co—make it difficult to determine the ground-state structure of E_4(4H) based on DFT-derived relative energies alone. To emphasize this issue, careful computational analyses carried out by the research groups of Ryde[137,146,148,149] and Bjornsson[139,147] have clearly shown that the exchange and correlation functional adopted in the DFT calculations largely affect the ordering of possible E_4 isomers, which differ on the location of the hydrides. This uncertainty is further aggravated by intrinsic deficiency of broken symmetry DFT calculations which are simply unable to capture the multideterminant character of the electronic structure of FeMo-co. A detailed discussion of all of these issues has been presented by Cao and Ryde.[146]

To determine how the Janus intermediate binds its two hydrides, exhaustive, high-resolution CW-stochastic ^{1}H-ENDOR experiments were performed using improved ENDOR methodologies and updated equipment.[150] Figure 11 illustrates the remarkable spectroscopic resolution and strong orientation selection that enabled the previously unattainable determination of absolute hyperfine-interaction signs. The important results for structural assessments were the findings that (i) the dipolar–electron–nuclear hyperfine coupling tensors for the two hydrides were coaxial, (ii) each had “rhombic symmetry” (two components with equal and opposite signs; one null component), and (iii) the *signed* tensor components for the two hydrides were permuted relative to each other.

These findings provided critical constraints on the structure of E_4(4H), but did not by themselves implicate a particular structure, and so experiment was coupled to the DFT computations. Just as the DFT computations could not discriminate among candidates for the E_4(4H) ground state, neither could they discriminate through computations of the dipolar hyperfine couplings. However, the DFT structures are robust and so the ENDOR measurements were coupled to DFT structural models through an analytical point-dipole Hamiltonian for the hydride electron–nuclear dipolar coupling to its “anchoring” Fe ions, an approach that overcomes limitations inherent in both experimental interpretation and computational accuracy. The simple point-dipole approximation was not expected to provide quantitatively accurate results for the magnitudes of the hyperfine tensor components because of the delocalized nature of the electron density in the FeMo-co.[147] Instead, for each of the DFT-derived candidate structures for E_4(4H) ground state the dipole approach was simply used to assess the relative *orientation* of the dipolar interaction tensors for the two hydrides of a structural model when each had a rhombic tensor, and this was compared to the experimentally determined relative tensor *orientation*.[146,147,150]

This comparison alone enabled discrimination among possible E_4(4H) isomers.[23,111] The result: the freeze-trapped, lowest-energy Janus intermediate structure is $E_4(4H)^{(a)}$, Figure 12. As the calculations indicated the presence of a number of isomers close in energy, [137,139,146,147,150] it was envisioned that at ambient temperatures the E_4(4H) hydrides become fluxional, with a dynamic population of multiple isomers.

As additional DFT computations are carried out, suggesting variations on the E_4(4H) structure, the results of this ENDOR study, in conjunction with the analytical point-dipole Hamiltonian, will continue to provide the benchmark against which those structures can be tested.

3.3.5. E_1 Forms by Reduction of Fe, Not Mo.—The E_1(H) state as prepared both by low-flux turnover and by radiolytic cryoreduction were investigated using a combination of Mo Kα-HERFD (high energy resolution fluorescence detection) and Fe K-edge PFY (partial-fluorescence yield) X-ray absorption spectroscopy techniques.[151] The results demonstrate that this state is formed by an Fe-centered reduction and that Mo does not change redox state, a further indication that Mo is only *in*directly involved in substrate reduction, which occurs at Fe. This conclusion is further supported by a recent Mo and Fe K-edge EXAFS (extended X-ray absorption fine structure) characterization of E_0 and E_1 states in combination with QM/MM calculations that supported protonation of a belt sulfide (S2B or S5A) in E_1.[152]

3.4. Kinetic Description of the Competing Reactions at E_4(4H)

As can be seen in Figure 13, the reactions of E_4(4H) can be viewed as a competition: the forward direction of the *re*/*oa* equilibrium, involving binding of N_2 and displacement of H_2, competes with the relaxation of E_4(4H) through hydride protonolysis (HP), which releases H_2 without N_2 binding.[153,154] The competition between these two reactions is defined by the ratio of their rate constants k_{re} for the forward reaction and k_{HP} for the relaxation reaction and modulated by the ratio of the partial pressures of N_2 and H_2. A kinetic model was developed that yields, under high electron flux conditions (high Fe protein to MoFe protein molar ratio), the values of these two rate constants from the fitting of the ratio, H_2 formed divided by N_2 reduced, as a function of the partial pressure of N_2. As can be seen in Figure 14[154] and from measurements by many groups, at 1 atm of N_2, Mo-nitrogenase shows $H_2/N_2 < 2$ and the ratio asymptotically approaches unity with increasing N_2 partial pressure. The fit to the data of Figure 14 yielded $k_{re}/k_{HP} = 5.1\ atm^{-1}$. This considerable preference for the forward reaction is truly remarkable when considering the expected reactivity of a metal hydride toward protonolysis as observed in many reductive catalysts. Corresponding suppression of the formation of H_2 by an HP reaction in synthetic catalysts for N_2 reduction is one of the grand challenges in catalyst design.

The two other isozyme of Mo-nitrogenase, the V- and Fe-nitrogenases, share similar architecture to the Mo-enzyme, but as noted above, have different polypeptides that present different active site environments and different active site metal clusters.[43,58] At 1 atm of N_2, it can be seen that the V- and Fe-nitrogenase show much higher ratios of H_2 formed per N_2 reduced (Figure 14). Application of the high-flux kinetic model to the V- and Fe-nitrogenases, revealed reduced values of the rate-constant ratio compared to Mo-nitrogenase, k_{re}/k_{HP}= 1.1 and 0.78 atm^{-1}, respectively.[154] Further analysis pinpointed that whereas the values for k_{re} for the V- and Fe- nitrogenases are as much as 10-fold smaller than k_{re} for the Mo enzyme, the values of k_{HP} differ by less than 2-fold. In short, the V- and Fe-nitrogenases are not better at the HP side-reaction, but rather are poorer at the productive *re* reaction. The

source of these differences among the three nitrogenase isozyme remains to be deduced.[153,154]

3.4.1. All Three Nitrogenases Employ the *re/oa* Mechanism.—

The differences in rate constants among the three isozymes might suggest a different mechanism for N_2 binding and activation. However, this is not so. The *re*/*oa* mechanism involves an equilibrium between the E_4(4H) state and the E_4(2N2H) state. This predicts H_2 inhibition of N_2 reduction and the formation of HD during turnover under mixed D_2 and N_2, both of which were found for all three isozymes. These observations establish that all three nitrogenase isoforms follow the same *re*/*oa* mechanism.[38,153,154]

3.5. Structure–Function Relationship During Nitrogenase Catalysis

One of the persistent challenges in nitrogenase research is to understand how protein and cluster dynamics might participate in the mechanism.[32,33,35–37,68,75,156–168] Many structural and spectroscopic studies have shown that the resting state of nitrogenase is largely unreactive, suggesting that motion of the surrounding protein or changes in ligation of FeMo-co might be essential in catalysis.[32,33,82,158] A number of calculations have suggested changes in FeMo-co that could be occurring during catalysis, including breaking of one or more the Fe–C bonds[126,140,141,169–171] or breaking one or more Fe–S bonds.[136,172–177] Recent structural studies have observed significant changes in the FeMo-co and FeV-co structures that might point to dynamics relevant to catalysis.[58,59,143,144,178] In one such study, it was observed that MoFe protein under turnover with CO shows the substitution of one of the belt sulfide ligand S2B by a bridging CO ligand[143] (see section 5.2 for more details). These studies point to lability in one or more of the Fe–S bonds during turnover.[178,179] This lability was seen in the computational study of the *re/oa* equilibrium described in sections 3.3.3 and 3.3.4.[136] Recently, a structure of the V-nitrogenase by Einsle et al. showed FeV-cofactor with two belt sulfide ligands substituted by a proposed carbonate and a light atom (N(H) or O(H), Figure 15).[59,155] Even though the identity of the light atom ligand is under debate, the plausible implication and relevance to the N_2 reduction mechanism by nitrogenase have initiated vigorous discussion.[156,180,181] The recent progress in spectroscopic studies on nitrogenase intermediates[162] and the X-ray structures of nitrogenase from turnover mixtures promises further progress in understanding the dynamics of the metalloclusters, especially the active site FeM-cofactor during substrate/inhibitor interaction.

4. NONPHYSIOLOGICAL N-BASED SUBSTRATES

4.1. Range of N-Based Substrates

An important property of nitrogenases is the ability to bind and reduce a number of nonphysiological substrates.[20,39,40] A common, but not universal, property of nitrogenase substrates is that they are small and contain double or triple bonds. The study of how these alternative substrates interact with nitrogenase has provided important mechanistic insights.[20,23,33,41,82] In this section, recent work on a number of alternative substrates that contain N is reviewed.

4.2. N_2H_x Substrates

As shown in the *re/oa* kinetic scheme of Figure 3, following the formation of E_4(2N2H), the catalytic cycle traverses four states that contain partially reduced species of N_2.[21,23] Researchers have long considered two competing proposals for this "second half" of the kinetic scheme, which invoke distinctly different intermediates, Figure 16. In the "distal" (**D**) pathway, utilized by N_2-fixing inorganic Mo complexes,[83,183–185] the distal N of Fe-bound N_2 is hydrogenated in three steps. The first NH_3 is then liberated with the addition of the fifth [e^-/H^+] overall, to generate the nitrido species, E_5. This nitrido-N is then hydrogenated three times to yield the second NH_3. In the "alternating" (**A**) pathway that has been suggested to apply to reaction at Fe of FeMo-co,[175,186] the two N's instead are hydrogenated alternately, with a four-electron and proton reduced species equivalent to hydrazine (N_2H_4) formed as the E_6 intermediate. In this case, the first NH_3 is only liberated during the next hydrogenation step, the formation of E_7 (Figure 16).[33,82] Peters et al. has proposed what might be called a hybrid-**A** pathway,[182] in which E_4 on the **D** pathway is converted to E_5 on the **A** pathway. Consequently, as with the limiting **A** pathway, the first NH_3 also is released with formation of E_7, as shown.

Previous studies demonstrated that the diazene analogs methyldiazene (CH_3-N=NH), dimethyldiazene (CH_3-N=N-CH_3) and diazirine (CH_2N_2) are substrates for nitrogenase, all being reduced to NH_3, and CH_x species.[187,188] The early studies on these substrates have been reviewed.[93] In 2007, the study of diazene (HN=NH) as a substrate for Mo-dependent nitrogenase was expanded through the use of in situ generation from azodiformate.[189] The 4 [e^-/H^+] reduction of diazene produced two equivalents of NH_3. The reduction of diazene was found to be inhibited by H_2, which is also an inhibitor of N_2 reduction.[189] As can now be understood, in both cases the inhibition is a consequence of the *re/oa* mechanism as described in section 3. This result implies that diazene *must* enter the reaction pathway by forming the same diazene-level intermediate, E_4(2N2H), as forms when N_2 reacts with E_4(4H).[23] The addition of H_2 then reverses the *re/oa* equilibrium, with the E_4(2N2H) undergoing *oa* with loss of N_2 to generate E_4(4H). The E_4(2N2H) could form in one of two ways: direct reaction with E_0 or, as proposed in 2012,[190] reaction with E_2(2H) with loss of H_2 through hydride protonation.

Recently it has also been shown that the 2 [e^-/H^+] reduction of hydrazine to produce two equivalents of NH_3[191] is efficiently achieved by remodeling of the α−70^{Val} residue around FeMo-cofactor of Mo-nitrogenase with a smaller side-chain amino acid (Ala).[192] In contrast to the H_2 inhibition of diazene and N_2 reduction, hydrazine reduction was not inhibited by H_2. This again is consistent with the scheme of Figure 3. Once the delivery of [e^-/H^+] to E_4(2N2H) has generated E_5, the enzyme has passed the *re/oa* equilibrium stage and is no longer susceptible to inhibition by H_2, while hydrazine appears on the **A** N_2 reduction pathway at E_6.[190]

Two common intermediates have been freeze-trapped using MoFe protein variants with both diazene substrates (CH_3-N=NH and HN=NH) and hydrazine N_2H_4 (Figure 17):[188,189,192,194] a broad, low-field resonance **H** (non-Kramers state, $S \geq 2$) EPR-detectable in Q-band at 2 K; a Kramers state, $S = 1/2$, with **g** = [2.09, 2.01, 1.98]), denoted, **I**.[190] These

intermediates have been fully characterized by X/Q-band EPR and ^{15}N, $^{1,2}H$-ENDOR, HYSCORE, and ESEEM spectroscopic studies. Their enzymatic and chemical assignments are $E_7(NH_2)$ = **H** with NH_2^- bound to FeMo-cofactor and $E_8(NH_3)$ = **I**, with a bound NH_3.[190]

4.3. NO_x Substrates

Nitrite (NO_2^-), nitrous oxide (N_2O), and hydroxylamine (NH_2OH) all are reduced by nitrogenase.[20] The recent characterization of nitrite as a nitrogenase substrate established that six-electron reduction of NO_2^- to NH_3 by nitrogenase proceeds without the obligatory H_2 evolution that is required for the reduction of N_2.[193] The kinetic observations and mechanistic implications of the first three of these substrates have been summarized in detail in an earlier review.[20] Hydroxylamine was recently reported as a nitrogenase substrate, being reduced by two electrons to NH_3 and H_2O.[193] The reduction of each of these substrates is not inhibited by H_2, as in the case in the reduction of hydrazine. As with hydrazine, these results are as expected for reactions that involve intermediates that correspond to E_n, $n > 4$ (see above).

Freeze-trapping α−$70^{Val\rightarrow Ala}$/α−$195^{His\rightarrow Gln}$ MoFe protein under turnover conditions with NO_2^- or NH_2OH as substrate resulted in the same two EPR-active species (S = 1/2 and $S \geq 2$) trapped with diazenes or hydrazine as substrate (Figure 18). As confirmed by ^1H and ^{15}N pulsed ENDOR study, the S = 1/2 intermediates of NO_2^- or NH_2OH are $E_8(NH_3)$ = **I**; $^{14/15}N$ ESEEM studies confirmed the identity of the non-Kramers intermediates as $E_7(NH_2)$ = **H** ($S \geq 2$) for NO_2^- or NH_2OH.[193]

4.4. Mechanisms and Insights

The study of these N-based alternative substrates has provided evidence regarding the nature of the reaction pathway for N_2 reduction: **D** or **A** (Figure 16). An alternating pathway for N_2 hydrogenation is supported by the observation that (i) hydrazine is a product of N_2 reduction by V-nitrogenase,[195] which also functions through the *re/oa* mechanism,[153,154] and (ii) hydrazine was detected as a product by acid or base quenching of Mo-nitrogenase during N_2 reduction.[86,87] Of course, as seen in Figure 16, in the **D** pathway the N-N bond is cleaved before hydrazine can be formed and so could not be formed during catalysis, thus indicating that the **A** pathway is followed by nitrogenase.

The kinetic and spectroscopic observations of nitrite and hydroxylamine reduction by nitrogenase led to the proposal of a [$6e^-/7H^+$] reduction mechanism of nitrite by nitrogenase (eq 6) as shown in the right panel of Figure 19.[193] In this mechanism, NO_2^- and one proton bind to FeMo-cofactor at the E_2 state. After one water molecule was released, the resulting **M**-[NO^+] species reacts with the hydride on the same cofactor to avoid the formation of an **M**-[NO] "thermodynamic sink".[196] The formation of an **M**-HNO species is similar to the reduction of heme-bound NO to bound HNO through hydride transfer from NADH by P450 NO reductase.[197] The **M**-HNO intermediate is then converted to further reduced species through a pathway analogous to the nitrite reduction by cytochrome c nitrite reductase (ccNIR),[198–201] including intermediates **H** (**M**-NH_2) and **I** (**M**-NH_3).[190]

$$NO_2^- + 6e^- + 7H^+ \rightarrow NH_3 + 2H_2O \quad (6)$$

Even though the binding and reduction mechanism of N_2 and NO_2^- are totally different, the generation of common intermediates **H** and **I** from both the di-N substrates (N_2H_2 and N_2H_4) and mono-N substrates (NO_2^- and NH_2OH) further confirmed the previous assignments of intermediate **H** to **M**-NH_2 and **I** to **M**-NH_3, and their assignment to E_7 and E_8, respectively.[190,193] These results are understood as arising from a convergence of the reduction pathways of N_2 and NO_2^- in the late stage of the corresponding catalytic cycles as highlighted in the red box in Figure 19.[193]

Hydrazine and hydroxylamine were proposed to bind to E_1 and undergo bond cleavage, forming the intermediate **H**, and NH_3 and H_2O, respectively.[190,193] These results are consistent with the proposed alternating N_2 reduction pathway by nitrogenase in which the first NH_3 is released after delivery of the seventh [e^-/H^+] to the N_2H_4-bound E_6 state to form intermediate **H**. The intermediate **H** accepts one last pair of [e^-/H^+] to form intermediate **I**, which regenerates the E_0 state to finish one catalytic cycle by releasing the second NH_3.[21,23,190]

5. C-BASED SUBSTRATES

In addition to the nonphysiological N-based substrates, nitrogenase interacts with a broad range of carbon (C)-based substrates/inhibitors. The utilization of these C-based substrates/inhibitors has greatly expanded the ability to probe nitrogenase mechanism, and their reduction has been reviewed.[20,39,40,203] In this section, we will focus on the progress in studying C-based substrates/inhibitors of nitrogenase since 2013,[40] referring to earlier work when necessary for clarity.

5.1. Alkyne Substrates

Alkynes were widely used as substrates and inhibitor in probing the substrate-binding sites and reduction mechanism of nitrogenase over the last half-century.[20,39,40,179] Acetylene was the first alkyne discovered early as an alternative substrate of nitrogenase,[204] with pioneering works studying the steady-state EPR of wild type[205] and α−195$^{\text{His}\rightarrow\text{Gln}}$-substituted MoFe protein[206] with acetylene as substrate. The X- and Q-band EPR spectra of the freeze-trapped species exhibited three simultaneously generated $S = 1/2$ signals: a rhombic S_{EPR1} signal with $g = 2.12, 1.98, 1.95$, a rhombic S_{EPR2} signal with $g = 2.007, 2.000, 1.992$, and a minor isotropic S_{EPR3} signal with $g \approx 1.97$.[206,207] Initial ^{13}C and ^1H ENDOR measurements on the S_{EPR1} signal suggested that it arises from a *substrate* complex, with two C_2H_2-derived species bound to the cofactor, one of them being a C_2H_2 bound to the FeMo-cofactor by bridging two Fe ions of the Fe2,3,6,7 face.[207] However, results described directly below, which were obtained for an intermediate trapped during turnover of the alkyne propargyl alcohol with the α−70 $^{\text{Val}\rightarrow\text{Ala}}$-substituted MoFe protein suggested that this interpretation be reexamined. Subsequent, improved ENDOR measurements on S_{EPR1}, which included ^{57}Fe ENDOR measurements, revealed interactions with three distinct carbon nuclei, again indicating that at least two C_2H_2-derived species are

bound to the cofactor, but they suggested that this intermediate in fact contains an ethylene *product* bound as a ferracycle to a single Fe of a two-electron reduced (E_2) FeMo-cofactor (Figure 20).[202]

It was long held that FeMo-cofactor contained within the MoFe protein required the accumulation of one or more electrons before any substrate or inhibitor could interact.[20,209] This conclusion was drawn from the lack of significant perturbations of the resting state (E_0) FeMo-cofactor EPR signal line shape upon the addition of any inhibitors or substrates.[20] This situation changed with the report that when the α−96^{Arg}, located on one FeS face of FeMo-cofactor within the MoFe protein, was substituted by a series of other amino acids, the resulting MoFe protein variants showed perturbations of the FeMo-cofactor EPR signal (S = 3/2, g = 4.26, 3.67, 2.00) upon incubation of the resting state enzyme with the substrate acetylene or the inhibitor cyanide (CN^-).[208] Both acetylene[204,210,211] and cyanide[212–214] were long ago reported as substrates for nitrogenase under turnover conditions, being reduced to ethylene (C_2H_4) and methane (CH_4) and ammonia (NH_3), respectively. Incubation of resting-state α−96$^{Arg\rightarrow Leu}$-substituted MoFe protein with acetylene or cyanide was found to decrease the normal FeMo-cofactor signal with appearance of new EPR signals having g = 4.50 and 3.50 (Figure 21), and g = 4.06, respectively. Subsequent ^{13}C ENDOR studies revealed direct, but weak, interactions between acetylene or CN^- and the resting-state FeMo-cofactor.[208] These observations were the first to show that substrates/inhibitors can interact with the resting state FeMo-cofactor contained within the MoFe protein.

Capitalizing on this finding, a recent X-ray crystallographic study of α−96$^{Arg\rightarrow Gln}$-substituted MoFe protein in the presence of acetylene resulted in the first crystal structure with a substrate molecule, acetylene, captured near the active site FeMo-cofactor.[215] In the 1.70 Å crystal structure, the acetylene is located 4–5 Å away from Fe6 atom, which was supported by DFT calculations (Figure 22).[215] These results are consistent with the previous findings that nitrogenase binds some substrates at the 4Fe4S face of FeMo-co approached by the side chains of α−70^{Val} and α−96^{Arg}.[33,36] An ^{1}H and ^{57}Fe ENDOR study using wild-type and *Nif V*$^-$ MoFe proteins from *Klebsiella pneumoniae* also revealed that acetylene binding to the resting-state MoFe protein can perturb the FeMo-cofactor environment.[216]

The first detailed characterization of alkyne-reduction intermediates, alluded to above, was carried out on states freeze-trapped during the turnover of nitrogenase modified by substitution of the valine at α−70 position in MoFe protein by alanine.[109,217,218] This substitution allows the reduction of longer-chain alkyne substrates,[219,220] such as propargyl alcohol ($HC{\equiv}CCH_2$-OH).[217] When the α−70$^{Val\rightarrow Ala}$-substituted MoFe protein was frozen in liquid nitrogen during steady-state turnover with propargyl alcohol as substrate, the S = 3/2 EPR spectrum of the FeMo-cofactor was changed to a new S = 1/2 signal.[217,218] Using ^{1,2}H- and ^{13}C-ENDOR spectroscopies, it was demonstrated that this S = 1/2 signal originates from the FeMo-cofactor having the alkene allyl alcohol ($H_2C{=}CHCH_2$-OH) reduction product bound as a ferracycle to a single Fe as shown in section 3 (Figure 4).[109]

This structural assignment was later supported by the EXAFS and NRVS examination of the same intermediate.[162] A similar S = 1/2 signal was also observed when propargyl alcohol was replaced by propargyl amine ($HC{\equiv}CCH_2$-NH_2) as substrate. Trapping of these two

intermediates was shown to be dependent on pH and the presence of histidine at α−195 position.[218] These results suggested that these intermediates are stabilized, and thereby trapped, by H-bonding interactions between either the −OH group or the $-NH_3^+$ group and the imidazole of α−195^{His}. Theoretical calculations refining the binding mode and site pointed to η^2 coordination at Fe6 of the FeMo-cofactor, as visualized in Figures 4 and 21.[218]

5.2. CO as Inhibitor and Substrate

CO was described as an inhibitor of wild-type Mo-nitrogenase in early studies, being shown to inhibit the reduction of all substrates except protons to make H_2.[20,93,221] CO inhibition of proton reduction was observed when the first sphere (substitution of homocitrate by citrate as in the $NifV^-$ mutant)[222,223] or secondary sphere environment of the FeMo-cofactor[222,224,225] was changed. Similar CO inhibition of proton reduction was also seen for Mo-nitrogenase under high pH conditions[226] and for V-nitrogenase.[227,228] Recently, CO was reported to *stimulate* the H_2 production catalyzed by three MoFe protein variants, α−277^{Cys}, α−192^{Asp}, and α−192^{Glu} under high-electron flux conditions but not under low-electron flux conditions. These intriguing observations are apparently at odds with the observation that CO displays either no inhibitory or inhibitory effect on proton reduction catalyzed by Mo- and V-nitrogenases, as noted above.[229]

Trapping of nitrogenase by freezing during turnover under CO revealed a loss of the EPR spectrum of the resting state FeMo-cofactor and appearance of two major different EPR signals.[205,230–234] In the presence of low concentrations of CO ([CO]:[FeMo-cofactor] ≤ 1:1), the S = 3/2 spectrum of FeMo-cofactor changed to an S = 1/2 spin state giving rise to a new rhombic EPR signal (denoted lo-CO) with g = 2.09, 1.97, 1.93. At higher concentrations of CO (≥0.5 atm), an axial EPR signal (S = 1/2, called hi-CO) was observed with g = 2.17, 2.06, 2.06.[205,231–234] In addition to these trapped CO complexes, a small population of species at S = 3/2 spin state, so-called hi(5)-CO, has been observed under high CO concentrations and higher electron flux in wild-type[233] and variant MoFe proteins.[222,234]

These trapped CO complexes of FeMo-cofactor have been well studied by advanced spectroscopic methods. ENDOR studies of lo-CO and hi-CO complexes using different isotopologues of CO and FeMo-cofactor characterized the two CO complexes.[202,230,235–238] Key conclusions from these studies were that in lo-CO the C of a single CO bridges two Fe ions (end-on mode) and in hi-CO, two CO terminally bind to two Fe ions in the “waist” of the FeMo-cofactor (Figure 23A). The hi(5)-CO complex has been suggested to contain two bridging CO molecules on the FeMo-cofactor.[222] Finally, EPR-monitored photolysis experiments revealed that a terminal CO of hi-CO complex is photolabile, causing the state to reversibly convert to lo-CO. In contrast, both lo-CO and hi(5)-CO complexes are photostable.[239]

The E_n level of lo-CO and hi-CO remain a matter of considerable interest. It has been reported that lo-CO and hi-CO can be interconverted by adding CO to the former or pumping CO off of the latter, without redox or catalytic processes, thus demonstrating that they are at the same E_n level.[233] In addition, lo-CO can be converted to E_0 by extensive pumping, which suggests that all three states are at the same, $M^N(E_0)$, redox level,[233] an

idea consistent with ^{57}Fe ENDOR measurements.[145,237] However, CO cannot bind to FeMo-cofactor in the resting state, and can only bind to the cofactor in a state formed during turnover under CO.[233] One possibility is that lo-CO is indeed an E_2 state, and we have discussed this possibility.[202] However, such a state should have the two reducing equivalents stored as a hydride, and no such ^{1}H ENDOR signal is observed.[150,236] Thus, it appears unlikely that lo-CO is an E_2 state. To explain the combined observations one might imagine that CO binds to FeMo-cofactor in an E_2 state, or in an E_1 state that then receives a second electron, and that the resulting CO-bound E_2 state loses H_2 to form the observed lo-CO, which indeed is at an E_0 redox level. The differing net spins, $S = 3/2$ for resting state, S = 1/2 for CO-bound states, would then merely reflect the influence of the CO binding. Clearly, a reexamination of the lo-CO state, including ^{95}Mo ENDOR and DFT computations, would seem to be in order.

Although EPR and ENDOR give the optimal insights into properties of intermediates with half-integer spin states ($S = 1/2, 3/2, 5/2, \ldots$), rarely (intermediate **H**, section 4.2) can it probe intermediates with integer spin ($S = 0, 1, 2, \ldots$).[190,193] Stopped-flow FTIR studies are equally effective for all spin states.[244–246] Recently, IR-monitored photolysis studies of complexes of wild-type and two MoFe protein variants trapped during turnover with low electron flux under hi-CO conditions displayed a more complex landscape of hi-CO complexes.[240–242] Three different hi-CO complexes (designated as Hi-1, Hi-2 or hi(5)-CO, and Hi-3) were observed with absorptions at different energy levels. All hi-CO complexes have two CO bound to FeMo-cofactor and can reversibly release one CO to generate lo-CO complexes with one terminal, bridging, or protonated CO species. The three hi-CO complexes all have one CO terminally bound to FeMo-cofactor with the other ligand as a terminal, semibridging, or bridging/protonated CO ligand (Figure 23B).[240–242] Further photolysis and DFT study of Hi-3 with C-O stretching frequencies at 1938 and 1911 cm^{-1} revealed that it has two terminal CO ligands bound to two adjacent Fe atoms in the FeMo-cofactor with an EPR silent $S = 0$ spin state.[241,242] DFT calculations of the C-O stretching frequencies of hi-CO complexes also suggested that C-O frequencies at 1973 and 1680 cm^{-1} in IR of Hi-1 species originated from a terminal −CO and a partially reduced −CHO ligands bound to two adjacent Fe sites as well, consistent with the EXAFS and NRVS observations for the wild-type enzyme.[242] Recent NRVS studies of nitrogenase under high CO conditions revealed that the FeMo-cofactor undergoes significant structural perturbation upon −CO/−CHO binding.[242] The identification of Fe-CO stretching and Fe-C-O bending modes in the range of 470–560 cm^{-1} in NRVS provided the first confirmation that binding is indeed at Fe sites,[23,110] extending the many studies noted above that showed the heterometal, Mo in FeMo-cofactor, may tune the properties of the cofactor, but is not directly involved in valence changes or substrate reduction.[114,151]

As described above, structures of the FeMo-cofactors with CO or CO-derived ligands have been proposed based on the different spectroscopic studies (Figure 23). In 2014, Rees et al.[143] reported the first X-ray crystal structure of a CO-bound state of the MoFe protein with 1.5 Å resolution, using crystals obtained from a solution, following turnover in the presence of CO and C_2H_2. Surprisingly, the structure showed the bridging CO proposed for lo-CO, but it was found to bind to the FeMo-cofactor by replacing one of the belt sulfide ligands,

S2B (Figure 23C). Correspondingly, a recent EPR study of the CO-modified MoFe protein generated under the same conditions that yielded the CO-modified crystals yielded a spectrum that almost exactly matches that reported for lo-CO.[243] The dissociation of a belt sulfide is a central factor in the developing view, noted above, that FeMo-cofactor is not structurally rigid[71,143] during turnover.

The exchange of CO for S^{2-} on the FeMo-cofactor is reversible under turnover conditions.[143] Thus, CO inhibition of acetylene reduction could be recovered when the CO-bound MoFe protein crystals were dissolved and incubated in an assay mixture, and the structure of MoFe protein crystals obtained from this mixture revealed the loss of the bridging CO ligand and the reinstallation of the belt sulfide, thus restoring the resting state FeMo-cofactor structure. Even though a plausible sulfide binding site (SBS) was proposed, the origin and mechanism of insertion of the belt sulfide ligand are still not clear.

About a decade ago, CO was discovered to be a substrate of V- and Mo-nitrogenases producing both CH_4 and short-chain hydrocarbons as products.[227,228,247] Two or more CO could be reduced and coupled to make multi-C hydrocarbons at low rates when turned over with Fe protein and MgATP. The reactivity of FeMo-co- and FeV-co-reconstituted apo-MoFe protein (apo-NifDK) toward CO reduction has also recently been explored.[248] It was found that both FeMo-co- and FeV-co-reconstituted NifDK protein showed similar hydrocarbon product profiles from CO to that of wild-type Mo-nitrogenases, with much lower rates compared to that by V-nitrogenase.[227,228] However, a ~100 times increase of hydrocarbon formation from CO reduction was observed when FeMo-cofactor was housed in a VFe protein scaffold compared to that housed in its native MoFe protein scaffold.[249] These results highlighted a combined contribution from the protein environment and cofactor properties toward CO reduction.

It has also been reported that CO can bind to the V-nitrogenase in the absence of Fe protein/MgATP (nonturn-over) as electron-delivery agent, but instead in the presence of the reductants dithionite (E^0 = −0.66 V), Eu^{II}-EGTA (E^0 = −0.88 V), and Eu^{II}-DTPA (E^0 = −1.14 V).[243] The comparison of the EPR spectrum of the CO-bound VFe protein to that of the CO-modified MoFe protein led the authors to propose replacement of a belt-sulfide by a bridging CO ligand (Figure 23C).[143,243] They reported that the CO of this CO-bound VFe protein could be further reduced to methane when subjected to turnover condition with Fe protein (VnfH)/MgATP and dithionite, revealing the relevance of this CO-bound state to the catalytic turnover of CO as substrate.[243]

It has been long believed that CO does not bind to FeMo-cofactor of Mo-nitrogenase in the resting state (E_0), which is further supported by a recent electrochemical study of CO interaction with FeMo-cofactor in MoFe protein with $Eu^{III/II}$-L (L = BAPTA, EGTA, DTPA) as electron mediators.[250] However, the binding of CO to FeV-cofactor in the absence of Fe protein/MgATP (resting-state VFe protein as suggested)[243] indicates that it might be risky to simply expand the concept of resting-state E_0 of Mo-nitrogenase to V- and Fe-nitrogenases without careful consideration of the fine-tuning effect of heterometals (Mo, V, and Fe) and secondary environments on the electronic structure of FeM-cofactor. For example, to date, the FeV-cofactor in as-isolated VFe protein always has a CO_3^{2-} ligand that does not exist in

any MoFe protein crystal structures observed.[58,59] Clearly, CO interacts with nitrogenases in complex ways, with some aspects still needing resolution.

In 2013, the possible connection between CO reduction and the interstitial carbide in the active site FeMo-cofactor was explored.[251] It was found that reconstitution of apo-MoFe protein with ^{14}C-labeled FeMo-cofactor in the resting state and upon turnover with acetylene and N_2 did not show any dilution of the ^{14}C-label in the active site, indicating that the interstitial carbide cannot be exchanged during turnover. Moreover, the GC-MS characterization of the hydrocarbon products from reaction mixtures with the combined use of $^{12/13}$C-enriched CO substrate and the carbide in the active site revealed that the interstitial carbide could not be used as a substrate and incorporated into the hydrocarbon products.[251] These results are consistent with a role for carbide in stabilizing the structural integrity of FeMo-cofactor[71] as it proceeds through different conformational states during catalysis.

5.3. CO_2 as Substrate

CO_2 was reported as a substrate for nitrogenase in 1995, being reduced by two electrons to CO.[252] The form of CO_2 (CO_3^{2-}, HCO_3^-, and CO_2) that is the substrate remains unclear. Recently, it was reported that in the crystal structures of V-nitrogenase a CO_3^{2-} ligand replaced one of the belt-sulfide ligands of the active site FeV-cofactor (Figure 2).[58] This proposed CO_3^{2-} ligand is also present in a plausible turnover-relevant structure of the FeV-cofactor,[59] further complicating the origin of this CO_3^{2-} ligand and the relevance to the CO_2 reducing ability of nitrogenases.

Later studies reported that CO_2 could be reduced by eight electrons/protons to methane (CH_4) by a remodeled Mo-nitrogenase having amino acid substitutions α−70$^{\text{Val}\rightarrow\text{Ala}}$/$\alpha$−195$^{\text{His}\rightarrow\text{Gln}}$.[254] In 2016, light-driven in vivo CO_2 reduction to CH_4 by an anoxygenic phototroph, *Rhodopseudomonas palustris* (*R. palustris*), which expressed the same remodeled Mo-nitrogenase, was reported.[255] This catalytic ability was conferred upon *R. palustris* by use of a variant of the transcription factor NifA that can activate expression of nitrogenase under all growth conditions.[256–259] More recently, the in vivo CH_4 production from CO_2 reduction has been confirmed to be catalyzed by the wild-type Fe-only nitrogenase from *R. palustris* and several other nitrogen-fixing bacteria.[260] The CH_4 production by the Fe-only nitrogenase in *R. palustris* was found sufficient to support the growth of an obligate CH_4-utilizing *Methylomonas* strain. These results suggest that active Fe-only nitrogenase, present in diverse organisms, contributes CH_4 that could shape microbial community interactions.[260]

Recently, it was discovered that Mo-nitrogenase catalytically reduces carbon dioxide (CO_2) to formate ($HCOO^-$) at rates >10 times faster than that of CO_2 reduction to CO and CH_4.[253] This reaction was not inhibited by H_2, indicating that CO_2 reduction does not involve the *re/oa* equilibrium central to N_2 binding/activation, as expected if the reduction occurs a E_n states with $n < 4$.[253] In fact, DFT calculations[136] on the doubly reduced FeMo-cofactor (E_2 state) with a Fe-bound hydride and S-bound proton favor a direct reaction of CO_2 with the hydride (direct hydride transfer reaction pathway, see Figure 24 and 25, lower blue pathway), with facile hydride transfer to CO_2 yielding formate. In contrast, a significant barrier is observed for reaction of Fe-bound CO_2 with the hydride (associative reaction

pathway, Figure 25, upper blue pathway), which leads to CO and CH_4. Importantly, computations revealed that protein residues above the reactive face of the FeMo-cofactor hamper the CO_2 access to the hydridic hydrogen. In particular, steric hindrance from the side chain of α−70^{Val} or α−96^{Arg} introduces a barrier for the direct hydride transfer favoring the competitive elimination of H_2 over $HCOO^-$ formation. Consistent with this finding, MoFe proteins with amino acid substitutions near FeMo-cofactor (α−70$^{Val\rightarrow Ala}$/α−195$^{His\rightarrow Gln}$) are found to significantly alter the distribution of products between formate and CO/CH_4.[253] The formate formation by Fe-nitrogenase reduction of CO_2 was also reported to have a higher efficiency than that of Mo-nitrogenase.[261]

The analysis of the electronic properties of FeMo-cofactor during the hydride transfer revealed a strong charge transfer from the σ(Fe-H) bonding orbital to the π^*(C=O) antibonding orbital, which results in the heterolytic Fe-H $\rightarrow$ $Fe^+ + H^-$ bond cleavage and the transfer of the hydride to CO_2. The exergonic nature of the direct hydride transfer (ΔG^0 = −26 kcal/mol) suggests that the hydricity of the E_2 state, ΔG_{H^-}, is sufficient to transfer a hydride to CO_2 to generate formate, that is, the hydricity is below that of formate ($HCOO^-$ $\rightarrow$ $CO_2 + H^-$, ΔG_{H^-} = +24.1 kcal/mol).[262]

The same computational investigation revealed a pathway leading to the formation of CO from E_2(2H)-CO_2, which starts with the exergonic transfer of the protic S-H hydrogen to one of the oxygen atoms of CO_2 (Figure 25, green pathway).[253] Although the small size of the adopted computational models introduces a rather large uncertainty, initial protonation of CO_2 by other ionizable residues, such as α−96^{Arg}, was found very unlikely. The formation of CO proceeds with the transfer of the Fe-H hydrogen (as a proton rather than a hydride) to that oxygen, which results in the exoergic dissociation of a water molecule.[253]

The competitive formation of H_2 from the E_2(2H) state was also investigated computationally (Figure 25, red pathway). It was found that the release of H_2 is a facile and exergonic process (ΔG^0 = −31.3 kcal/mol). The exergonic nature of the formation of H_2 is consistent with the observation that H_2 cannot reduce FeMo-cofactor. It is of interest to point out that, as with the direct hydride pathway for the CO_2 reduction, the Fe-H behaves as a hydride that is protonated by S-H, with the overall H_2 elimination driven by a σ(Fe-H) to σ^*(S-H) charge transfer.[253]

In a separate study of CO_2 reduction by nitrogenases, it was found that both Mo- and V-nitrogenases can reduce CO_2 to CO yielding substoichiometric amounts of product compared to the amount of the proteins used.[263,264] Different from its Mo-counterpart, the V-nitrogenase can further reduce CO_2 to CD_4, C_2D_4, and C_2D_6 in D_2O buffer with substoichiometric amounts of products after 3 h incubation. The product profile of CO_2 reduction was further expanded to ≤C_4 hydrocarbons in an ATP-independent study of V-nitrogenase with Eu^{II}-DTPA as reductant, with all products showing a turnover number (TON) < 1.[264,265]

5.4. Other C Substrates

As analogs of carbon dioxide, isocyanic acid/cyanate ($HNCO/OCN^-$), thiocyanate (SCN^-), and carbon disulfide (CS_2) are substrates of wild-type Mo-nitrogenase.[252,266] The slow

turnover rates for the reduction of these substrates allowed trapping intermediates by rapid freeze-quench. Dependent on pH and isocyanic acid concentration, the EPR spectra of nitrogenase during turnover in the presence of HNCO displayed signals with g-values corresponding to lo-CO and hi-CO complexes indicating the production of CO.[266] The initial EPR study of trapped intermediates from thiocyanate and carbon disulfide reduction by nitrogenase revealed a similar $S = 1/2$ spin state signal (denoted "c"), indicating a sulfur-containing intermediate bound to FeMo-cofactor.[266] Further detailed EPR and ^{13}C-ENDOR study[267] revealed the presence of three sequentially formed intermediates trapped during CS_2 reduction: "a" with $g = 2.035, 1.982, 1.973$; "b" with $g = 2.111, 2.002, 1.956$; and a previously observed "c" with $g = 2.211, 1.996, 1.978$. All three intermediates were suggested to have CS_2-derived fragments bound to one or two Fe atoms on FeMo-cofactor. The first formed intermediate "a" might contain an activated CS_2 bound to FeMo-cofactor in side-on mode, and the third intermediate "c" was suggested to contain a "C≡S" species terminally bound to the cofactor through C atom.[267]

Recently, the potential of selenocyanate ($SeCN^-$) as nitrogenase substrate and inhibitor was evaluated.[144] Compared to SCN^- and cyanide (CN^-), it was found that $SeCN^-$ is a poor substrate in terms of methane production. In addition, $SeCN^-$ is a potent, yet reversible inhibitor of acetylene reduction by nitrogenase with an inhibition constant (K_i ($SeCN^-$) = 410 ± 30 μM)[144] 30 times lower than that observed for SCN^- (K_i (SCN^-) = 12.7 ± 1.2 mM).[266] In contrast to full inhibition of acetylene reduction by $SeCN^-$, the proton reduction was inhibited to a lesser extent.[144]

Rees et al. resolved a MoFe protein crystal structure at 1.6 Å resolution isolated from an assay mixture that included 25 mM $SeCN^-$, revealing a quantitative substitution of the belt sulfide S2B by a selenide ligand.[144] A time course series of crystallographic structures demonstrated the migration of the selenide ligand from the original Se2B position to the other two belt sulfide positions (S5A and S3A) during acetylene reduction, as opposed to little or no migration of Se2B during proton reduction. The Se was completely lost and replaced by S after a sufficient number of catalytic turnovers of acetylene. Turning over of the Se-incorporated MoFe protein in the presence of CO and C_2H_2 resulted in the migration of Se from 2B position to the other two belt positions and high occupancy of bridging CO ligand in the Se2B position (Figure 26).[144] The lability of the S2B position toward ligand exchange during substrate reduction confirms the long-proposed Fe2-Fe6 edge as a primary interaction site for substrates and inhibitors.[23,33,36,40,59,110,144,156] Application of advanced X-ray absorption spectroscopies to these Se- and CO-substituted FeMo-cofactors revealed a significant asymmetry with regard to the electronic distribution about the cluster, and a redox reorganization mechanism within the cluster has been postulated.[268]

As discussed above, the migration of Se2B into the other two belt positions displayed a reversible and substrate-dependent pattern.[144] This apparent "ratcheting" motion of the selenide in three belt positions on the FeMo-co suggests a dynamic structural change (e.g., the interchange of the belt sulfides through swapping Fe-S partners in the prismatic 6Fe core) of the cluster, while still bound in the protein upon turnover.[144,269] The mechanism of this apparent "ratcheting" motion is not yet clear. On basis of the DFT calculations,[179] the rotation of the prismatic part of the FeMo-co as a whole is less possible. Other pathways

involving small molecules, such as S and Se atom carriers, has been suggested and is worth considering.[179] The motion might be substrate specific.[269] These studies open the door to further exploration of structure-function relationships of the active site of nitrogenase during nitrogen fixation. Moreover, the mutual substitution reactions between different small molecule ligands, S^{2-}, Se^{2-}, CO, and possibly acetylene, should be considered in light of the relative bond dissociation energy between different Fe-L bonds, where L = S, Se, or C.

6. CONCLUDING REMARKS

Remarkable progress has been achieved in understanding aspects of the mechanism of nitrogenase reduction of a wide range of substrates, including protons and N_2, nonphysiological N substrates, and C substrates. For N_2 and proton reduction, studies over the last 10 years have provided an understanding of the critical E_4 step where N_2 binds, and H_2 is released. Many lines of evidence have revealed the enzyme functions with the limiting $8e^-$ stoichiometry of eq 1 and Figure 3 because the *re* and release of H_2 is required to drive one of the most challenging reactions in biology, cleavage of the N≡N triple bond. This exoergic loss of H_2 from E_4(4H), the Janus intermediate drives N_2 binding and formation of the first stage in actual N_2 reduction, the E_4(2N2H) state. The enzyme *mechanistically* couples exothermic H_2 formation to endothermic cleavage of the N≡N triple bond in the nearly thermoneutral *re/oa* equilibrium.

One of the tasks remaining is to determine whether there is an alternative pathway, with H_2 *re* and release at E_3(3H), as also proposed by Lowe and Thorneley. The evidence for this process is not strong, and the question must be re-examined. In the future, it would be useful to develop direct spectroscopic probes of the E_n FeMo-cofactor intermediates with odd-*n* (even-electron) that could give the types of insight that have been gained using EPR on even-*n* (odd-electron) species.

The additional questions about the mechanism of nitrogenase reduction of N-substrates include the following. Foremost is unambiguously distinguishing between alternating (**A**) and distal (**D**) pathways for N_2 reduction. The fundamental difference between these two pathways is the stage at which the N-N bond is cleaved and the first NH_3 formed: E_5 for **D** versus E_7 for **A**. The two trapped reduction intermediates, **H** and **I**, do not directly distinguish, as they are respectively E_7 and E_8, stages past N-N cleavage. However, the weight of the evidence provided by studies of the non-native N-substrates points to the **A** pathway, as described above. Nonetheless, more studies are needed, in particular, trapping and characterization of the odd-electron E_6 state. An initial step in this direction is studies of E_1, and it has been suggested, but not confirmed, that a recent crystal structure of VFe represents E_6 or E_7.[59]

In delivering each [e^-/H^+] to FeMo-cofactor, the critical step is the P → M electron transfer that must be accompanied by H^+ delivery. One might well ask whether this occurs through proton coupled electron transfer (PCET) or coupled electron–proton transfer (CEPT). The ability to observe by EPR *both* E_7 and E_8 (**H** and **I**) provides a chance to study the conversion of **H** to **I** by cryoreduction/annealing, as has been done for the E_0 to E_1 conversion.

For nonphysiological N substrates, an important question is understanding how the N species is hydrogenated. Is this through migratory insertion of FeMo-cofactor bound hydride species? Is there any significant structural rearrangement/change that plays important roles during binding/activation/hydrogenation? Answers to such questions will take our understanding of the mechanism to the next level.

Progress in understanding nitrogenase reduction of C-based substrates spans decades, with the most recent advances coming for acetylene, CO, and CO_2. A clearer picture of the mechanism for CO_2 and CO reduction is emerging, with the Fe-hydrides again at the center of the chemistry. Clearly understanding how nitrogenase reduces these C-bound substrates is important in gaining insights into the chemistry that can be achieved at the active site metal clusters. These reactions have also been suggested as a possible avenue for advancing biotechnology for hydrocarbon production. However, the direct use of nitrogenase or its cofactors to contribute to the production of feedstocks or CO_2 sequestration at a useful scale is likely to be an insurmountable challenge given the lack of robustness of the enzymes and their associated cofactors.

Nitrogenase first became available for critical studies in its purified form more than half a century ago.[61,62,270] This was followed by steady progress in understanding the catalytic function of this complex enzyme, with rapid recent progress in determining the enzyme mechanism as described in this Review. Similar progress in addressing the many remaining issues, including those just mentioned, is expected.

ACKNOWLEDGMENTS

The work in the Seefeldt and Dean groups was supported by grants from the US Department of Energy (DOE), Office of Science, Basic Energy Sciences (BES) (Grants DESC0010687 and DESC0010834). The work of Raugei was supported by the US DOE, Office of Science, BES, Division of Chemical Sciences, Geosciences, and Biosciences. Work in the Hoffman Laboratory was supported by the National Science Foundation (Grant) and the National Institutes of Health (Grant GM111097) and the US Department of Energy (DOE), Office of Science, Basic Energy Sciences (BES) (Grant DE-SC0019342).

Biographies

Lance C. Seefeldt received a B.S. degree in chemistry from the University of Redlands in California and a Ph.D. in biochemistry from the University of California at Riverside. He was a postdoctoral fellow at the Center for Metalloenzyme Studies at the University of Georgia before joining the faculty of the Chemistry and Biochemistry Department at Utah State University, where he is now Professor and Department Head. He was recently awarded the D. Wynne Thorne Career Research Award and was elected a Fellow of the American Association for the Advancement of Science. Over the past 30 years, his research has focused on elucidating the mechanism of nitrogenase.

Zhi-Yong Yang received a B.S. degree in chemistry in 2001 and a Ph.D. degree in organic chemistry in 2006 from Nankai University in Tianjin, China. Following a position at Shanghai ChemPartner as an organic chemist, he joined Prof. Lance Seefeldt’s lab at Utah State University and was awarded with a Ph.D. degree in biochemistry in 2013. After a postdoctoral training in the same group, he was promoted to Researcher in 2017. During the

past 19 years, his research has covered biomimetic chemistry of hydrogenases and the mechanism of nitrogenase. His research interest is in understanding the mechanism of small molecule activation catalyzed by biological and synthetic catalysts, including kinetics, thermodynamics, electron transfer, and energy transduction.

Dmitriy A. Lukoyanov received a M.S. degree and a Ph.D. from Kazan State University. He is a Research Associate at Northwestern University. During the last 14 years, his research work has focused on investigation of nitrogenase catalysis with application of various Electron Paramagnetic Resonance (EPR) techniques.

Derek F. Harris received a B.S. in biology from Dixie State University and a M.S. and Ph.D. in biochemistry from Utah State University. He continues to study nitrogenase enzymes as a postdoctoral fellow at Utah State University.

Dennis R. Dean received a B.A. from Wabash College and a Ph.D. from Purdue University. He is currently a University Distinguished Professor at Virginia Tech, where he has also served as the Director of the Fralin Life Sciences Institute, the Virginia Bioinformatics Institute and Vice President for Research. He is a Fellow of the American Association for the Advancement of Science and a Fellow of the American Academy of Microbiology.

Simone Raugei obtained a Ph.D. in theoretical chemistry from the University of Florence (Italy) in 2000 with Prof. Vincenzo Schettino. In 1997–1998, he studied at the Max Planck Institute for Solid State Physics in Stuttgart (Germany) under the supervision of Prof. Michele Parrinello. From 2000 to 2002, he joined the University of Pennsylvania (USA) as a postdoctoral fellow in the group of Prof. Michael L. Klein. From 2002 to 2009, he was an Assistant Professor at the School for Advanced Studies in Trieste (Italy). Since 2010, he has been a senior Scientist at the Pacific Northwest National Laboratory. His current scientific activity focuses on the computational and theoretical modeling of chemical and biochemical processes for energy storage and energy delivery.

Brian M. Hoffman is the Charles E. and Emma H. Morrison Professor of Chemistry and Professor of Molecular Biosciences at Northwestern University. His undergraduate studies were at the University of Chicago, PhD with Harden McConnell at the California Institute of Technology, and Postdoctoral work at the Massachusetts Institute of Technology with Alex Rich. His research in Bioinorganic Chemistry has included measurements of long-range electron transfer between proteins, in addition to determinations of metalloenzyme mechanisms through development and implementation of electron–nuclear double resonance (ENDOR) techniques. He is a member of the National Academy of Sciences and the American Academy of Arts and Sciences.

REFERENCES

(1). Smil V Enriching the Earth: Fritz Haber, Carl Bosch, and the Transformation of World Food Production; MIT Press: Cambridge, MA, 2004.

(2). Erisman JW; Galloway JN; Dise NB; Sutton MA; Bleeker A; Grizzetti B; Leach AM; de Vries W Nitrogen: Too Much of a Vital Resource; Science Brief; WWF Nederland, 2015.

(3). Chen JG; Crooks RM; Seefeldt LC; Bren KL; Bullock RM; Darensbourg MY; Holland PL; Hoffman B; Janik MJ; Jones AK; et al. Beyond Fossil Fuel–Driven Nitrogen Transformations. Science 2018, 360, No. eaar6611. [PubMed: 29798857]

(4). Dawson CJ; Hilton J Fertiliser Availability in a Resource-Limited World: Production and Recycling of Nitrogen and Phosphorus. Food Policy 2011, 36, S14–S22.

(5). Erisman JW; Galloway JN; Seitzinger S; Bleeker A; Dise NB; Petrescu AMR; Leach AM; de Vries W Consequences of Human Modification of the Global Nitrogen Cycle. Philos. Trans. R. Soc., B 2013, 368, 20130116.

(6). Galloway JN; Townsend AR; Erisman JW; Bekunda M; Cai Z; Freney JR; Martinelli LA; Seitzinger SP; Sutton MA Transformation of the Nitrogen Cycle: Recent Trends, Questions, and Potential Solutions. Science 2008, 320, 889–892. [PubMed: 18487183]

(7). Erisman JW; Sutton MA; Galloway J; Klimont Z; Winiwarter W How a Century of Ammonia Synthesis Changed the World. Nat. Geosci 2008, 1, 636–639.

(8). Fowler D; Coyle M; Skiba U; Sutton MA; Cape JN; Reis S; Jenkins A; Grizzetti B; Galloway JN; Vitousek P; et al. The Global Nitrogen Cycle in the Twenty-First Century. Philos. Trans. R. Soc., B 2013, 368, 20130164.

(9). Gruber N; Galloway JN An Earth-System Perspective of the Global Nitrogen Cycle. Nature 2008, 451, 293–296. [PubMed: 18202647]

(10). Thamdrup B New Pathways and Processes in the Global Nitrogen Cycle. Annu. Rev. Ecol. Evol. Syst 2012, 43, 407–428.

(11). Raymond J; Siefert JL; Staples CR; Blankenship RE The Natural History of Nitrogen Fixation. Mol. Biol. Evol 2004, 21, 541–554. [PubMed: 14694078]

(12). Zhang X; Davidson EA; Mauzerall DL; Searchinger TD; Dumas P; Shen Y Managing Nitrogen for Sustainable Development. Nature 2015, 528, 51–59. [PubMed: 26595273]

(13). Haber FÜber die Darstellung des Ammoniaks aus Stickstoff und Wasserstoff. Naturwissenschaften 1922, 10, 1041–1049.

(14). Ertl G Reactions at Surfaces: From Atoms to Complexity. Angew. Chem., Int. Ed 2008, 47, 3524–3535.

(15). Haber F The History of the Ammonia Process. Naturwissenschaften 1923, 11, 339–340.

(16). Burris RH; Roberts GP Biological Nitrogen Fixation. Annu. Rev. Nutr 1993, 13, 317–335. [PubMed: 8369149]

(17). Cheng Q Perspectives in Biological Nitrogen Fixation Research. J. Integr. Plant Biol 2008, 50, 786–798. [PubMed: 18713389]

(18). Boyd ES; Hamilton TL; Peters JW An Alternative Path for the Evolution of Biological Nitrogen Fixation. Front. Microbiol 2011, 2, 205. [PubMed: 22065963]

(19). Simpson FB; Burris RHA Nitrogen Pressure of 50 atm Does Not Prevent Evolution of Hydrogen by Nitrogenase. Science 1984, 224, 1095–1097. [PubMed: 6585956]

(20). Burgess BK; Lowe DJ Mechanism of Molybdenum Nitrogenase. Chem. Rev 1996, 96, 2983–3012. [PubMed: 11848849]

(21). Hoffman BM; Lukoyanov D; Dean DR; Seefeldt LC Nitrogenase: A Draft Mechanism. Acc. Chem. Res 2013, 46, 587–595. [PubMed: 23289741]

(22). Yang Z-Y; Khadka N; Lukoyanov D; Hoffman BM; Dean DR; Seefeldt LC On Reversible H_2 Loss upon N_2 Binding to FeMo-cofactor of Nitrogenase. Proc. Natl. Acad. Sci. U. S. A 2013, 110, 16327–16332. [PubMed: 24062454]

(23). Hoffman BM; Lukoyanov D; Yang Z-Y; Dean DR; Seefeldt LC Mechanism of Nitrogen Fixation by Nitrogenase: The next Stage. Chem. Rev 2014, 114, 4041–4062. [PubMed: 24467365]

(24). Rafiqul I; Weber C; Lehmann B; Voss A Energy Efficiency Improvements in Ammonia Production—Perspectives and Uncertainties. Energy 2005, 30, 2487–2504.

(25). Neet KE Enzyme Catalytic Power Minireview Series. J. Biol. Chem 1998, 273, 25527–25528. [PubMed: 9748210]

(26). Knowles JR Enzyme Catalysis: Not Different, Just Better. Nature 1991, 350, 121–124. [PubMed: 2005961]

(27). Benkovic SJ; Hammes-Schiffer S A Perspective on Enzyme Catalysis. Science 2003, 301, 1196–1202. [PubMed: 12947189]

(28). Yang Z-Y; Ledbetter R; Shaw S; Pence N; Tokmina-Lukaszewska M; Eilers B; Guo Q; Pokhrel N; Cash VL; Dean DR; et al. Evidence That the Pi Release Event Is the Rate-Limiting Step in the Nitrogenase Catalytic Cycle. Biochemistry 2016, 55, 3625–3635. [PubMed: 27295169]

(29). Badalyan A; Yang Z-Y; Seefeldt LC A Voltammetric Study of Nitrogenase Catalysis Using Electron Transfer Mediators. ACS Catal. 2019, 9, 1366–1372.

(30). Mortenson LE; Thorneley RN Structure and Function of Nitrogenase. Annu. Rev. Biochem 1979, 48, 387–418. [PubMed: 224803]

(31). Thorneley RNF; Lowe DJ Kinetics and Mechanism of the Nitrogenase Enzyme In Molybdenum Enzymes; Spiro TG, Ed.; Metal Ions in Biology; Wiley-Interscience Publications: New York, 1985; Vol. 7, pp 221–284.

(32). Howard JB; Rees DC How Many Metals Does It Take to Fix N_2? A Mechanistic Overview of Biological Nitrogen Fixation. Proc. Natl. Acad. Sci. U. S. A 2006, 103, 17088–17093. [PubMed: 17088547]

(33). Seefeldt LC; Hoffman BM; Dean DR Mechanism of Mo-Dependent Nitrogenase. Annu. Rev. Biochem 2009, 78, 701–722. [PubMed: 19489731]

(34). Seefeldt LC; Dean DR Role of Nucleotides in Nitrogenase Catalysis. Acc. Chem. Res 1997, 30, 260–266.

(35). Igarashi RY; Seefeldt LC Nitrogen Fixation: The Mechanism of the Mo-Dependent Nitrogenase. Crit. Rev. Biochem. Mol. Biol 2003, 38, 351–384. [PubMed: 14551236]

(36). Dos Santos PC; Igarashi RY; Lee H-I; Hoffman BM; Seefeldt LC; Dean DR Substrate Interactions with the Nitrogenase Active Site. Acc. Chem. Res 2005, 38, 208–214. [PubMed: 15766240]

(37). Tezcan FA; Kaiser JT; Mustafi D; Walton MY; Howard JB; Rees DC Nitrogenase Complexes: Multiple Docking Sites for a Nucleotide Switch Protein. Science 2005, 309, 1377–1380. [PubMed: 16123301]

(38). Harris DF; Lukoyanov DA; Shaw S; Compton P; Tokmina-Lukaszewska M; Bothner B; Kelleher N; Dean DR; Hoffman BM; Seefeldt LC Mechanism of N_2 Reduction Catalyzed by Fe-Nitrogenase Involves Reductive Elimination of H_2. Biochemistry 2018, 57, 701–710. [PubMed: 29283553]

(39). Burgess BK Substrate Reactions of Nitrogenase In Metal Ions in Biology: Molybdenum Enzymes; Spiro TG, Ed.; John Wiley and Sons: New York, 1985; pp 161–220.

(40). Seefeldt LC; Yang Z-Y; Duval S; Dean DR Nitrogenase Reduction of Carbon-Containing Compounds. Biochim. Biophys. Acta, Bioenerg 2013, 1827, 1102–1111.

(41). Eady RR Structure–Function Relationships of Alternative Nitrogenases. Chem. Rev 1996, 96, 3013–3030. [PubMed: 11848850]

(42). Hu Y; Lee CC; Ribbe MW Vanadium Nitrogenase: A Two-Hit Wonder? Dalton Trans 2012, 41, 1118–1127. [PubMed: 22101422]

(43). Schneider K; Müller A Iron-Only Nitrogenase: Exceptional Catalytic, Structural and Spectroscopic Features In Catalysts for Nitrogen Fixation: Origins, Applications, and Research Progress; Springer: Dordrecht, 2004; pp 281–307.

(44). Hales BJ Alternative Nitrogenase. Adv. Inorg. Biochem 1990, 8, 165–198. [PubMed: 2206026]

(45). McGlynn SE; Boyd ES; Peters JW; Orphan VJ Classifying the Metal Dependence of Uncharacterized Nitrogenases. Front. Microbiol 2013, 3, 419. [PubMed: 23440025]

(46). Waugh SI; Paulsen DM; Mylona PV; Maynard RH; Premakumar R; Bishop PE The Genes Encoding the Delta Subunits of Dinitrogenases 2 and 3 Are Required for Mo-Independent Diazotrophic Growth by *Azotobacter vinelandii*. J. Bacteriol 1995, 177, 1505–1510. [PubMed: 7883707]

(47). Bishop PE; Hawkins ME; Eady RR Nitrogen Fixation in Molybdenum-Deficient Continuous Culture by a Strain of *Azotobacter vinelandii* Carrying a Deletion of the Structural Genes for Nitrogenase (*nif HDK*). Biochem. J 1986, 238, 437–442. [PubMed: 3467721]

(48). Bishop PE; Premakumar R; Dean DR; Jacobson MR; Chisnell JR; Rizzo TM; Kopczynski J Nitrogen Fixation by *Azotobacter vinelandii* Strains Having Deletions in Structural Genes for Nitrogenase. Science 1986, 232, 92–94. [PubMed: 17774003]

(49). Betancourt DA; Loveless TM; Brown JW; Bishop PE Characterization of Diazotrophs Containing Mo-Independent Nitrogenases, Isolated from Diverse Natural Environments. Appl. Environ. Microbiol 2008, 74, 3471–3480. [PubMed: 18378646]

(50). Dos Santos PC; Fang Z; Mason SW; Setubal JC; Dixon R Distribution of Nitrogen Fixation and Nitrogenase-like Sequences amongst Microbial Genomes. BMC Genomics 2012, 13, 162. [PubMed: 22554235]

(51). Boyd ES; Costas AMG; Hamilton TL; Mus F; Peters JW Evolution of Molybdenum Nitrogenase during the Transition from Anaerobic to Aerobic Metabolism. J. Bacteriol 2015, 197, 1690–1699. [PubMed: 25733617]

(52). Bishop PE; Jarlenski DM; Hetherington DR Evidence for an Alternative Nitrogen Fixation System in *Azotobacter vinelandii*. Proc. Natl. Acad. Sci. U. S. A 1980, 77, 7342–7346. [PubMed: 6938981]

(53). Sippel D; Schlesier J; Rohde M; Trncik C; Decamps L; Djurdjevic I; Spatzal T; Andrade SLA; Einsle O Production and Isolation of Vanadium Nitrogenase from *Azotobacter vinelandii* by Molybdenum Depletion. JBIC, J. Biol. Inorg. Chem 2017, 22, 161–168. [PubMed: 27928630]

(54). Georgiadis MM; Komiya H; Chakrabarti P; Woo D; Kornuc JJ; Rees DC Crystallographic Structure of the Nitrogenase Iron Protein from *Azotobacter vinelandii*. Science 1992, 257, 1653–1659. [PubMed: 1529353]

(55). Kim J; Rees DC Structural Models for the Metal Centers in the Nitrogenase Molybdenum-Iron Protein. Science 1992, 257, 1677–1682. [PubMed: 1529354]

(56). Einsle O; Tezcan FA; Andrade SLA; Schmid B; Yoshida M; Howard JB; Rees DC Nitrogenase MoFe-Protein at 1.16 Å Resolution: A Central Ligand in the FeMo-cofactor. Science 2002, 297, 1696–1700. [PubMed: 12215645]

(57). Spatzal T; Aksoyoglu M; Zhang L; Andrade SLA; Schleicher E; Weber S; Rees DC; Einsle O Evidence for Interstitial Carbon in Nitrogenase FeMo Cofactor. Science 2011, 334, 940–940. [PubMed: 22096190]

(58). Sippel D; Einsle O The Structure of Vanadium Nitrogenase Reveals an Unusual Bridging Ligand. Nat. Chem. Biol 2017, 13, 956–960. [PubMed: 28692069]

(59). Sippel D; Rohde M; Netzer J; Trncik C; Gies J; Grunau K; Djurdjevic I; Decamps L; Andrade SLA; Einsle O A Bound Reaction Intermediate Sheds Light on the Mechanism of Nitrogenase. Science 2018, 359, 1484–1489. [PubMed: 29599235]

(60). Rohde M; Trncik C; Sippel D; Gerhardt S; Einsle O Crystal Structure of VnfH, the Iron Protein Component of Vanadium Nitrogenase. JBIC, J. Biol. Inorg. Chem 2018, 23, 1049–1056. [PubMed: 30141094]

(61). Bulen WA; LeComte JR The Nitrogenase System from Azotobacter: Two-Enzyme Requirement for N_2 Reduction, ATP-Dependent H_2 Evolution, and ATP Hydrolysis. Proc. Natl. Acad. Sci. U. S. A 1966, 56, 979–986. [PubMed: 5230193]

(62). Mortenson LE Components of Cell-Free Extracts of Clostridium Pasteurianum Required for ATP-Dependent H_2 Evolution from Dithionite and for N_2 Fixation. Biochim. Biophys. Acta, Gen. Subj 1966, 127, 18–25.

(63). Roberts GP; MacNeil T; MacNeil D; Brill WJ Regulation and Characterization of Protein Products Coded by the *nif* (Nitrogen Fixation) Genes of *Klebsiella pneumoniae*. J. Bacteriol 1978, 136, 267–279. [PubMed: 361694]

(64). Robson R; Woodley P; Jones R Second Gene (*Nif H*) Coding for a Nitrogenase Iron Protein in *Azotobacter chroococcum* Is Adjacent to a Gene Coding for a Ferredoxin-like Protein. EMBO J. 1986, 5, 1159–1163. [PubMed: 15966103]

(65). Joerger RD; Wolfinger ED; Bishop PE The Gene Encoding Dinitrogenase Reductase 2 Is Required for Expression of the Second Alternative Nitrogenase from *Azotobacter vinelandii*. J. Bacteriol 1991, 173, 4440–4446. [PubMed: 1906063]

(66). Joerger RD; Bishop PE; Evans HJ Bacterial Alternative Nitrogen Fixation Systems. Crit. Rev. Microbiol 1988, 16, 1–14. [PubMed: 3053048]

(67). Joerger RD; Jacobson MR; Premakumar R; Wolfinger ED; Bishop PE Nucleotide Sequence and Mutational Analysis of the Structural Genes (*anf HDGK*) for the Second Alternative Nitrogenase from *Azotobacter vinelandii*. J. Bacteriol 1989, 171, 1075–1086. [PubMed: 2644222]

(68). Howard JB; Rees DC Structural Basis of Biological Nitrogen Fixation. Chem. Rev 1996, 96, 2965–2982. [PubMed: 11848848]

(69). Lancaster KM; Roemelt M; Ettenhuber P; Hu Y; Ribbe MW; Neese F; Bergmann U; DeBeer S X-Ray Emission Spectroscopy Evidences a Central Carbon in the Nitrogenase Iron-Molybdenum Cofactor. Science 2011, 334, 974–977. [PubMed: 22096198]

(70). Shah VK; Brill WJ Isolation of an Iron-Molybdenum Cofactor from Nitrogenase. Proc. Natl. Acad. Sci. U. S. A 1977, 74, 3249–3253. [PubMed: 410019]

(71). Grunenberg J The Interstitial Carbon of the Nitrogenase FeMo Cofactor Is Far Better Stabilized than Previously Assumed. Angew. Chem., Int. Ed 2017, 56, 7288–7291.

(72). Rees JA; Bjornsson R; Schlesier J; Sippel D; Einsle O; DeBeer S The Fe–V Cofactor of Vanadium Nitrogenase Contains an Interstitial Carbon Atom. Angew. Chem., Int. Ed 2015, 54, 13249–13252.

(73). Fay AW; Blank MA; Lee CC; Hu Y; Hodgson KO; Hedman B; Ribbe MW Characterization of Isolated Nitrogenase FeVco. J. Am. Chem. Soc 2010, 132, 12612–12618. [PubMed: 20718463]

(74). Peters JW; Fisher K; Newton WE; Dean DR Involvement of the P-Cluster in Intramolecular Electron Transfer within the Nitrogenase MoFe Protein. J. Biol. Chem 1995, 270, 27007–27013. [PubMed: 7592949]

(75). Seefeldt LC; Hoffman BM; Peters JW; Raugei S; Beratan DN; Antony E; Dean DR Energy Transduction in Nitrogenase. Acc. Chem. Res 2018, 51, 2179–2186. [PubMed: 30095253]

(76). Poudel S; Colman DR; Fixen KR; Ledbetter RN; Zheng Y; Pence N; Seefeldt LC; Peters JW; Harwood CS; Boyd ES Electron Transfer to Nitrogenase in Different Genomic and Metabolic Backgrounds. J. Bacteriol 2018, 200, e00757–17. [PubMed: 29483165]

(77). Katz FEH; Owens CP; Tezcan FA Electron Transfer Reactions in Biological Nitrogen Fixation. Isr. J. Chem 2016, 56, 682–692.

(78). Münck E; Rhodes H; Orme-Johnson WH; Davis LC; Brill WJ; Shah VK Nitrogenase. VIII. Mössbauer and EPR Spectroscopy. The MoFe Protein Component from *Azotobacter vinelandii* OP. Biochim. Biophys. Acta, Protein Struct 1975, 400, 32–53.

(79). Harris TV; Szilagyi RK Comparative Assessment of the Composition and Charge State of Nitrogenase FeMo-cofactor. Inorg. Chem 2011, 50, 4811–4824. [PubMed: 21545160]

(80). Krahn E; Weiss B; Kröckel M; Groppe J; Henkel G; Cramer S; Trautwein A; Schneider K; Müller A The Fe-Only Nitrogenase from *Rhodobacter capsulatus*: Identification of the Cofactor, an Unusual, High-Nuclearity Iron-Sulfur Cluster, by Fe K-Edge EXAFS and ^{57}Fe Mössbauer Spectroscopy. JBIC, J. Biol. Inorg. Chem 2002, 7, 37–45. [PubMed: 11862539]

(81). Wilson PE; Nyborg AC; Watt GD Duplication and Extension of the Thorneley and Lowe Kinetic Model for *Klebsiella pneumoniae* Nitrogenase Catalysis Using a MATHEMATICA Software Platform. Biophys. Chem 2001, 91, 281–304. [PubMed: 11551440]

(82). Hoffman BM; Dean DR; Seefeldt LC Climbing Nitrogenase: Toward a Mechanism of Enzymatic Nitrogen Fixation. Acc. Chem. Res 2009, 42, 609–619. [PubMed: 19267458]

(83). Pickett CJ The Chatt Cycle and the Mechanism of Enzymic Reduction of Molecular Nitrogen. JBIC, J. Biol. Inorg. Chem 1996, 1, 601–606.

(84). Henderson RA Metal Hydride Intermediates in Hydro-genases and Nitrogenases: Enzymological and Model Studies In Recent Advances in Hydride Chemistry; Peruzzini M, Poli R, Eds.; Elsevier: Amsterdam, 2001; pp 463–505.

(85). Jackson EK; Parshall GW; Hardy RWF Hydrogen Reactions of Nitrogenase. Formation of the Molecule HD by Nitrogenase and by an Inorganic Model. J. Biol. Chem 1968, 243, 4952–4958. [PubMed: 4234468]

(86). Thorneley RNF; Eady RR; Lowe DJ Biological Nitrogen Fixation by Way of an Enzyme-Bound Dinitrogen-Hydride Intermediate. Nature 1978, 272, 557–558.

(87). Thorneley RN; Lowe DJ The Mechanism of *Klebsiella pneumoniae* Nitrogenase Action: Pre-Steady-State Kinetics of an Enzyme-Bound Intermediate in N_2 Reduction and of NH_3 Formation. Biochem. J 1984, 224, 887–894. [PubMed: 6395862]

(88). Guth JH; Burris RH Inhibition of Nitrogenase-Catalyzed Ammonia Formation by Hydrogen. Biochemistry 1983, 22, 5111–5122. [PubMed: 6360203]

(89). Jensen BB; Burris RH Effect of High pN_2 and High pD_2 on Ammonia Production, Hydrogen Evolution, and Hydrogen Deuteride Formation by Nitrogenases. Biochemistry 1985, 24, 1141–1147. [PubMed: 3913463]

(90). Burgess BK; Wherland S; Newton WE; Stiefel EI Nitrogenase Reactivity: Insight into the Nitrogen-Fixing Process through Hydrogen-Inhibition and HD-Forming Reactions. Biochemistry 1981, 20, 5140–5146. [PubMed: 6945872]

(91). Leigh GJ The Mechanism of Dinitrogen Reduction by Molybdenum Nitrogenases. Eur. J. Biochem 1995, 229, 14–20. [PubMed: 7744024]

(92). Thorneley RNF; Lowe DJ Nitrogenase: Substrate Binding and Activation. JBIC, J. Biol. Inorg. Chem 1996, 1, 576–580.

(93). Rivera-Ortiz JM; Burris RH Interactions among Substrates and Inhibitors of Nitrogenase. J. Bacteriol 1975, 123, 537–545. [PubMed: 1150625]

(94). Strandberg GW; Wilson PW Formation of the Nitrogen-Fixing Enzyme System in *Azotobacter vinelandii*. Can. J. Microbiol 1968, 14, 25–31. [PubMed: 5644401]

(95). Hwang JC; Chen CH; Burris RH Inhibition of Nitrogenase-Catalyzed Reductions. Biochim. Biophys. Acta, Bioenerg 1973, 292, 256–270.

(96). Hoch GE; Schneider KC; Burris RH Hydrogen Evolution and Exchange, and Conversion of N_2O to N_2 by Soybean Root Nodules. Biochim. Biophys. Acta 1960, 37, 273–279. [PubMed: 14402169]

(97). Wherland S; Burgess BK; Stiefel EI; Newton WE Nitrogenase Reactivity: Effects of Component Ratio on Electron Flow and Distribution during Nitrogen Fixation. Biochemistry 1981, 20, 5132–5140. [PubMed: 6945871]

(98). Li J-L; Burris RH Influence of pN_2 and pD_2 on HD Formation by Various Nitrogenases. Biochemistry 1983, 22, 4472–4480. [PubMed: 6354256]

(99). Dilworth MJ; Fisher K; Kim C-H; Newton WE Effects on Substrate Reduction of Substitution of Histidine-195 by Glutamine in the α-Subunit of the MoFe Protein of *Azotobacter vinelandii* Nitrogenase. Biochemistry 1998, 37, 17495–17505. [PubMed: 9860864]

(100). Fisher K; Dilworth MJ; Newton WE Differential Effects on N_2 Binding and Reduction, HD Formation, and Azide Reduction with α−195^{His}- and α−191^{Gln}-Substituted MoFe Proteins of *Azotobacter vinelandii* Nitrogenase. Biochemistry 2000, 39, 15570–15577. [PubMed: 11112544]

(101). Ashby GA; Dilworth MJ; Thorneley RNF *Klebsiella pneumoniae* Nitrogenase. Inhibition of Hydrogen Evolution by Ethylene and the Reduction of Ethylene to Ethane. Biochem. J 1987, 247, 547–554. [PubMed: 3322266]

(102). Lowe DJ; Fisher K; Thorneley RN *Klebsiella pneumoniae* Nitrogenase: Mechanism of Acetylene Reduction and Its Inhibition by Carbon Monoxide. Biochem. J 1990, 272, 621–625. [PubMed: 2268290]

(103). Leigh GJ; McMahon CN The Organometallic Chemistry of Nitrogenases. J. Organomet. Chem 1995, 500, 219–225.

(104). Chatt J; Richards RL The Reactions of Dinitrogen in Its Metal Complexes. J. Organomet. Chem 1982, 239, 65–77.

(105). Crabtree RH Dihydrogen Binding in Hydrogenase and Nitrogenase. Inorg. Chim. Acta 1986, 125, L7–L8.

(106). Ogo S; Kure B; Nakai H; Watanabe Y; Fukuzumi S Why Do Nitrogenases Waste Electrons by Evolving Dihydrogen? Appl. Organomet. Chem 2004, 18, 589–594.

(107). MacKay BA; Fryzuk MD Dinitrogen Coordination Chemistry: On the Biomimetic Borderlands. Chem. Rev 2004, 104, 385–402. [PubMed: 14871129]

(108). Ballmann J; Munhá RF; Fryzuk MD The Hydride Route to the Preparation of Dinitrogen Complexes. Chem. Commun 2010, 46, 1013–1025.

(109). Lee H-I; Igarashi RY; Laryukhin M; Doan PE; Dos Santos PC; Dean DR; Seefeldt LC; Hoffman BM An Organometallic Intermediate during Alkyne Reduction by Nitrogenase. J. Am. Chem. Soc 2004, 126, 9563–9569. [PubMed: 15291559]

(110). Seefeldt LC; Dance IG; Dean DR Substrate Interactions with Nitrogenase: Fe versus Mo. Biochemistry 2004, 43, 1401–1409. [PubMed: 14769015]

(111). Igarashi RY; Laryukhin M; Dos Santos PC; Lee H-I; Dean DR; Seefeldt LC; Hoffman BM Trapping H^- Bound to the Nitrogenase FeMo-cofactor Active Site during H_2 Evolution: Characterization by ENDOR Spectroscopy. J. Am. Chem. Soc 2005, 127, 6231–6241. [PubMed: 15853328]

(112). Barney BM; Igarashi RY; Dos Santos PC; Dean DR; Seefeldt LC Substrate Interaction at an Iron-Sulfur Face of the FeMo-cofactor during Nitrogenase Catalysis. J. Biol. Chem 2004, 279, 53621–53624. [PubMed: 15465817]

(113). Lukoyanov D; Barney BM; Dean DR; Seefeldt LC; Hoffman BM Connecting Nitrogenase Intermediates with the Kinetic Scheme for N_2 Reduction by a Relaxation Protocol and Identification of the N_2 Binding State. Proc. Natl. Acad. Sci. U. S. A 2007, 104, 1451–1455. [PubMed: 17251348]

(114). Lukoyanov D; Yang Z-Y; Dean DR; Seefeldt LC; Hoffman BM Is Mo Involved in Hydride Binding by the Four-Electron Reduced (E_4) Intermediate of the Nitrogenase MoFe Protein? J. Am. Chem. Soc 2010, 132, 2526–2527. [PubMed: 20121157]

(115). Lukoyanov D; Khadka N; Yang Z-Y; Dean DR; Seefeldt LC; Hoffman BM Reductive Elimination of H_2 Activates Nitrogenase to Reduce the N≡N Triple Bond: Characterization of the E_4(4H) Janus Intermediate in Wild-Type Enzyme. J. Am. Chem. Soc 2016, 138, 10674–10683. [PubMed: 27529724]

(116). Lukoyanov D; Khadka N; Yang Z-Y; Dean DR; Seefeldt LC; Hoffman BM Reversible Photoinduced Reductive Elimination of H_2 from the Nitrogenase Dihydride State, the E_4(4H) Janus Intermediate. J. Am. Chem. Soc 2016, 138, 1320–1327. [PubMed: 26788586]

(117). Hartwig J Organotransition Metal Chemistry: From Bonding to Catalysis; University Science Books: Sausalito, CA, 2010.

(118). Crabtree RH The Organometallic Chemistry of the Transition Metals, 5th ed.; Wiley: Hoboken, NJ, 2009.

(119). Peruzzini M; Poli R Recent Advances in Hydride Chemistry; Elsevier Science B. V.: Amsterdam, The Netherlands, 2001.

(120). Fisher K; Newton WE; Lowe DJ Electron Paramagnetic Resonance Analysis of Different *Azotobacter vinelandii* Nitrogenase MoFe-Protein Conformations Generated during Enzyme Turnover: Evidence for $S = 3/2$ Spin States from Reduced MoFe-Protein Intermediates. Biochemistry 2001, 40, 3333–3339. [PubMed: 11258953]

(121). Fisher K; Lowe DJ; Tavares P; Pereira AS; Huynh BH; Edmondson D; Newton WE Conformations Generated during Turnover of the *Azotobacter vinelandii* Nitrogenase MoFe Protein and Their Relationship to Physiological Function. J. Inorg. Biochem 2007, 101, 1649–1656. [PubMed: 17845818]

(122). Lukoyanov D; Yang Z-Y; Duval S; Danyal K; Dean DR; Seefeldt LC; Hoffman BM A Confirmation of the Quench-Cryoannealing Relaxation Protocol for Identifying Reduction States of Freeze-Trapped Nitrogenase Intermediates. Inorg. Chem 2014, 53, 3688–3693. [PubMed: 24635454]

(123). Lukoyanov DA; Khadka N; Yang Z-Y; Dean DR; Seefeldt LC; Hoffman BM Hydride Conformers of the Nitrogenase FeMo-cofactor Two-Electron Reduced State E_2(2H), Assigned Using Cryogenic Intra Electron Paramagnetic Resonance Cavity Photolysis. Inorg. Chem 2018, 57, 6847–6852. [PubMed: 29575898]

(124). Lukoyanov D; Yang Z-Y; Khadka N; Dean DR; Seefeldt LC; Hoffman BM Identification of a Key Catalytic Intermediate Demonstrates That Nitrogenase Is Activated by the Reversible Exchange of N_2 for H_2. J. Am. Chem. Soc 2015, 137, 3610–3615. [PubMed: 25741750]

(125). Lukoyanov D; Khadka N; Dean DR; Raugei S; Seefeldt LC; Hoffman BM Photoinduced Reductive Elimination of H_2 from the Nitrogenase Dihydride (Janus) State Involves a FeMo-cofactor-H_2 Intermediate. Inorg. Chem 2017, 56, 2233–2240. [PubMed: 28177622]

(126). Siegbahn PEM Model Calculations Suggest That the Central Carbon in the FeMo-cofactor of Nitrogenase Becomes Protonated in the Process of Nitrogen Fixation. J. Am. Chem. Soc 2016, 138, 10485–10495. [PubMed: 27454704]

(127). Gurbiel RJ; Bolin JT; Ronco AE; Mortenson L; Hoffman BM Single-Crystal EPR and ENDOR Study of Nitrogenase from *Clostridium pasteurianum*. J. Magn. Reson 1991, 91, 227–240.

(128). Yu Y; Sadique AR; Smith JM; Dugan TR; Cowley RE; Brennessel WW; Flaschenriem CJ; Bill E; Cundari TR; Holland PL The Reactivity Patterns of Low-Coordinate Iron-Hydride Complexes. J. Am. Chem. Soc 2008, 130, 6624–6638. [PubMed: 18444648]

(129). Smith JM; Sadique AR; Cundari TR; Rodgers KR; Lukat-Rodgers G; Lachicotte RJ; Flaschenriem CJ; Vela J; Holland PL Studies of Low-Coordinate Iron Dinitrogen Complexes. J. Am. Chem. Soc 2006, 128, 756–769. [PubMed: 16417365]

(130). Dugan TR; Holland PL New Routes to Low-Coordinate Iron Hydride Complexes: The Binuclear Oxidative Addition of H_2. J. Organomet. Chem 2009, 694, 2825–2830.

(131). Colombo M; George MW; Moore JN; Pattison DI; Perutz RN; Virrels IG; Ye T-Q Ultrafast Reductive Elimination of Hydrogen from a Metal Carbonyl Dihydride Complex; a Study by Time-Resolved IR and Visible Spectroscopy. J. Chem. Soc., Dalton Trans 1997, 0, 2857–2860.

(132). Perutz RN Metal Dihydride Complexes: Photochemical Mechanisms for Reductive Elimination. Pure Appl. Chem 1998, 70, 2211–2220.

(133). Perutz RN; Procacci B Photochemistry of Transition Metal Hydrides. Chem. Rev 2016, 116, 8506–8544. [PubMed: 27380829]

(134). Ozin GA; McCaffrey JG The Photoreversible Oxidative-Addition, Reductive-Elimination Reactions Fe + $H_2 \rightleftharpoons FeH_2$ in Low-Temperature Matrixes. J. Phys. Chem 1984, 88, 645–648.

(135). Whittlesey MK; Mawby RJ; Osman R; Perutz RN; Field LD; Wilkinson MP; George MW Transient and Matrix Photochemistry of $Fe(Dmpe)_2H_2$ (Dmpe = $Me_2PCH_2CH_2Me_2$): Dynamics of C-H and H-H Activation. J. Am. Chem. Soc 1993, 115, 8627–8637.

(136). Raugei S; Seefeldt LC; Hoffman BM Critical Computational Analysis Illuminates the Reductive-Elimination Mechanism That Activates Nitrogenase for N_2 Reduction. Proc. Natl. Acad. Sci. U. S. A 2018, 115, E10521–E10530. [PubMed: 30355772]

(137). Cao L; Ryde U Extremely Large Differences in DFT Energies for Nitrogenase Models. Phys. Chem. Chem. Phys 2019, 21, 2480–2488. [PubMed: 30652711]

(138). Siegbahn PEM; Blomberg MRA A Systematic DFT Approach for Studying Mechanisms of Redox Active Enzymes. Front. Chem 2018, 6, 644. [PubMed: 30627530]

(139). Benediktsson B; Bjornsson R QM/MM Study of the Nitrogenase MoFe Protein Resting State: Broken-Symmetry States, Protonation States, and QM Region Convergence in the FeMoco Active Site. Inorg. Chem 2017, 56, 13417–13429. [PubMed: 29053260]

(140). Siegbahn PEM Is There Computational Support for an Unprotonated Carbon in the E_4 State of Nitrogenase? J. Comput. Chem 2018, 39, 743–747. [PubMed: 29265384]

(141). Siegbahn PEM The Mechanism for Nitrogenase Including All Steps. Phys. Chem. Chem. Phys 2019, 21, 15747–15759. [PubMed: 31276128]

(142). McKee MLA New Nitrogenase Mechanism Using a CFe_8S_9 Model: Does H_2 Elimination Activate the Complex to N_2 Addition to the Central Carbon Atom? J. Phys. Chem. A 2016, 120, 754–764. [PubMed: 26821350]

(143). Spatzal T; Perez KA; Einsle O; Howard JB; Rees DC Ligand Binding to the FeMo-cofactor: Structures of CO-Bound and Reactivated Nitrogenase. Science 2014, 345, 1620–1623. [PubMed: 25258081]

(144). Spatzal T; Perez KA; Howard JB; Rees DC Catalysis-Dependent Selenium Incorporation and Migration in the Nitrogenase Active Site Iron-Molybdenum Cofactor. eLife 2015, 4, No. e11620. [PubMed: 26673079]

(145). Doan PE; Telser J; Barney BM; Igarashi RY; Dean DR; Seefeldt LC; Hoffman BM ^{57}Fe ENDOR Spectroscopy and 'Electron Inventory' Analysis of the Nitrogenase E_4 Intermediate Suggest the Metal-Ion Core of FeMo-cofactor Cycles through Only One Redox Couple. J. Am. Chem. Soc 2011, 133, 17329–17340. [PubMed: 21980917]

(146). Cao L; Ryde U What Is the Structure of the E_4 Intermediate in Nitrogenase? J. Chem. Theory Comput 2020, DOI: 10.1021/acs.jctc.9b01254.

(147). Thorhallsson A. Th.; Benediktsson B; Bjornsson R A Model for Dinitrogen Binding in the E_4 State of Nitrogenase. Chem. Sci 2019, 10, 11110–11124. [PubMed: 32206260]

(148). Cao L; Caldararu O; Ryde U Protonation States of Homocitrate and Nearby Residues in Nitrogenase Studied by Computational Methods and Quantum Refinement. J. Phys. Chem. B 2017, 121, 8242–8262. [PubMed: 28783353]

(149). Cao L; Caldararu O; Ryde U Protonation and Reduction of the FeMo Cluster in Nitrogenase Studied by Quantum Mechanics/Molecular Mechanics (QM/MM) Calculations. J. Chem. Theory Comput 2018, 14, 6653–6678. [PubMed: 30354152]

(150). Hoeke V; Tociu L; Case DA; Seefeldt LC; Raugei S; Hoffman BM High-Resolution ENDOR Spectroscopy Combined with Quantum Chemical Calculations Reveals the Structure of Nitrogenase Janus Intermediate E_4(4H). J. Am. Chem. Soc 2019, 141, 11984–11996. [PubMed: 31310109]

(151). Van Stappen C; Davydov R; Yang Z-Y; Fan R; Guo Y; Bill E; Seefeldt LC; Hoffman BM; DeBeer S Spectroscopic Description of the E_1 State of Mo Nitrogenase Based on Mo and Fe X-Ray Absorption and Mössbauer Studies. Inorg. Chem 2019, 58, 12365–12376. [PubMed: 31441651]

(152). Van Stappen C; Thorhallsson AT; Decamps L; Bjornsson R; DeBeer S Resolving the Structure of the E_1 State of Mo Nitrogenase through Mo and Fe K-Edge EXAFS and QM/MM Calculations. Chem. Sci 2019, 10, 9807–9821. [PubMed: 32055350]

(153). Harris DF; Yang Z-Y; Dean DR; Seefeldt LC; Hoffman BM Kinetic Understanding of N_2 Reduction versus H_2 Evolution at the E_4(4H) Janus State in the Three Nitrogenases. Biochemistry 2018, 57, 5706–5714. [PubMed: 30183278]

(154). Harris DF; Lukoyanov DA; Kallas H; Trncik C; Yang Z-Y; Compton P; Kelleher N; Einsle O; Dean DR; Hoffman BM; et al. Mo-, V-, and Fe-Nitrogenases Use a Universal Eight-Electron Reductive-Elimination Mechanism To Achieve N_2 Reduction. Biochemistry 2019, 58, 3293–3301. [PubMed: 31283201]

(155). Benediktsson B; Thorhallsson A. Th.; Bjornsson R QM/MM Calculations Reveal a Bridging Hydroxo Group in a Vanadium Nitrogenase Crystal Structure. Chem. Commun 2018, 54, 7310–7313.

(156). Rohde M; Sippel D; Trncik C; Andrade SLA; Einsle O The Critical E_4 State of Nitrogenase Catalysis. Biochemistry 2018, 57, 5497–5504. [PubMed: 29965738]

(157). Peters JW; Stowell MHB; Soltis SM; Finnegan MG; Johnson MK; Rees DC Redox-Dependent Structural Changes in the Nitrogenase P-Cluster. Biochemistry 1997, 36, 1181–1187. [PubMed: 9063865]

(158). Peters JW; Szilagyi RK Exploring New Frontiers of Nitrogenase Structure and Mechanism. Curr. Opin. Chem. Biol 2006, 10, 101–108. [PubMed: 16510305]

(159). Keable SM; Zadvornyy OA; Johnson LE; Ginovska B; Rasmussen AJ; Danyal K; Eilers BJ; Prussia GA; LeVan AX; Raugei S; et al. Structural Characterization of the P^{1+} Intermediate State of the P-Cluster of Nitrogenase. J. Biol. Chem 2018, 293, 9629–9635. [PubMed: 29720402]

(160). Seefeldt LC; Peters JW; Beratan DN; Bothner B; Minteer SD; Raugei S; Hoffman BM Control of Electron Transfer in Nitrogenase. Curr. Opin. Chem. Biol 2018, 47, 54–59. [PubMed: 30205289]

(161). Xiao Y; Fisher K; Smith MC; Newton WE; Case DA; George SJ; Wang H; Sturhahn W; Alp EE; Zhao J; et al. How Nitrogenase Shakes – Initial Information about P–Cluster and FeMo-cofactor Normal Modes from Nuclear Resonance Vibrational Spectroscopy (NRVS). J. Am. Chem. Soc 2006, 128, 7608–7612. [PubMed: 16756317]

(162). George SJ; Barney BM; Mitra D; Igarashi RY; Guo Y; Dean DR; Cramer SP; Seefeldt LC EXAFS and NRVS Reveal a Conformational Distortion of the FeMo-cofactor in the MoFe Nitrogenase Propargyl Alcohol Complex. J. Inorg. Biochem 2012, 112, 85–92. [PubMed: 22564272]

(163). Mitra D; George SJ; Guo Y; Kamali S; Keable S; Peters JW; Pelmenschikov V; Case DA; Cramer SP Characterization of [4Fe-4S] Cluster Vibrations and Structure in Nitrogenase Fe Protein at Three Oxidation Levels via Combined NRVS, EXAFS, and DFT Analyses. J. Am. Chem. Soc 2013, 135, 2530–2543. [PubMed: 23282058]

(164). Mao Z; Liou S-H; Khadka N; Jenney FE; Goodin DB; Seefeldt LC; Adams MWW; Cramer SP; Larsen DS Cluster-Dependent Charge-Transfer Dynamics in Iron–Sulfur Proteins. Biochemistry 2018, 57, 978–990. [PubMed: 29303562]

(165). Gee LB; Leontyev I; Stuchebrukhov A; Scott AD; Pelmenschikov V; Cramer SP Docking and Migration of Carbon Monoxide in Nitrogenase: The Case for Gated Pockets from Infrared Spectroscopy and Molecular Dynamics. Biochemistry 2015, 54, 3314–3319. [PubMed: 25919807]

(166). Owens CP; Katz FEH; Carter CH; Luca MA; Tezcan FA Evidence for Functionally Relevant Encounter Complexes in Nitrogenase Catalysis. J. Am. Chem. Soc 2015, 137, 12704–12712. [PubMed: 26360912]

(167). Owens CP; Katz FEH; Carter CH; Oswald VF; Tezcan FA Tyrosine-Coordinated P-Cluster in *G. diazotrophicus* Nitrogenase: Evidence for the Importance of O-Based Ligands in Conformationally Gated Electron Transfer. J. Am. Chem. Soc 2016, 138, 10124–10127. [PubMed: 27487256]

(168). Rutledge HL; Rittle J; Williamson LM; Xu WA; Gagnon DM; Tezcan FA Redox-Dependent Metastability of the Nitrogenase P-Cluster. J. Am. Chem. Soc 2019, 141, 10091–10098. [PubMed: 31146522]

(169). Hinnemann B; Nørskov JK Chemical Activity of the Nitrogenase FeMo Cofactor with a Central Nitrogen Ligand: Density Functional Study. J. Am. Chem. Soc 2004, 126, 3920–3927. [PubMed: 15038746]

(170). Dance I The Mechanistically Significant Coordination Chemistry of Dinitrogen at FeMo-Co, the Catalytic Site of Nitrogenase. J. Am. Chem. Soc 2007, 129, 1076–1088. [PubMed: 17263388]

(171). Pelmenschikov V; Case DA; Noodleman L Ligand-Bound $S = 1/2$ FeMo-cofactor of Nitrogenase: Hyperfine Interaction Analysis and Implication for the Central Ligand X Identity. Inorg. Chem 2008, 47, 6162–6172. [PubMed: 18578487]

(172). Hallmen PP; Kästner J N_2 Binding to the FeMo-cofactor of Nitrogenase. Z. Anorg. Allg. Chem 2015, 641, 118–122.

(173). Varley JB; Wang Y; Chan K; Studt F; Nørskov JK Mechanistic Insights into Nitrogen Fixation by Nitrogenase Enzymes. Phys. Chem. Chem. Phys 2015, 17, 29541–29547. [PubMed: 26366854]

(174). Schimpl J; Petrilli HM; Blöchl PE Nitrogen Binding to the FeMo-cofactor of Nitrogenase. J. Am. Chem. Soc 2003, 125, 15772–15778. [PubMed: 14677967]

(175). Kästner J; Blöchl PE Towards an Understanding of the Workings of Nitrogenase from DFT Calculations. ChemPhysChem 2005, 6, 1724–1726. [PubMed: 16013077]

(176). Kästner J; Blöchl PE Model for Acetylene Reduction by Nitrogenase Derived from Density Functional Theory. Inorg. Chem 2005, 44, 4568–4575. [PubMed: 15962963]

(177). Kästner J; Blöchl PE Ammonia Production at the FeMo Cofactor of Nitrogenase: Results from Density Functional Theory. J. Am. Chem. Soc 2007, 129, 2998–3006. [PubMed: 17309262]

(178). Spatzal T The Center of Biological Nitrogen Fixation: FeMo-cofactor. Z. Anorg. Allg. Chem 2015, 641, 10–17.

(179). Dance I Mechanisms of the S/CO/Se Interchange Reactions at FeMo-co, the Active Site Cluster of Nitrogenase. Dalton Trans 2016, 45, 14285–14300. [PubMed: 27534727]

(180). Skubi KL; Holland PL So Close, yet Sulfur Away: Opening the Nitrogenase Cofactor Structure Creates a Binding Site. Biochemistry 2018, 57, 3540–3541. [PubMed: 29927241]

(181). Čorić I; Holland PL Insight into the FeMoco of Nitrogenase from Synthetic Iron Complexes with Sulfur, Carbon, and Hydride Ligands. J. Am. Chem. Soc 2016, 138, 7200–7211. [PubMed: 27171599]

(182). Rittle J; Peters JC An Fe-N_2 Complex That Generates Hydrazine and Ammonia via Fe=NNH_2: Demonstrating a Hybrid Distal-to-Alternating Pathway for N_2 Reduction. J. Am. Chem. Soc 2016, 138, 4243–4248. [PubMed: 26937584]

(183). Schrock RR Catalytic Reduction of Dinitrogen to Ammonia at a Single Molybdenum Center. Acc. Chem. Res 2005, 38, 955–962. [PubMed: 16359167]

(184). Neese F The Yandulov/Schrock Cycle and the Nitrogenase Reaction: Pathways of Nitrogen Fixation Studied by Density Functional Theory. Angew. Chem., Int. Ed 2006, 45, 196–199.

(185). MacLeod KC; Holland PL Recent Developments in the Homogeneous Reduction of Dinitrogen by Molybdenum and Iron. Nat. Chem 2013, 5, 559–565. [PubMed: 23787744]

(186). Dance I The Chemical Mechanism of Nitrogenase: Calculated Details of the Intramolecular Mechanism for Hydrogenation of η^2-N_2 on FeMo-co to NH_3. Dalton Trans 2008, No. 43, 5977–5991.

(187). McKenna CE; Simeonov AM; Eran H; Bravo-Leerabhandh M Reduction of Cyclic and Acyclic Diazene Derivatives by *Azotobacter vinelandii* Nitrogenase: Diazirine and Trans-Dimethyldiazene. Biochemistry 1996, 35, 4502–4514. [PubMed: 8605200]

(188). Barney BM; Lukoyanov D; Yang T-C; Dean DR; Hoffman BM; Seefeldt LC A Methyldiazene (HN=N-CH_3)-Derived Species Bound to the Nitrogenase Active-Site FeMo Cofactor: Implications for Mechanism. Proc. Natl. Acad. Sci. U. S. A 2006, 103, 17113–17118. [PubMed: 17088552]

(189). Barney BM; McClead J; Lukoyanov D; Laryukhin M; Yang T-C; Dean DR; Hoffman BM; Seefeldt LC Diazene (HN=NH) Is a Substrate for Nitrogenase: Insights into the Pathway of N_2 Reduction. Biochemistry 2007, 46, 6784–6794. [PubMed: 17508723]

(190). Lukoyanov D; Yang Z-Y; Barney BM; Dean DR; Seefeldt LC; Hoffman BM Unification of Reaction Pathway and Kinetic Scheme for N_2 Reduction Catalyzed by Nitrogenase. Proc. Natl. Acad. Sci. U. S. A 2012, 109, 5583–5587. [PubMed: 22460797]

(191). Davis LC Hydrazine as a Substrate and Inhibitor of *Azotobacter vinelandii* Nitrogenase. Arch. Biochem. Biophys 1980, 204, 270–276. [PubMed: 6932825]

(192). Barney BM; Laryukhin M; Igarashi RY; Lee H-I; Dos Santos PC; Yang T-C; Hoffman BM; Dean DR; Seefeldt LC Trapping a Hydrazine Reduction Intermediate on the Nitrogenase Active Site. Biochemistry 2005, 44, 8030–8037. [PubMed: 15924422]

(193). Shaw S; Lukoyanov D; Danyal K; Dean DR; Hoffman BM; Seefeldt LC Nitrite and Hydroxylamine as Nitrogenase Substrates: Mechanistic Implications for the Pathway of N_2 Reduction. J. Am. Chem. Soc 2014, 136, 12776–12783. [PubMed: 25136926]

(194). Barney BM; Yang T-C; Igarashi RY; Dos Santos PC; Laryukhin M; Lee H-I; Hoffman BM; Dean DR; Seefeldt LC Intermediates Trapped during Nitrogenase Reduction of N≡N, CH_3-N=NH, and H_2N-NH_2. J. Am. Chem. Soc 2005, 127, 14960–14961. [PubMed: 16248599]

(195). Dilworth MJ; Eady RR Hydrazine Is a Product of Dinitrogen Reduction by the Vanadium-Nitrogenase from *Azotobacter chroococcum*. Biochem. J 1991, 277, 465–468. [PubMed: 1859374]

(196). Maia LB; Moura JJG How Biology Handles Nitrite. Chem. Rev 2014, 114, 5273–5357. [PubMed: 24694090]

(197). Riplinger C; Neese F The Reaction Mechanism of Cytochrome P450 NO Reductase: A Detailed Quantum Mechanics/Molecular Mechanics Study. ChemPhysChem 2011, 12, 3192–3203. [PubMed: 22095732]

(198). Einsle O; Messerschmidt A; Huber R; Kroneck PMH; Neese F Mechanism of the Six-Electron Reduction of Nitrite to Ammonia by Cytochrome *c* Nitrite Reductase. J. Am. Chem. Soc 2002, 124, 11737–11745. [PubMed: 12296741]

(199). Bykov D; Neese F Substrate Binding and Activation in the Active Site of Cytochrome *c* Nitrite Reductase: A Density Functional Study. JBIC, J. Biol. Inorg. Chem 2011, 16, 417–430. [PubMed: 21125303]

(200). Bykov D; Neese F Reductive Activation of the Heme Iron–Nitrosyl Intermediate in the Reaction Mechanism of Cytochrome *c* Nitrite Reductase: A Theoretical Study. JBIC, J. Biol. Inorg. Chem 2012, 17, 741–760. [PubMed: 22454108]

(201). Bykov D; Plog M; Neese F Heme-Bound Nitroxyl, Hydroxylamine, and Ammonia Ligands as Intermediates in the Reaction Cycle of Cytochrome *c* Nitrite Reductase: A Theoretical Study. JBIC, J. Biol. Inorg. Chem 2014, 19, 97–112. [PubMed: 24271207]

(202). Lee H-I; Sørlie M; Christiansen J; Yang T-C; Shao J; Dean DR; Hales BJ; Hoffman BM Electron Inventory, Kinetic Assignment (E_n), Structure, and Bonding of Nitrogenase Turnover Intermediates with C_2H_2 and CO. J. Am. Chem. Soc 2005, 127, 15880–15890. [PubMed: 16277531]

(203). Newton WE; Dilworth MJ Assays of Nitrogenase Reaction Products In Nitrogen Fixation: Methods and Protocols; Ribbe MW, Ed.; Methods in Molecular Biology; Humana Press: Totowa, NJ, 2011; pp 105–127.

(204). Dilworth MJ Acetylene Reduction by Nitrogen-Fixing Preparations from *Clostridium pasteurianum*. Biochim. Biophys. Acta, Gen. Subj 1966, 127, 285–294.

(205). Lowe DJ; Eady RR; Thorneley NF Electron-Paramagnetic-Resonance Studies on Nitrogenase of *Klebsiella pneumoniae*: Evidence for Acetylene- and Ethylene-Nitrogenase Transient Complexes. Biochem. J 1978, 173, 277–290. [PubMed: 210766]

(206). Sørlie M; Christiansen J; Dean DR; Hales BJ Detection of a New Radical and FeMo-cofactor EPR Signal during Acetylene Reduction by the α-H195Q Mutant of Nitrogenase. J. Am. Chem. Soc 1999, 121, 9457–9458.

(207). Lee HI; Sørlie M; Christiansen J; Song RT; Dean DR; Hales BJ; Hoffman BM Characterization of an Intermediate in the Reduction of Acetylene by the Nitrogenase α-Gln^{195} MoFe Protein by Q-Band EPR and ^{13}C,^{1}H ENDOR. J. Am. Chem. Soc 2000, 122, 5582–5587.

(208). Benton PMC; Mayer SM; Shao J; Hoffman BM; Dean DR; Seefeldt LC Interaction of Acetylene and Cyanide with the Resting State of Nitrogenase α−96-Substituted MoFe Proteins. Biochemistry 2001, 40, 13816–13825. [PubMed: 11705370]

(209). Burgess BK The Iron-Molybdenum Cofactor of Nitrogenase. Chem. Rev 1990, 90, 1377–1406.

(210). Hardy RWF; Jackson EK Reduction of Model Substrates—Nitriles and Acetylenes—by Nitrogenase (N_2Ase). Fed. Proc 1967, 28, 725.

(211). Schöllhorn R; Burris RH Acetylene as a Competitive Inhibitor of N_2 Fixation. Proc. Natl. Acad. Sci. U. S. A 1967, 58, 213–216. [PubMed: 5231601]

(212). Hardy RW; Knight EJ ATP-Dependent Reduction of Azide and HCN by N_2-Fixing Enzymes of *Azotobacter vinelandii* and *Clostridium pasteurianum*. Biochim. Biophys. Acta 1967, 139, 69–90. [PubMed: 4291834]

(213). Li J; Burgess BK; Corbin JL Nitrogenase Reactivity: Cyanide as Substrate and Inhibitor. Biochemistry 1982, 21, 4393–4402. [PubMed: 6982070]

(214). Lowe DJ; Fisher K; Thorneley RNF; Vaughn SA; Burgess BK Kinetics and Mechanism of the Reaction of Cyanide with Molybdenum Nitrogenase from *Azotobacter vinelandii*. Biochemistry 1989, 28, 8460–8466. [PubMed: 2605195]

(215). Keable SM; Vertemara J; Zadvornyy OA; Eilers BJ; Danyal K; Rasmussen AJ; De Gioia L; Zampella G; Seefeldt LC; Peters JW Structural Characterization of the Nitrogenase Molybdenum-Iron Protein with the Substrate Acetylene Trapped near the Active Site. J. Inorg. Biochem 2018, 180, 129–134. [PubMed: 29275221]

(216). McLean PA; True A; Nelson MJ; Lee HI; Hoffman BM; Orme-Johnson WH Effects of Substrates (Methyl Isocyanide, C_2H_2) and Inhibitor (CO) on Resting-State Wild-Type and $NifV^-$ *Klebsiella pneumoniae* MoFe Proteins. J. Inorg. Biochem 2003, 93, 18–32. [PubMed: 12538049]

(217). Benton PMC; Laryukhin M; Mayer SM; Hoffman BM; Dean DR; Seefeldt LC Localization of a Substrate Binding Site on the FeMo-cofactor in Nitrogenase: Trapping Propargyl Alcohol with an α−70-Substituted MoFe Protein. Biochemistry 2003, 42, 9102–9109. [PubMed: 12885243]

(218). Igarashi RY; Dos Santos PC; Niehaus WG; Dance IG; Dean DR; Seefeldt LC Localization of a Catalytic Intermediate Bound to the FeMo-cofactor of Nitrogenase. J. Biol. Chem 2004, 279, 34770–34775. [PubMed: 15181010]

(219). Mayer SM; Niehaus WG; Dean DR Reduction of Short Chain Alkynes by a Nitrogenase α −70^{Ala}-Substituted MoFe Protein. J. Chem. Soc., Dalton Trans 2002, No. 5, 802–807.

(220). Dos Santos PC; Mayer SM; Barney BM; Seefeldt LC; Dean DR Alkyne Substrate Interaction within the Nitrogenase MoFe Protein. J. Inorg. Biochem 2007, 101, 1642–1648. [PubMed: 17610955]

(221). Lockshin A; Burris RH Inhibitors of Nitrogen Fixation in Extracts from *Clostridium pasteurianum*. Biochim. Biophys. Acta, Gen. Subj 1965, 111, 1–10.

(222). Maskos Z; Fisher K; Sørlie M; Newton WE; Hales BJ Variant MoFe Proteins of *Azotobacter vinelandii*: Effects of Carbon Monoxide on Electron Paramagnetic Resonance Spectra Generated during Enzyme Turnover. JBIC, J. Biol. Inorg. Chem 2005, 10, 394–406. [PubMed: 15887041]

(223). Liang J; Madden M; Shah VK; Burris RH Citrate Substitutes for Homocitrate in Nitrogenase of a *nif V* Mutant of *Klebsiella pneumoniae*. Biochemistry 1990, 29, 8577–8581. [PubMed: 2271541]

(224). Scott DJ; Dean DR; Newton WE Nitrogenase-catalyzed Ethane Production and CO-sensitive Hydrogen Evolution from MoFe Proteins Having Amino Acid Substitutions in an α-Subunit FeMo Cofactor-Binding Domain. J. Biol. Chem 1992, 267, 20002–20010. [PubMed: 1328190]

(225). Yang Z-Y Substrate Binding and Reduction Mechanism of Molybdenum Nitrogenase; Utah State University: Logan, UT, 2013.

(226). Pham DN; Burgess BK Nitrogenase Reactivity: Effects of pH on Substrate Reduction and Carbon Monoxide Inhibition. Biochemistry 1993, 32, 13725–13731. [PubMed: 8257707]

(227). Lee CC; Hu Y; Ribbe MW Vanadium Nitrogenase Reduces CO. Science 2010, 329, 642. [PubMed: 20689010]

(228). Hu Y; Lee CC; Ribbe MW Extending the Carbon Chain: Hydrocarbon Formation Catalyzed by Vanadium/Molybdenum Nitrogenases. Science 2011, 333, 753–755. [PubMed: 21817053]

(229). Fisher K; Hare ND; Newton WE Another Role for CO with Nitrogenase? CO Stimulates Hydrogen Evolution Catalyzed by Variant *Azotobacter vinelandii* Mo-Nitrogenases. Biochemistry 2014, 53, 6151–6160. [PubMed: 25203280]

(230). Pollock RC; Lee H.-In.; Cameron LM; DeRose VJ; Hales BJ; Orme-Johnson WH; Hoffman BM Investigation of CO Bound to Inhibited Forms of Nitrogenase MoFe Protein by ^{13}C ENDOR. J. Am. Chem. Soc 1995, 117, 8686–8687.

(231). Yates MG Nitrogenase of *Azotobacter chroococcum* : A New Electronparamagnetic-Resonance Signal Associated with a Transient Species of the MoFe Protein during Catalysis. FEBS Lett. 1976, 72, 127. [PubMed: 1001455]

(232). Davis LC; Henzl MT; Burris RH; Orme-Johnson WH Iron-Sulfur Clusters in the Molybdenum-Iron Protein Component of Nitrogenase. Electron Paramagnetic Resonance of the Carbon Monoxide Inhibited State. Biochemistry 1979, 18, 4860–4869. [PubMed: 228701]

(233). Cameron LM; Hales BJ Investigation of CO Binding and Release from Mo-Nitrogenase during Catalytic Turnover. Biochemistry 1998, 37, 9449–9456. [PubMed: 9649328]

(234). Sørlie M; Christiansen J; Lemon BJ; Peters JW; Dean DR; Hales BJ Mechanistic Features and Structure of the Nitrogenase α-Gln^{195} MoFe Protein. Biochemistry 2001, 40, 1540–1549. [PubMed: 11327812]

(235). Christie PD; Lee H.-In.; Cameron LM; Hales BJ; Orme-Johnson WH; Hoffman BM Identification of the CO-Binding Cluster in Nitrogenase MoFe Protein by ENDOR of ^{57}Fe Isotopomers. J. Am. Chem. Soc 1996, 118, 8707–8709.

(236). Lee H-I; Cameron LM; Hales BJ; Hoffman BM CO Binding to the FeMo Cofactor of CO-Inhibited Nitrogenase: ^{13}CO and ^{1}H Q-Band ENDOR Investigation. J. Am. Chem. Soc 1997, 119, 10121–10126.

(237). Lee H-I; Hales BJ; Hoffman BM Metal-Ion Valencies of the FeMo Cofactor in CO-Inhibited and Resting State Nitrogenase by ^{57}Fe Q-Band ENDOR. J. Am. Chem. Soc 1997, 119, 11395–11400.

(238). Lee HI; Cameron LM; Sorlie M; Pollock RC; Christie PD; Christiansen J; Ryle MJ; Peters JW; DeRose VJ; Seefeldt LC; et al. Study of Substrate Inhibitor Interactions in Nitrogenase MoFe Protein by Advanced Paramagnetic Resonance. J. Inorg. Biochem 1999, 74, 202–202.

(239). Maskos Z; Hales BJ Photo-Lability of CO Bound to Mo-Nitrogenase from *Azotobacter vinelandii*. J. Inorg. Biochem 2003, 93, 11–17. [PubMed: 12538048]

(240). Yan L; Dapper CH; George SJ; Wang H; Mitra D; Dong W; Newton WE; Cramer SP Photolysis of Hi-CO Nitrogenase – Observation of a Plethora of Distinct CO Species Using Infrared Spectroscopy. Eur. J. Inorg. Chem 2011, 2064–2074. [PubMed: 27630531]

(241). Yan L; Pelmenschikov V; Dapper CH; Scott AD; Newton WE; Cramer SP IR-Monitored Photolysis of CO-Inhibited Nitrogenase: A Major EPR-Silent Species with Coupled Terminal CO Ligands. Chem. - Eur. J 2012, 18, 16349–16357. [PubMed: 23136072]

(242). Scott AD; Pelmenschikov V; Guo Y; Yan L; Wang H; George SJ; Dapper CH; Newton WE; Yoda Y; Tanaka Y; et al. Structural Characterization of CO-Inhibited Mo-Nitrogenase by Combined Application of Nuclear Resonance Vibrational Spectroscopy, Extended X-Ray

Absorption Fine Structure, and Density Functional Theory: New Insights into the Effects of CO Binding and the Role of the Interstitial Atom. J. Am. Chem. Soc 2014, 136, 15942–15954. [PubMed: 25275608]

(243). Lee CC; Fay AW; Weng T-C; Krest CM; Hedman B; Hodgson KO; Hu Y; Ribbe MW Uncoupling Binding of Substrate CO from Turnover by Vanadium Nitrogenase. Proc. Natl. Acad. Sci. U. S. A 2015, 112, 13845–13849. [PubMed: 26515097]

(244). George SJ; Ashby GA; Wharton CW; Thorneley RNF Time-Resolved Binding of Carbon Monoxide to Nitrogenase Monitored by Stopped-Flow Infrared Spectroscopy. J. Am. Chem. Soc 1997, 119, 6450–6451.

(245). Tolland JD; Thorneley RNF Stopped-Flow Fourier Transform Infrared Spectroscopy Allows Continuous Monitoring of Azide Reduction, Carbon Monoxide Inhibition, and ATP Hydrolysis by Nitrogenase. Biochemistry 2005, 44, 9520–9527. [PubMed: 15996106]

(246). Yang Z-Y; Seefeldt LC; Dean DR; Cramer SP; George SJ Steric Control of the Hi-CO MoFe Nitrogenase Complex Revealed by Stopped-Flow Infrared Spectroscopy. Angew. Chem., Int. Ed 2011, 50, 272–275.

(247). Yang Z-Y; Dean DR; Seefeldt LC Molybdenum Nitrogenase Catalyzes the Reduction and Coupling of CO to Form Hydrocarbons. J. Biol. Chem 2011, 286, 19417–19421. [PubMed: 21454640]

(248). Lee CC; Tanifuji K; Newcomb M; Liedtke J; Hu Y; Ribbe MW A Comparative Analysis of the CO-Reducing Activities of MoFe Proteins Containing Mo- and V-Nitrogenase Cofactors. ChemBioChem 2018, 19, 649–653. [PubMed: 29363247]

(249). Rebelein JG; Lee CC; Newcomb M; Hu Y; Ribbe MW Characterization of an M-Cluster-Substituted Nitrogenase VFe Protein. mBio 2018, 9, E00310–18. [PubMed: 29535200]

(250). Paengnakorn P; Ash PA; Shaw S; Danyal K; Chen T; Dean DR; Seefeldt LC; Vincent KA Infrared Spectroscopy of the Nitrogenase MoFe Protein under Electrochemical Control: Potential-Triggered CO Binding. Chem. Sci 2017, 8, 1500–1505. [PubMed: 28616146]

(251). Wiig JA; Lee CC; Hu Y; Ribbe MW Tracing the Interstitial Carbide of the Nitrogenase Cofactor during Substrate Turnover. J. Am. Chem. Soc 2013, 135, 4982–4983. [PubMed: 23514429]

(252). Seefeldt LC; Rasche ME; Ensign SA Carbonyl Sulfide and Carbon Dioxide as New Substrates, and Carbon Disulfide as a New Inhibitor, of Nitrogenase. Biochemistry 1995, 34, 5382–5389. [PubMed: 7727396]

(253). Khadka N; Dean DR; Smith D; Hoffman BM; Raugei S; Seefeldt LC CO_2 Reduction Catalyzed by Nitrogenase: Pathways to Formate, Carbon Monoxide, and Methane. Inorg. Chem 2016, 55, 8321–8330. [PubMed: 27500789]

(254). Yang Z-Y; Moure VR; Dean DR; Seefeldt LC Carbon Dioxide Reduction to Methane and Coupling with Acetylene to Form Propylene Catalyzed by Remodeled Nitrogenase. Proc. Natl. Acad. Sci. U. S. A 2012, 109, 19644–19648. [PubMed: 23150564]

(255). Fixen KR; Zheng Y; Harris DF; Shaw S; Yang Z-Y; Dean DR; Seefeldt LC; Harwood CS Light-Driven Carbon Dioxide Reduction to Methane by Nitrogenase in a Photosynthetic Bacterium. Proc. Natl. Acad. Sci. U. S. A 2016, 113, 10163–10167. [PubMed: 27551090]

(256). Rey FE; Heiniger EK; Harwood CS Redirection of Metabolism for Biological Hydrogen Production. Appl. Environ. Microbiol 2007, 73, 1665–1671. [PubMed: 17220249]

(257). McKinlay JB; Harwood CS Carbon Dioxide Fixation as a Central Redox Cofactor Recycling Mechanism in Bacteria. Proc. Natl. Acad. Sci. U. S. A 2010, 107, 11669–11675. [PubMed: 20558750]

(258). Heiniger EK; Oda Y; Samanta SK; Harwood CS How Posttranslational Modification of Nitrogenase Is Circumvented in *Rhodopseudomonas palustris* Strains That Produce Hydrogen Gas Constitutively. Appl. Environ. Microbiol 2012, 78, 1023–1032. [PubMed: 22179236]

(259). Demtröder L; Pfänder Y; Schäkermann S; Bandow JE; Masepohl B NifA Is the Master Regulator of Both Nitrogenase Systems in *Rhodobacter capsulatus*. MicrobiologyOpen 2019, 8, No. e921. [PubMed: 31441241]

(260). Zheng Y; Harris DF; Yu Z; Fu Y; Poudel S; Ledbetter RN; Fixen KR; Yang Z-Y; Boyd ES; Lidstrom ME; et al. A Pathway for Biological Methane Production Using Bacterial Iron-only Nitrogenase. Nat. Microbiol 2018, 3, 281–286. [PubMed: 29335552]

(261). Hu B; Harris DF; Dean DR; Liu TL; Yang Z-Y; Seefeldt LC Electrocatalytic CO_2 Reduction Catalyzed by Nitrogenase MoFe and FeFe Proteins. Bioelectrochemistry 2018, 120, 104–109. [PubMed: 29223886]

(262). Connelly SJ; Wiedner ES; Appel AM Predicting the Reactivity of Hydride Donors in Water: Thermodynamic Constants for Hydrogen. Dalton Trans 2015, 44, 5933–5938. [PubMed: 25697077]

(263). Rebelein JG; Hu Y; Ribbe MW Differential Reduction of CO_2 by Molybdenum and Vanadium Nitrogenases. Angew. Chem., Int. Ed 2014, 53, 11543–11546.

(264). Sickerman NS; Hu Y; Ribbe MW Activation of CO_2 by Vanadium Nitrogenase. Chem. - Asian J 2017, 12, 1985–1996. [PubMed: 28544649]

(265). Rebelein JG; Hu Y; Ribbe MW Widening the Product Profile of Carbon Dioxide Reduction by Vanadium Nitrogenase. ChemBioChem 2015, 16, 1993–1996. [PubMed: 26266490]

(266). Rasche ME; Seefeldt LC Reduction of Thiocyanate, Cyanate, and Carbon Disulfide by Nitrogenase: Kinetic Characterization and EPR Spectroscopic Analysis. Biochemistry 1997, 36, 8574–8585. [PubMed: 9214303]

(267). Ryle MJ; Lee HI; Seefeldt LC; Hoffman BM Nitrogenase Reduction of Carbon Disulfide: Freeze-Quench EPR and ENDOR Evidence for Three Sequential Intermediates with Cluster-Bound Carbon Moieties. Biochemistry 2000, 39, 1114–1119. [PubMed: 10653657]

(268). Henthorn JT; Arias RJ; Koroidov S; Kroll T; Sokaras D; Bergmann U; Rees DC; DeBeer S Localized Electronic Structure of Nitrogenase FeMoco Revealed by Selenium K-Edge High Resolution X-Ray Absorption Spectroscopy. J. Am. Chem. Soc 2019, 141, 13676–13688. [PubMed: 31356071]

(269). Chen PY-T; Wittenborn EC; Drennan CL Waltzing around Cofactors. eLife 2016, 5, No. e13977. [PubMed: 26843316]

(270). Kennedy IR; Morris JA; Mortenson LE N_2 Fixation by Purified Components of the N_2-Fixing System of *Clostridium pasteurianum*. Biochim. Biophys. Acta, Bioenerg 1968, 153, 777–786.

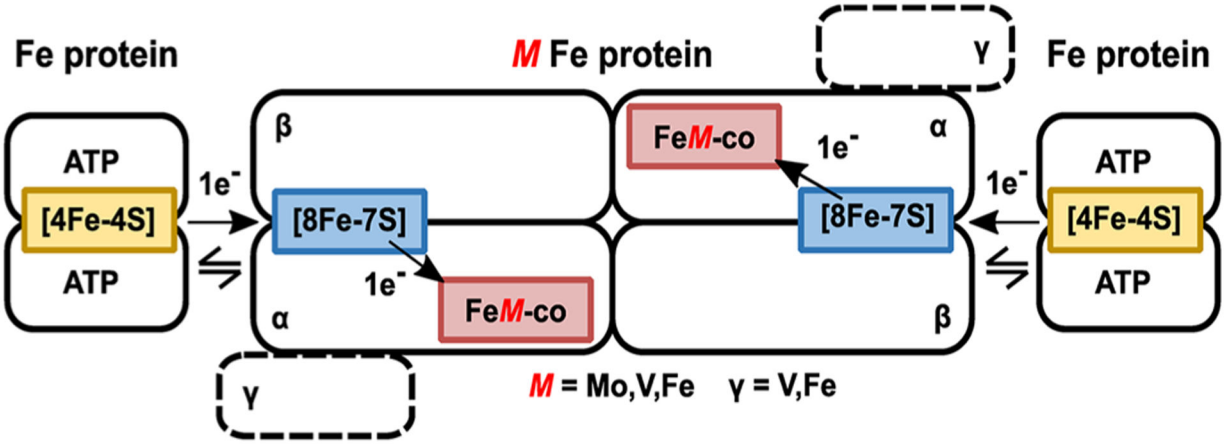

Figure 1.

<j/>General nitrogenase architecture. Schematic of nitrogenase structures showing the electron delivery Fe protein component and the catalytic MFe protein component (M = Mo, V, Fe). MoFe protein is an $\alpha_2\beta_2$, and VFe and FeFe proteins are $\alpha_2\beta_2\gamma_2$ heterohexamers. Adapted with permission from ref 38. Copyright 2018 American Chemical Society.

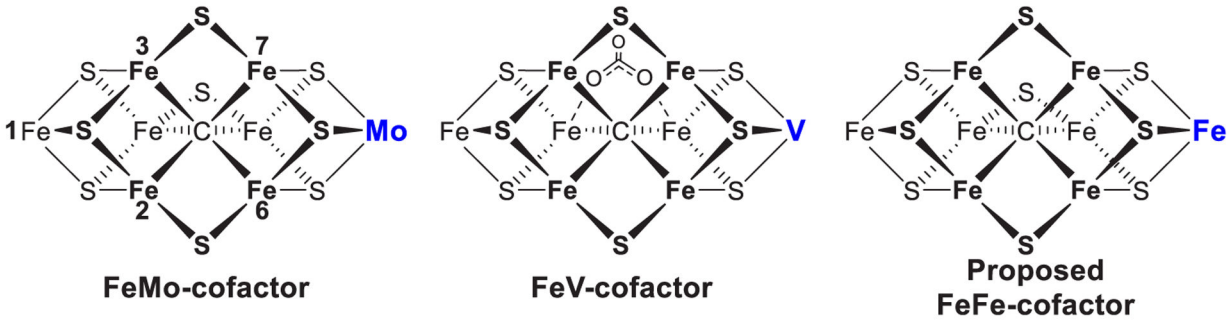

Figure 2.

Structures of the FeMo-cofactor of Mo-nitrogenase,[56,57,69,79] FeV-cofactor of V-nitrogenase,[58,72] and proposed structure of the FeFe-cofactor of Fe-nitrogenase.[80] View is looking down on the Fe2, 3, 6, 7 face as indicated by the Fe atom numbering on FeMo-cofactor. Not shown are the cysteine coordinating Fe1, and the histidine and the *R*-homocitrate tail that ligate the Mo, V, or Fe are shown in blue.

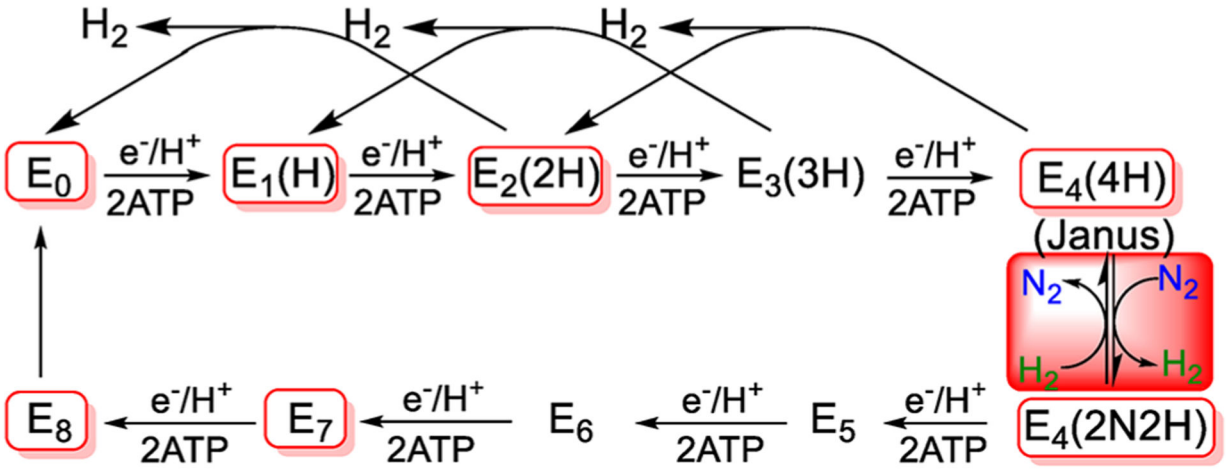

Figure 3.

Simplified 8[e^-/H^+] kinetic scheme for nitrogen reduction. In the Lowe–Thorneley E_n notation, n = number of [e^-/H^+] added to FeMo-co; in parentheses, the stoichiometry of H/N bound to FeMo-co. The *re/oa* equilibrium is highlighted in red, and the intermediates in red boxes have been freeze trapped for spectroscopic study.

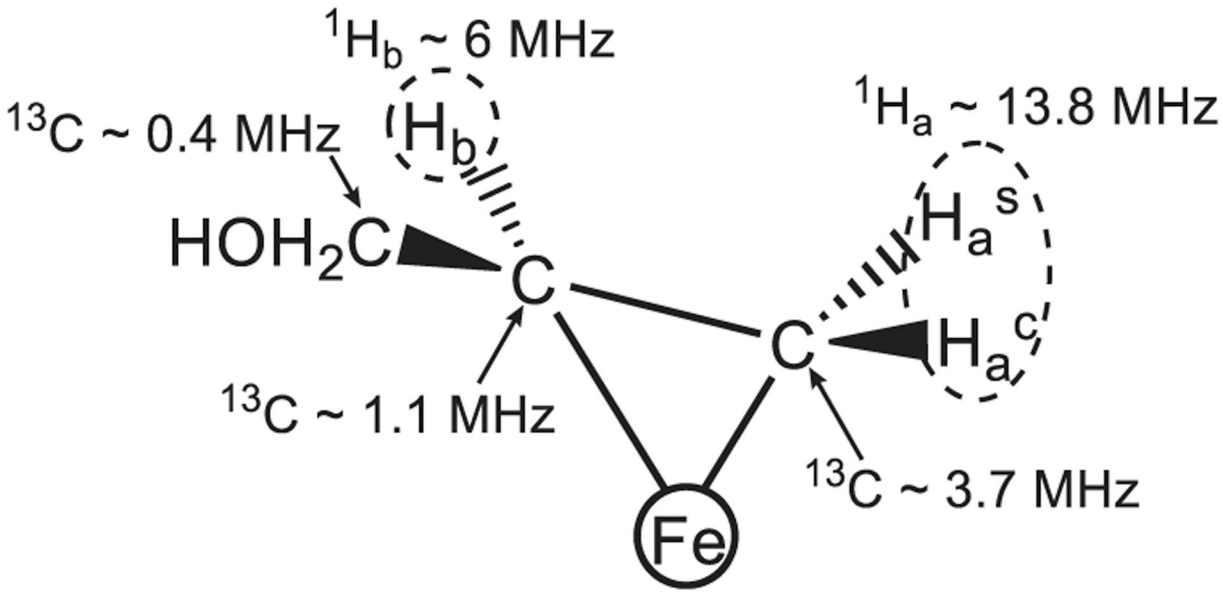

Figure 4.
Propargyl alcohol reduction intermediate with hyperfine couplings indicated. Reproduced with permission from ref 109. Copyright 2004 American Chemical Society.

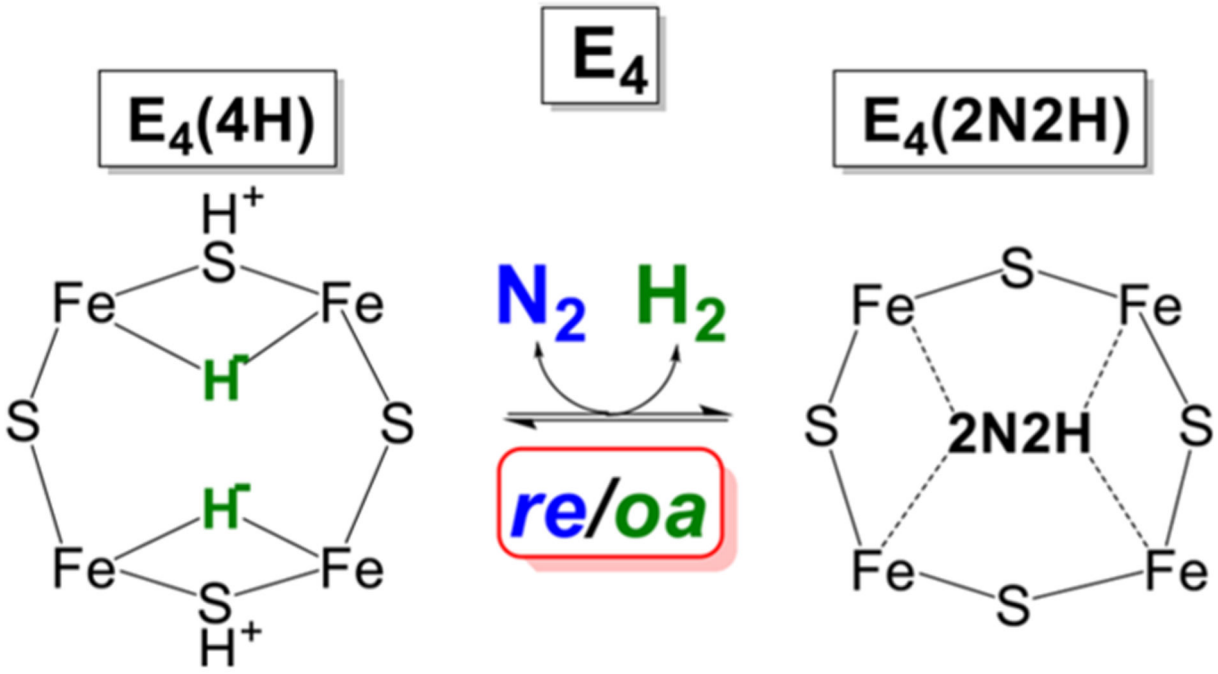

Figure 5.
Schematic of *re/oa* equilibrium. In the indicated equilibrium, the binding and activation of N_2 is mechanistically coupled to the *re* of H_2, as described in the text. Adapted with permission from ref 116. Copyright 2016 American Chemical Society.

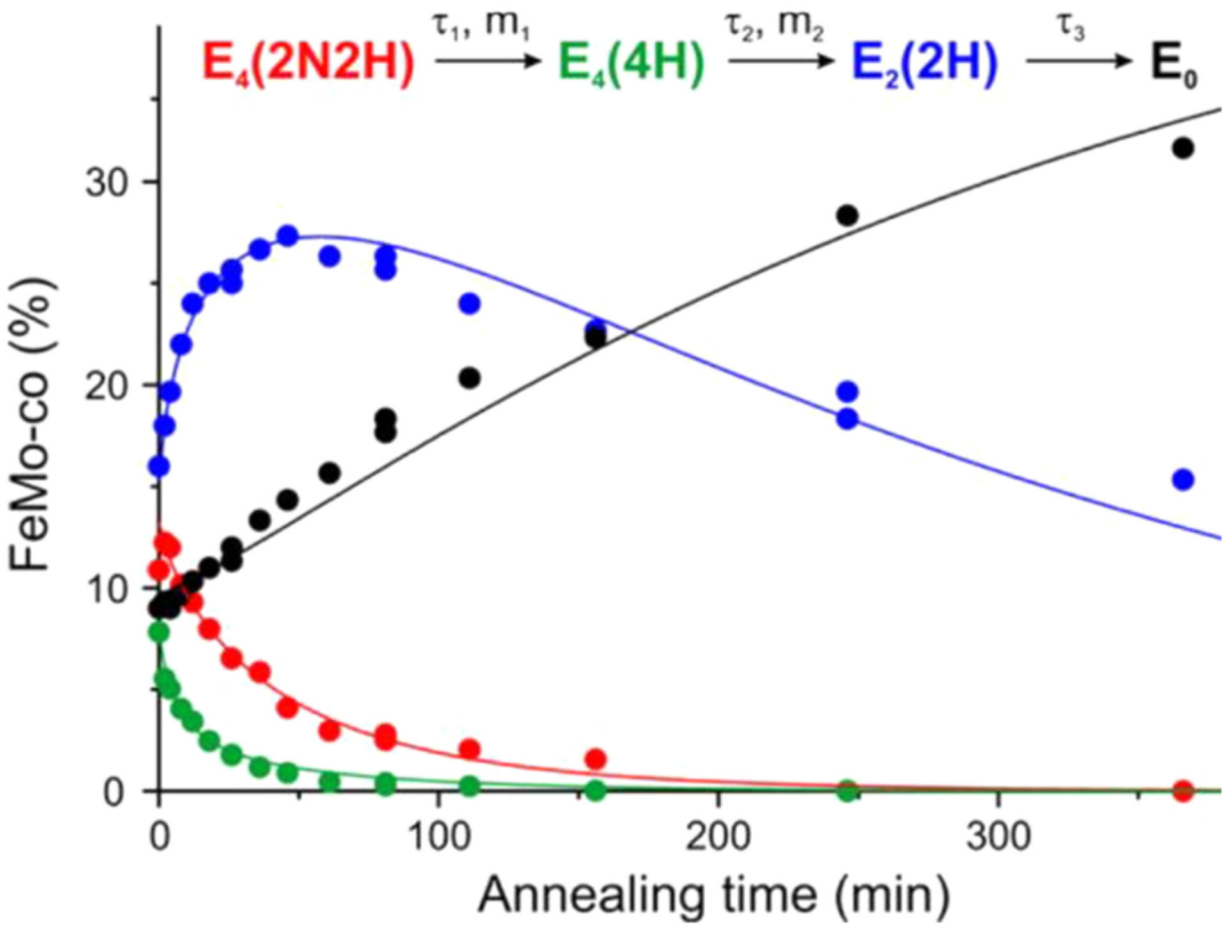

Figure 6.

Time courses of four EPR detected states during −50 °C cryoannealing of WT low $P(N_2)$ ~ 0.05 atm turnover in H_2O. The data colors correspond to those in the kinetic scheme (top) and the lines correspond to fits to that scheme. Stretched exponential $\exp(-(t/\tau)^m)$ parameters of the first two fast steps are τ_1 = 43 min, m_1 = 0.79 and τ_2 = 6 min, m_2 = 0.8, and the third slow step fitted as exponential with τ_3 = 330 min. Reproduced with permission from 115. Copyright 2016 American Chemical Society.

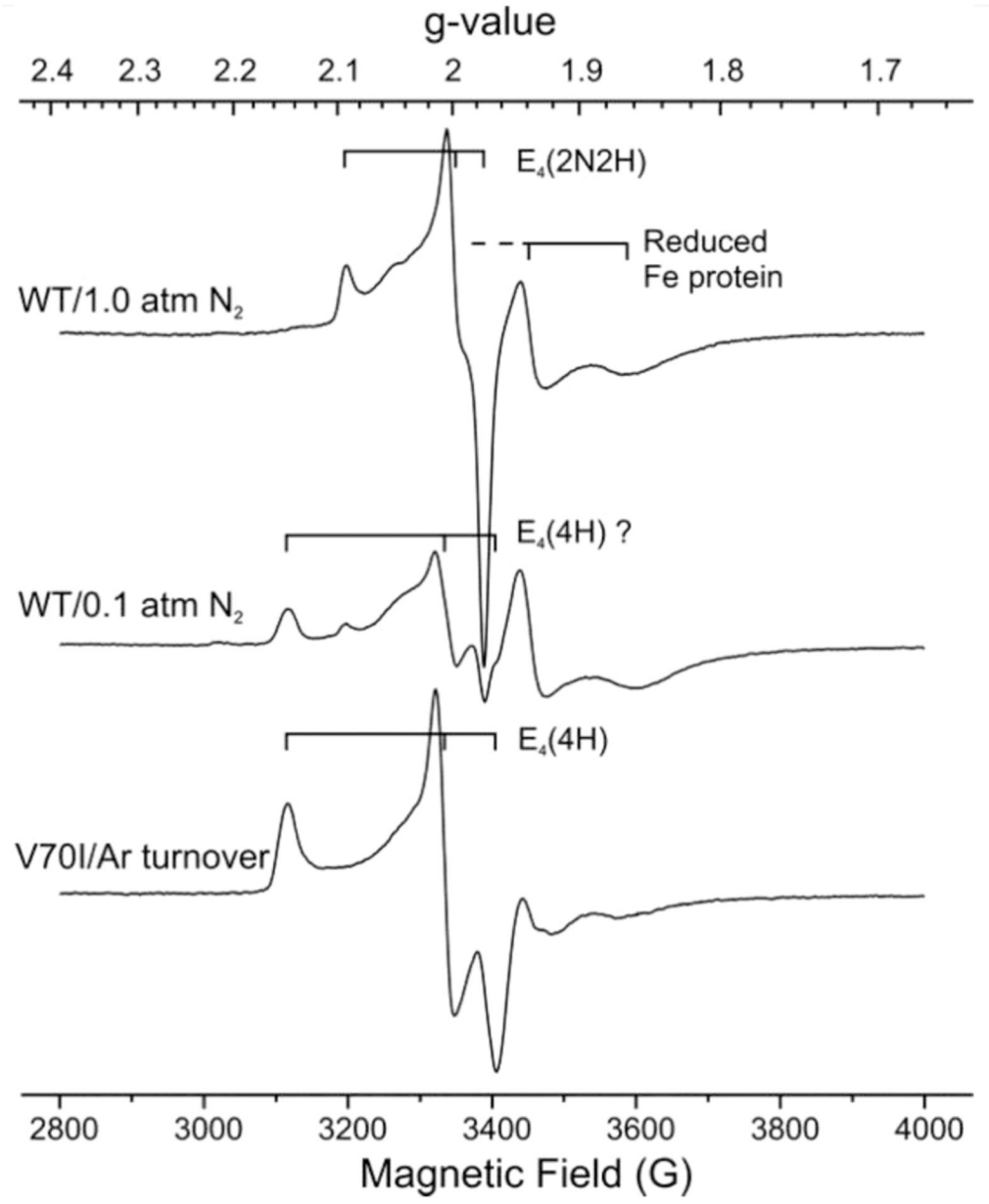

Figure 7.

X-band EPR spectra of WT nitrogenase turnover samples trapped under 1 atm of N_2 (with stirring to facilitate transfer of H_2 formed during turnover into the headspace[124]), and under low $P(N_2)$ in H_2O buffer (without stirring) shown in comparison with spectrum of $E_4(4H)$ state trapped during turnover of α−$70^{Val\rightarrow Ile}$ MoFe protein of the same concentration. Reproduced with permission from ref 115. Copyright 2016 American Chemical Society.

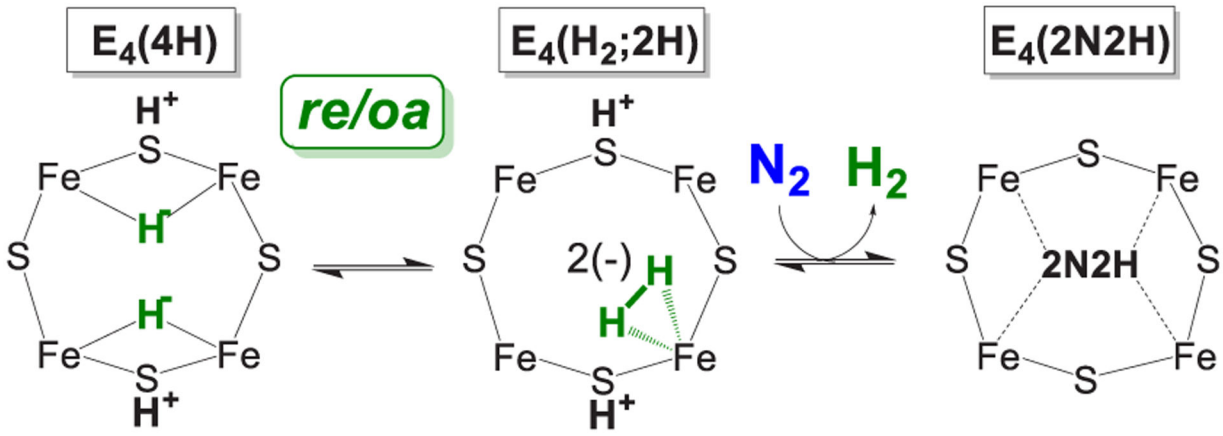

Figure 8.

Cartoon version of suggested catalytic pathway for *re/oa* activation of FeMo-co for N_2 reduction. Reproduced with permission from ref 125. Copyright 2017 American Chemical Society.

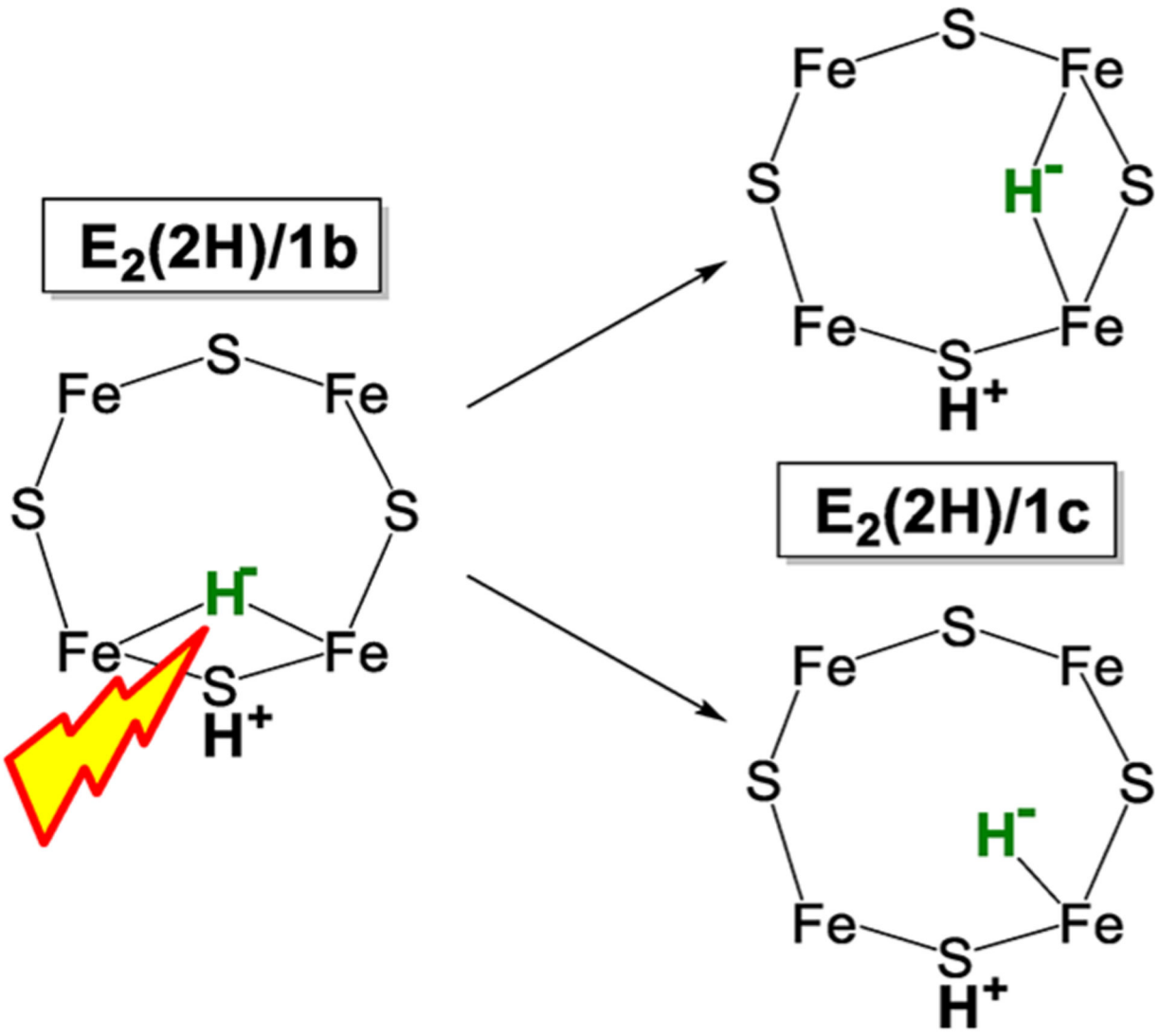

Figure 9.

Schematic representation of photolysis conversion of [Fe-H-Fe] hydride bridge of $E_2(2H)/1b$ into isomer $E_2(2H)/1c$ with either a hydride bridge between a different pair of Fe ions or an Fe-H terminal hydride. Adapted with permission from ref 123. Copyright 2018 American Chemical Society

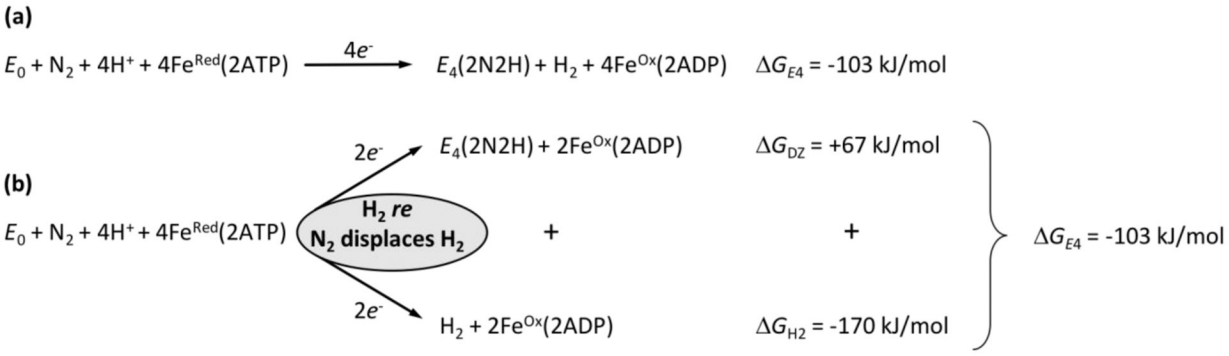

Figure 10.

Energetics of formation of E_4(2N2H) from the enzymatic reactants and its decomposition into two individual two-electron, two-proton processes, each involving the hydrolysis of 2ATP per electron: the formation of E_4(2N2H) and of H_2, which are coupled through displaces and releases H_2 formed by *re* from E_4(4H). Adapted with permission from 136. Copyright 2018 National Academy of Sciences.

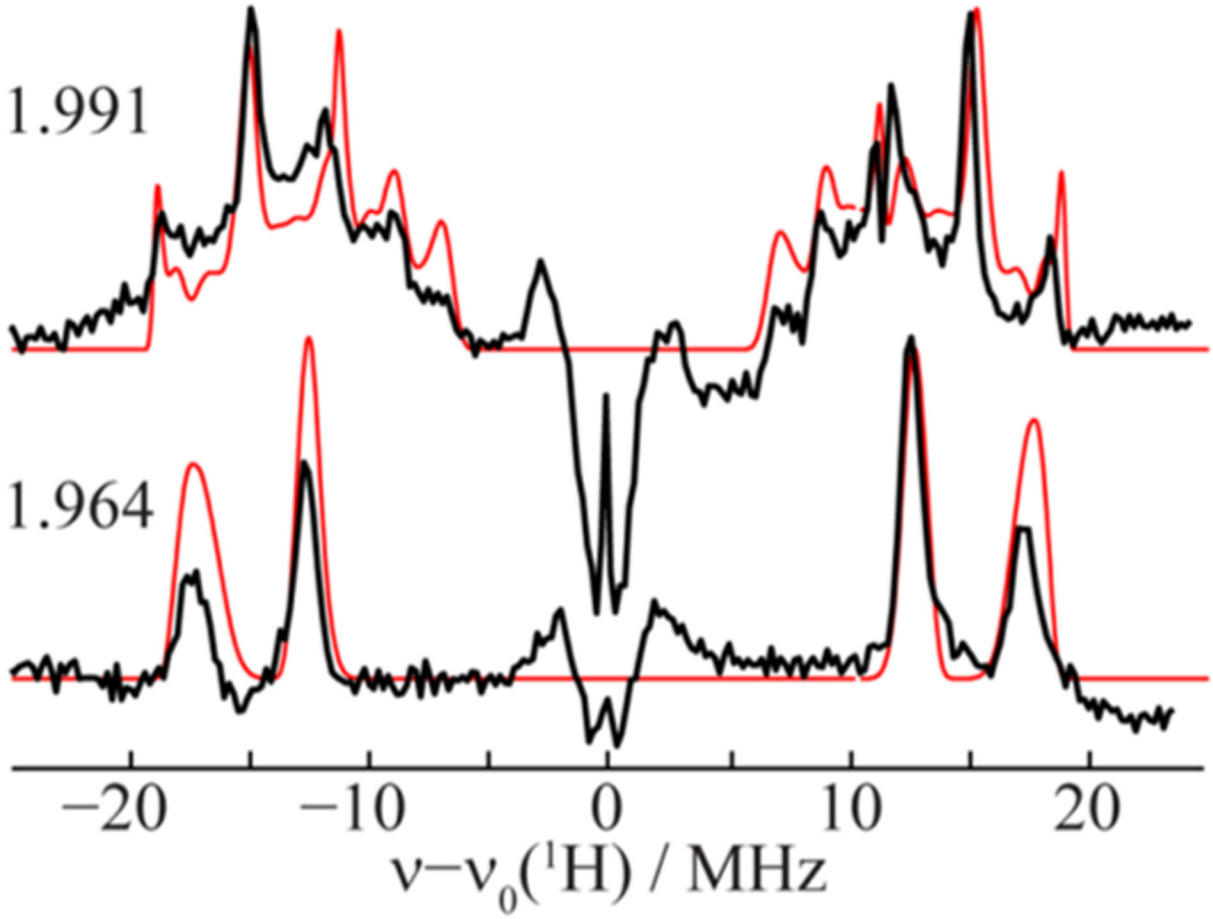

Figure 11.

35 GHz ^{1}H stochastic-field modulation detected (stochastic CW) ENDOR spectra of E_4(4H) in $70^{Val\rightarrow Ile}/\alpha{-}195^{His\rightarrow Gln}$ MoFe protein, acquired at g = 1.991 and 1.964 (black) and summed simulations (red). The signal with $\nu_0(^1H)$ ± ~3 MHz, with both positive and negative features, represents transient responses from weakly coupled, more distant protons. Reproduced with permission ref 150. Copyright 2019 American Chemical Society.

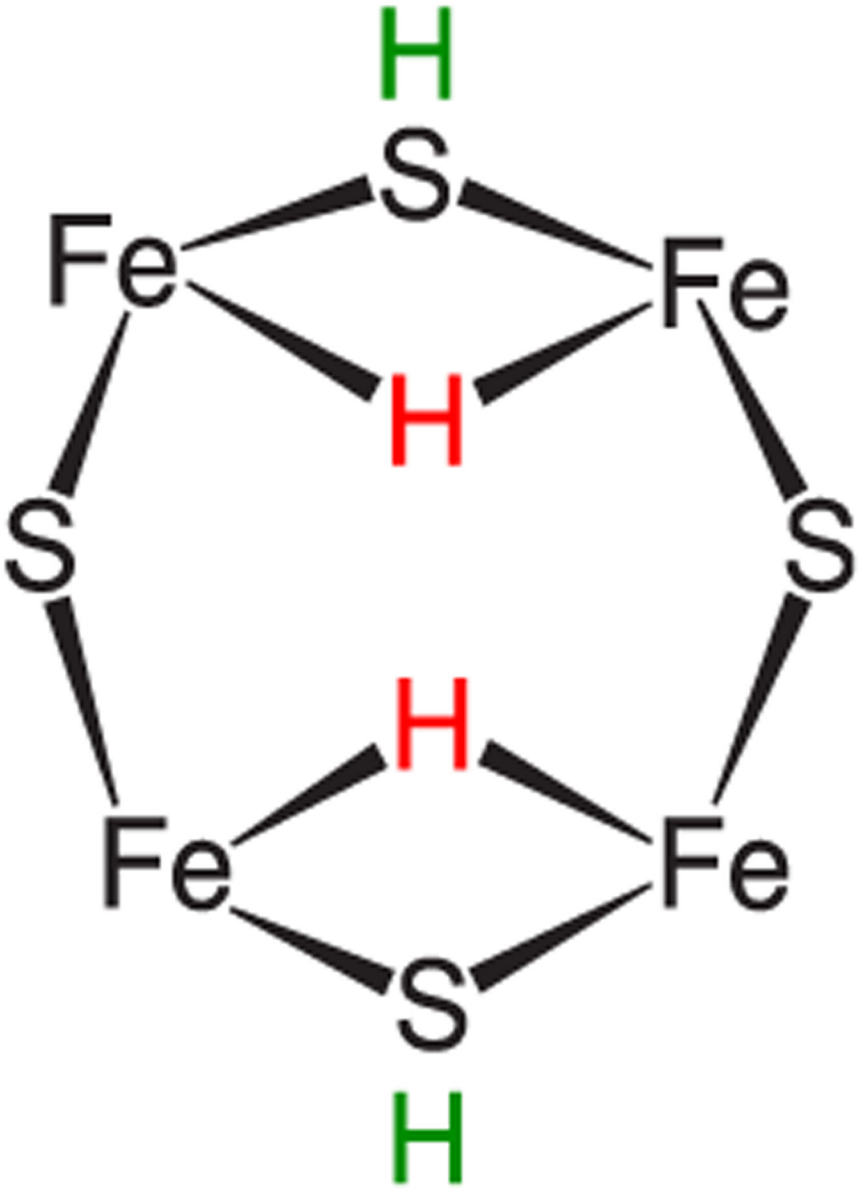

Figure 12.

Cartoon of the 2,3,6,7 face of the ground state isomer of $E_4(4H)$, denoted $E_4(4H)^{[a]}$ as found by BS-DFT computation. Reproduced with permission from ref 150. Copyright 2019 American Chemical Society.

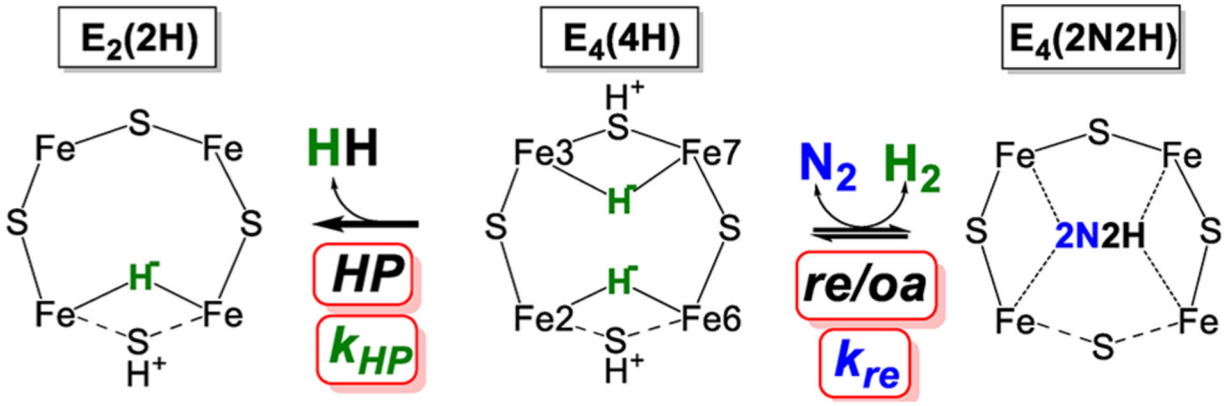

Figure 13.

Reactions of the E_4 state. N_2 binds through *re* with rate constant k_{re} to the right. H_2 evolves through HP with rate constant k_{HP} to the left. Reproduced with permission 153. Copyright 2018 American Chemical Society.

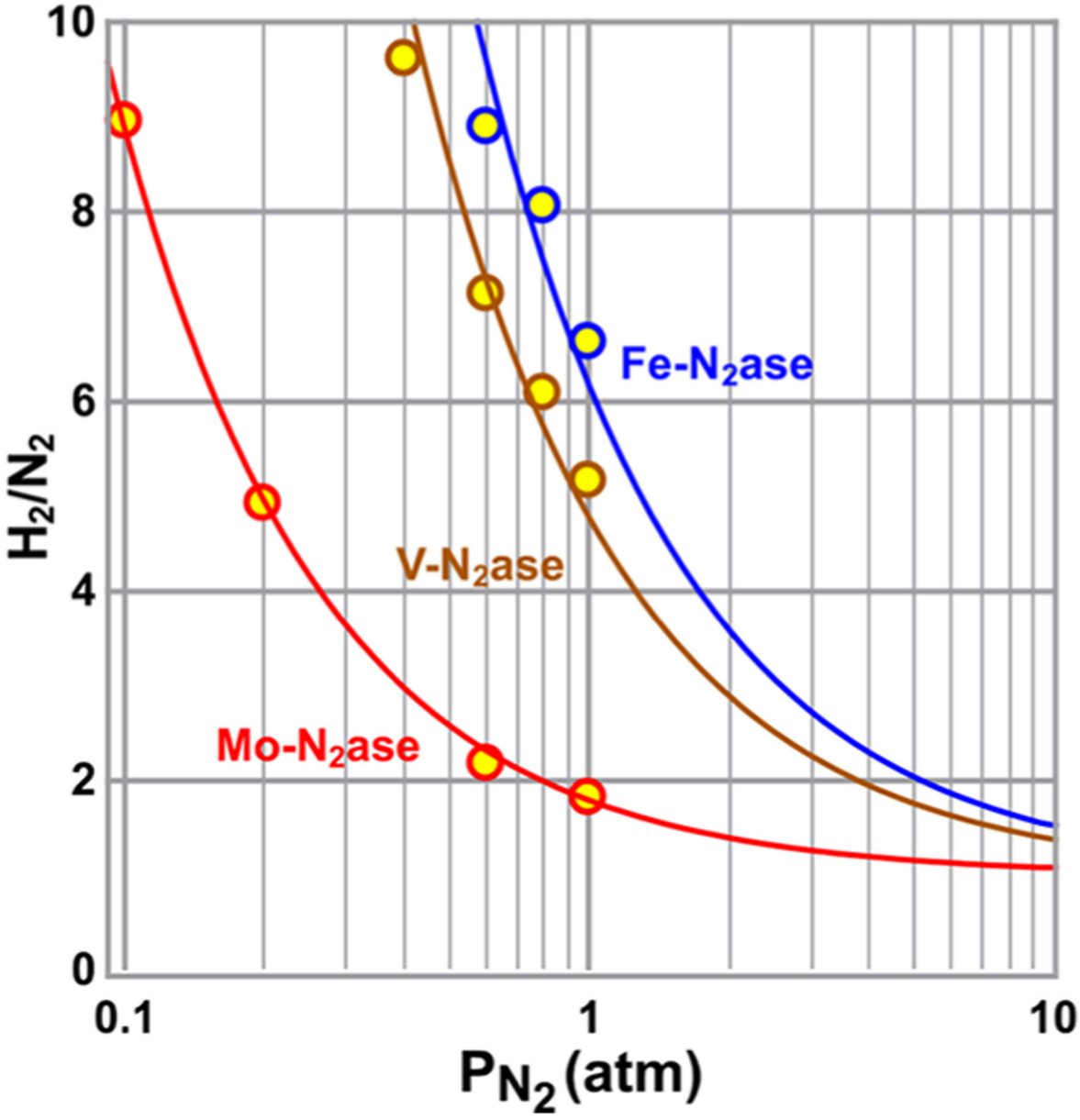

Figure 14.

Ratio of H_2 evolved to N_2 reduced as a function of partial pressure N_2 for all three nitrogenase isozymes. The fits to this data for each enzyme produce the value of its parameter $\rho = k_{re}/k_{HP}$ Reproduced with permission from ref 154. Copyright 2019 American Chemical Society.

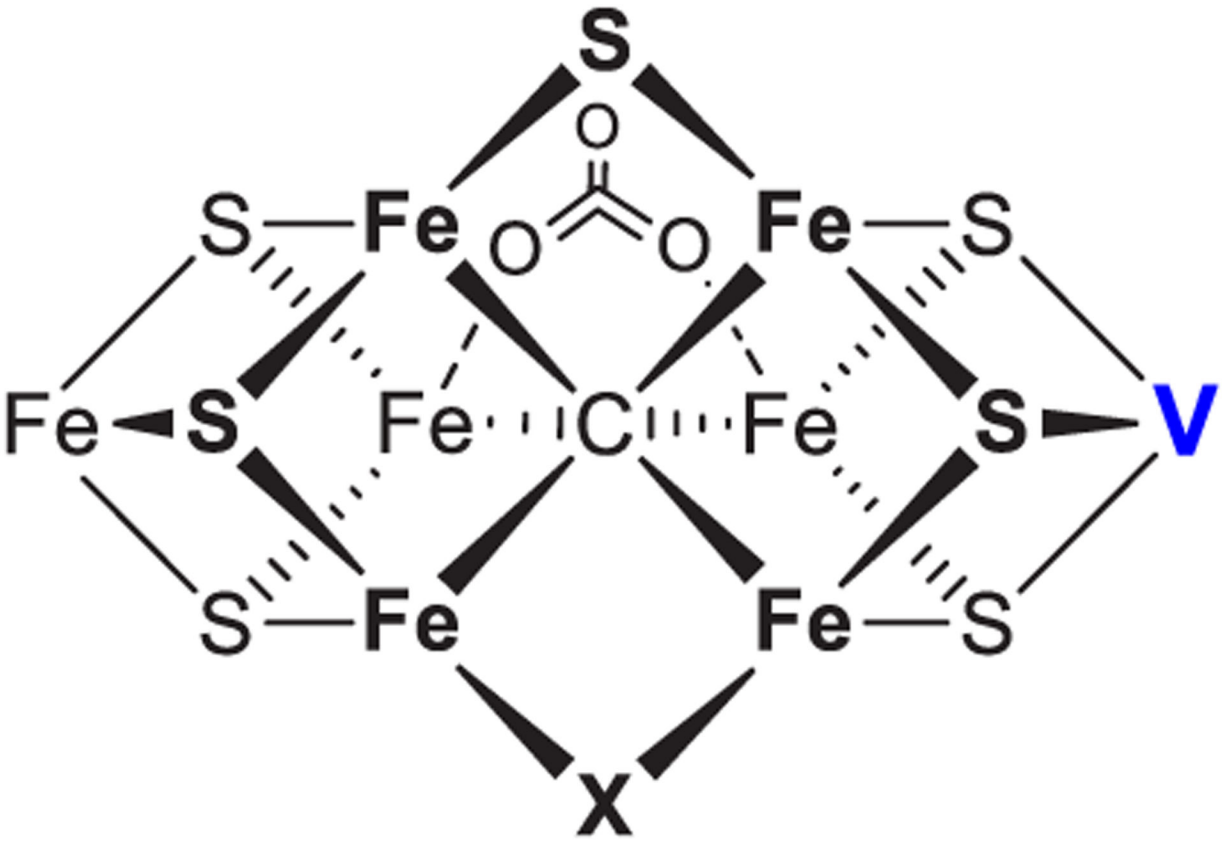

Figure 15.

FeV-cofactor structure proposed by X-ray structure (X = NH)[59] and theoretical calculations (X = OH).[155]

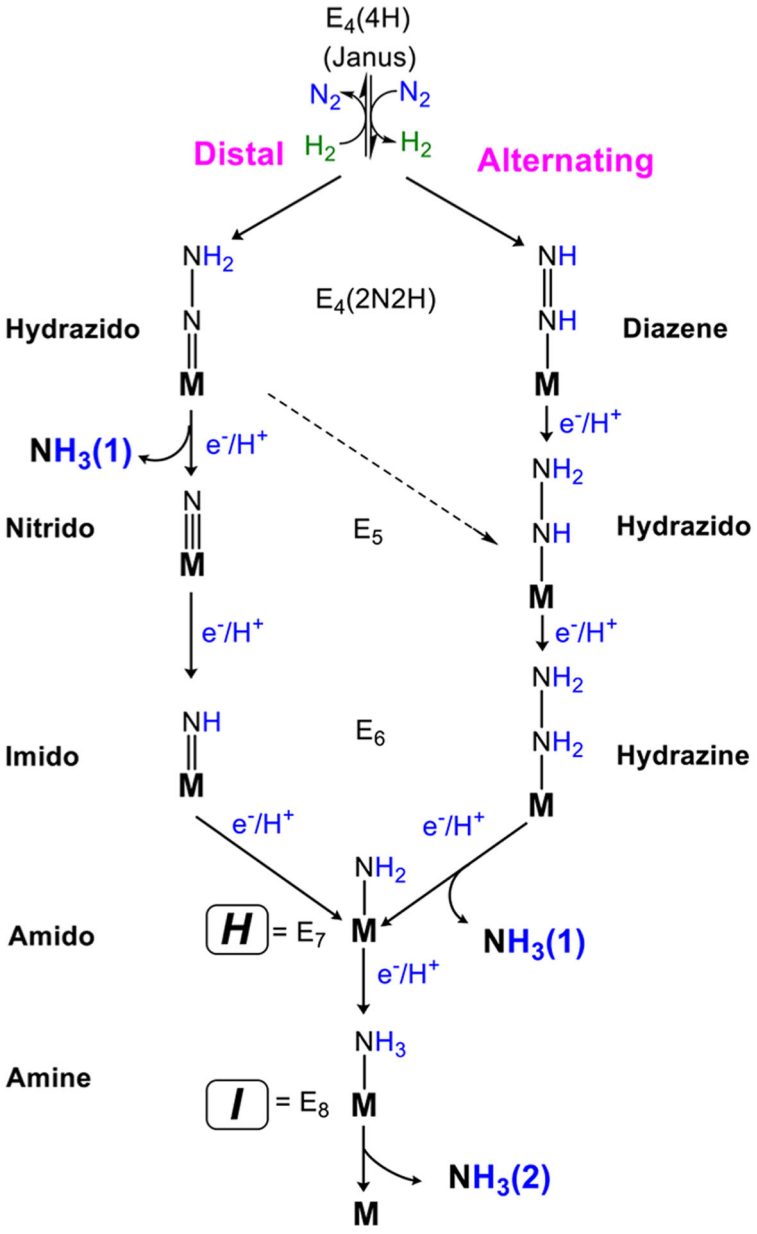

Figure 16.

Proposed N_2 reduction pathways with **M** representing the active site FeMo-cofactor. A distal reduction pathway (**D**) and an alternating reduction pathway (**A**) are displayed with plausible key intermediates. The hybrid-**A** pathway is indicated by a dashed arrow.[182]

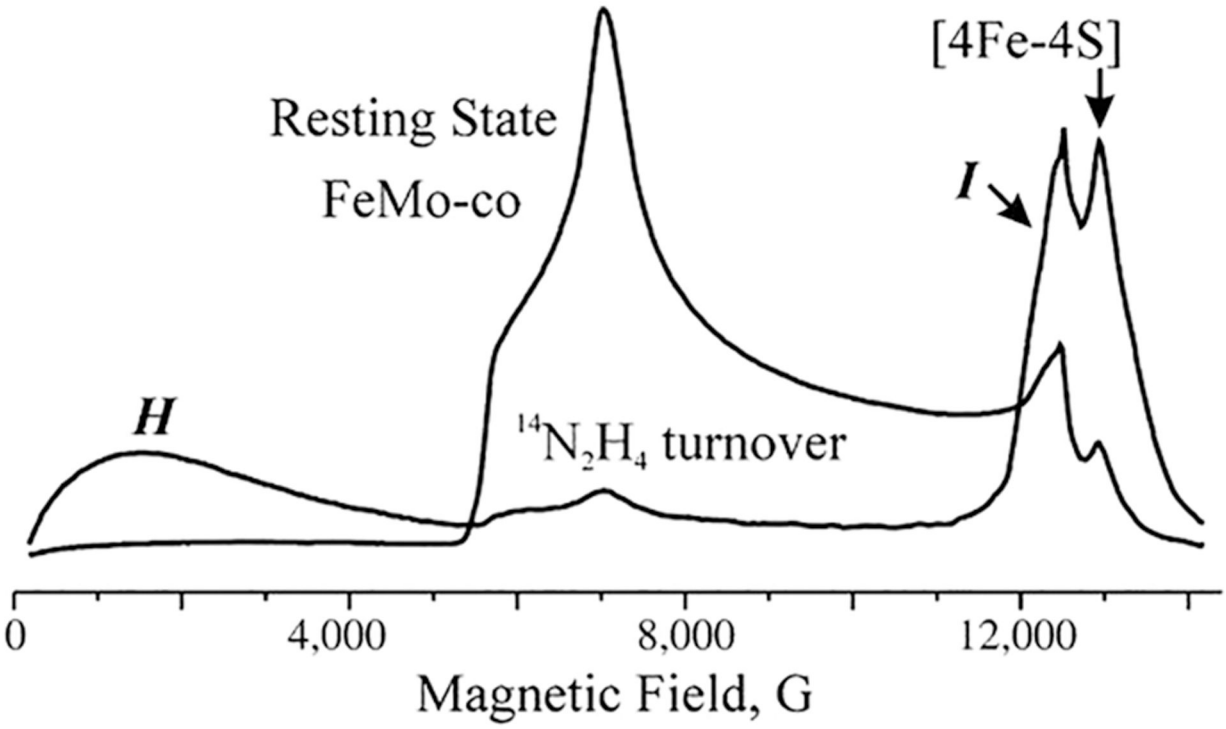

Figure 17.

Q-band CW EPR spectrum of α−70$^{Val\rightarrow Ala}$/α−195$^{His\rightarrow Gln}$ MoFe protein in the resting state and trapped during turnover with $^{14}N_2H_4$ as substrate. Kramers intermediate **I** and non-Kramers intermediate, H, are noted in the turnover spectrum. Reproduced with permission from ref 190. Copyright 2012 Authors. Published by PNAS.

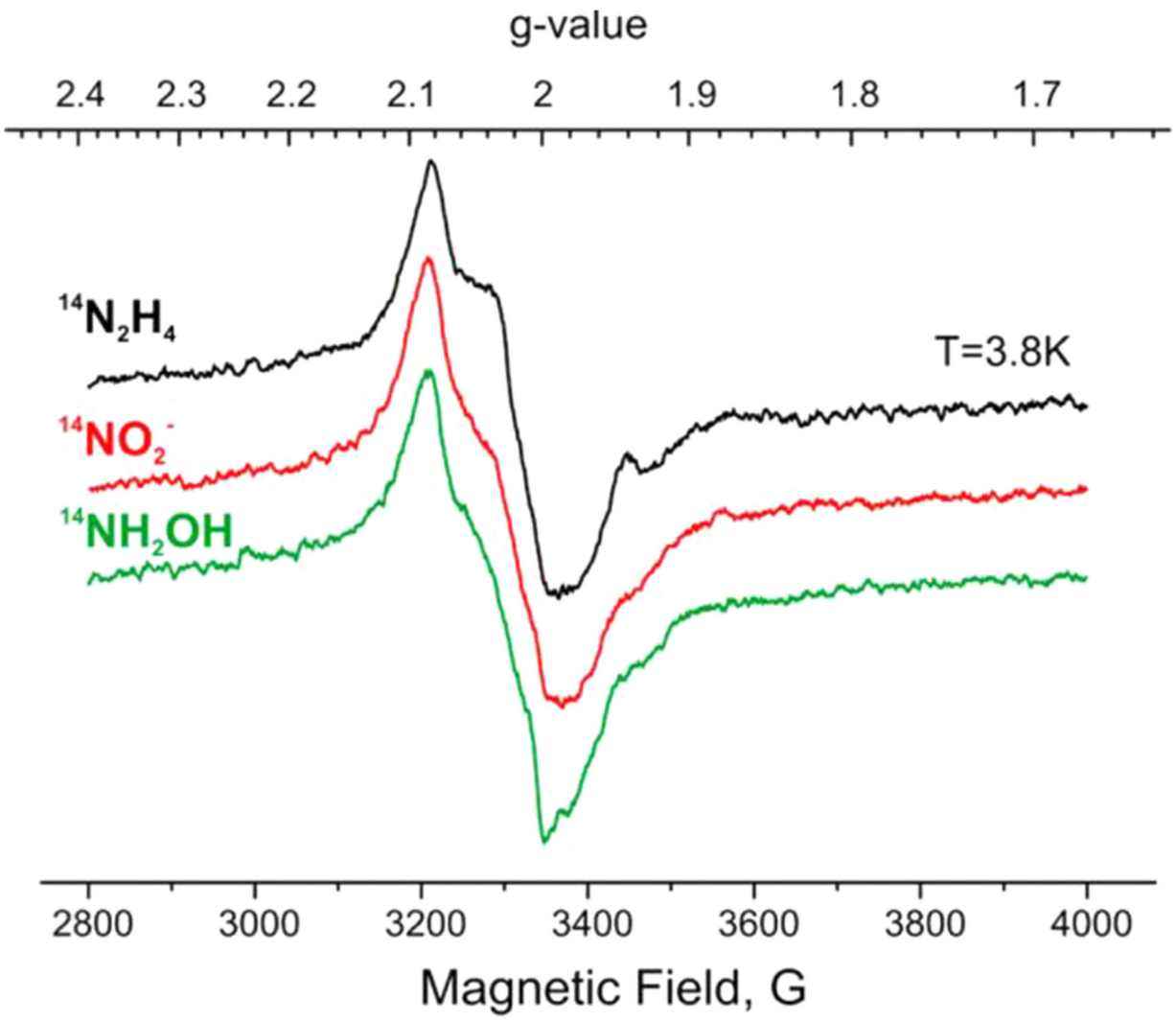

Figure 18.

X-band EPR spectra of α−70^{Ala}/α−195^{Gln} MoFe protein turnover samples prepared with N_2H_4 (black), NO_2^- (red), and NH_2OH (green) substrates. Reproduced with permission 193. Copyright 2014 American Chemical Society.

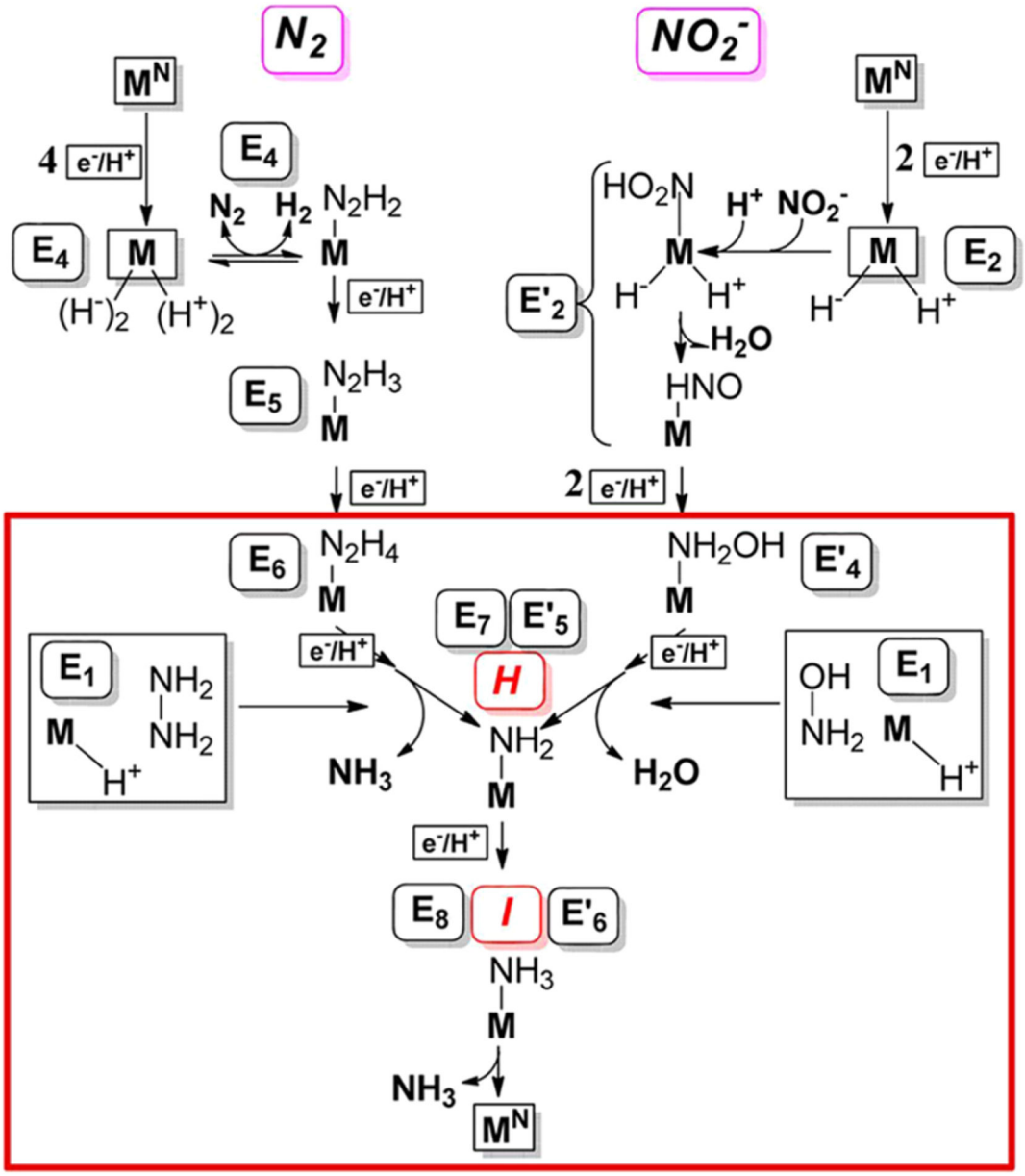

Figure 19.

Comparison of the proposed reduction pathways of N_2 (left) and nitrite (right) by nitrogenase (**M** represents FeMo-cofactor). An intermediate, labeled E_n on N_2 pathway and $E_{m'}$ on nitrite pathway, has accumulated n or m [e^-/H^+]. (Boxed Region) Convergence of pathways for nitrite and N_2 reduction by nitrogenase, as discussed in the text. Within this region, boxed reactions of E_1 show the most direct routes by which N_2H_4 and NH_2OH join their respective pathways. Reproduced with permission from ref 193. Copyright 2014 American Chemical Society.

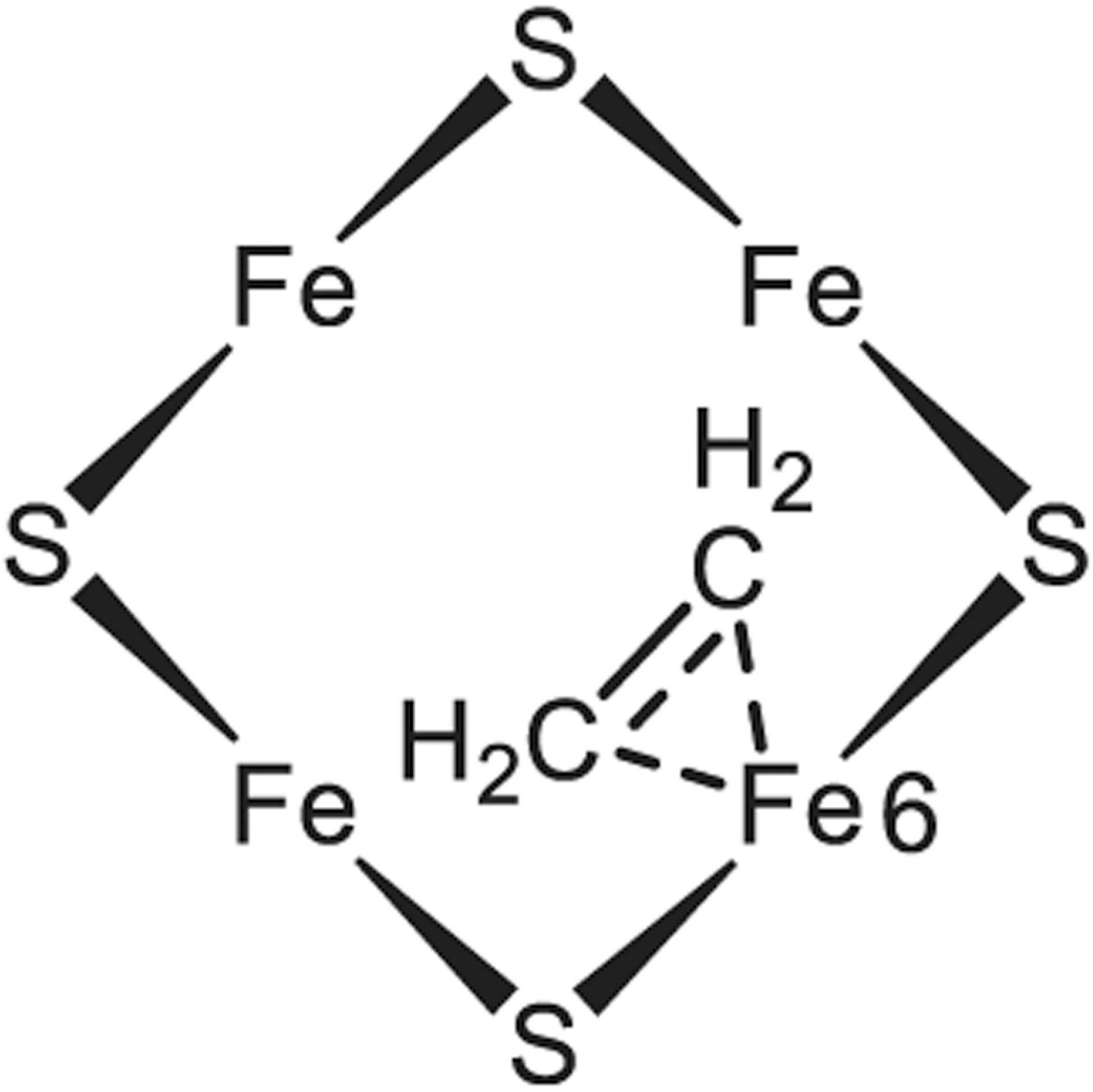

Figure 20.

Schematic representation of chemical structure of S_{EPR1} species at E_2 state, highlighting the ferracycle formed by C_2H_4 binding to Fe_6 as proposed in literature.[202] The 4Fe4S face represents the same orientation as in Figure 2.

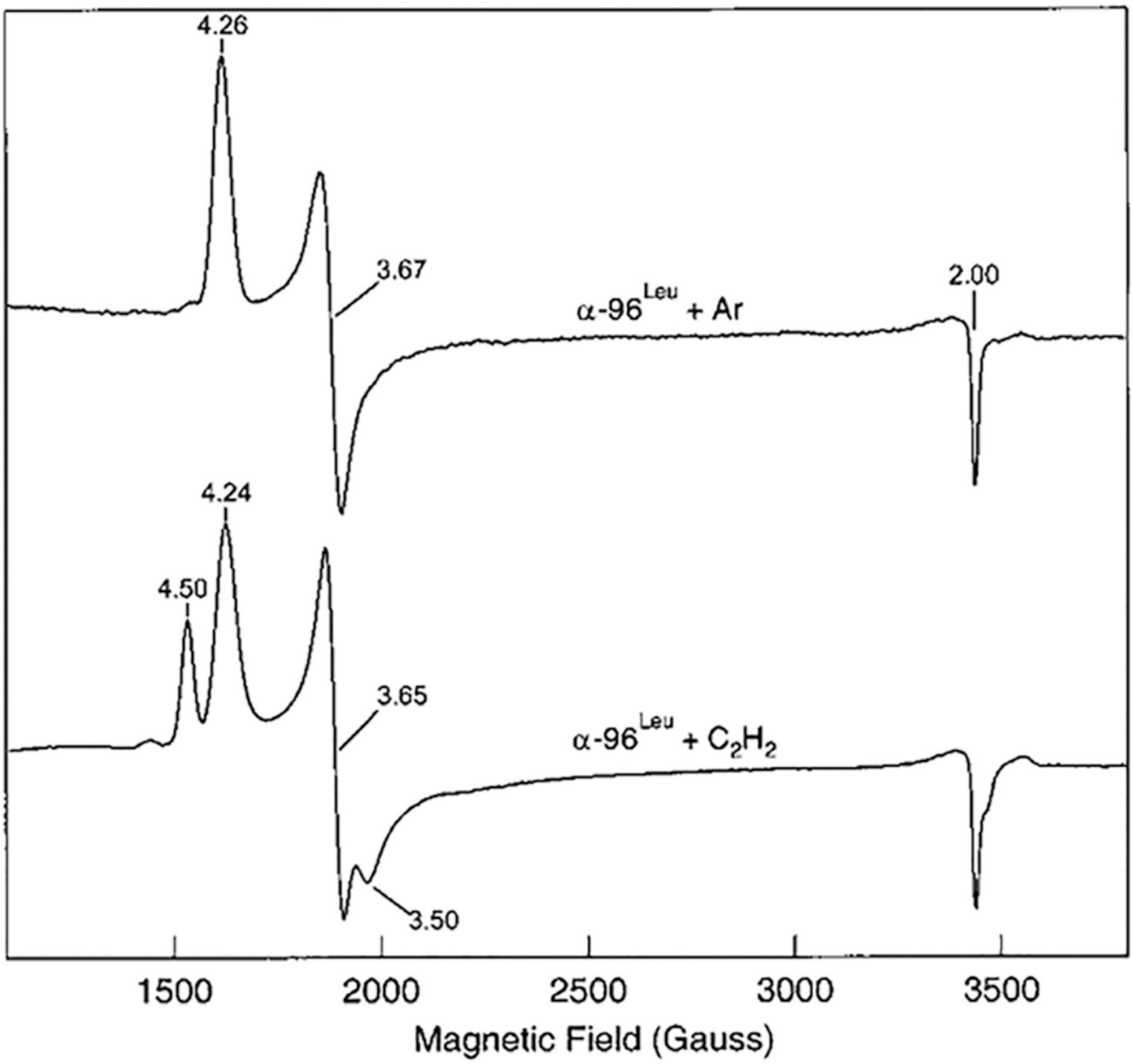

Figure 21.

X-band EPR spectra of α−96^{Leu} MoFe protein under nonturnover conditions in the absence (top trace) and presence (bottom trace) of acetylene. Reproduced with permission from ref 208. Copyright 2001 American Chemical Society.

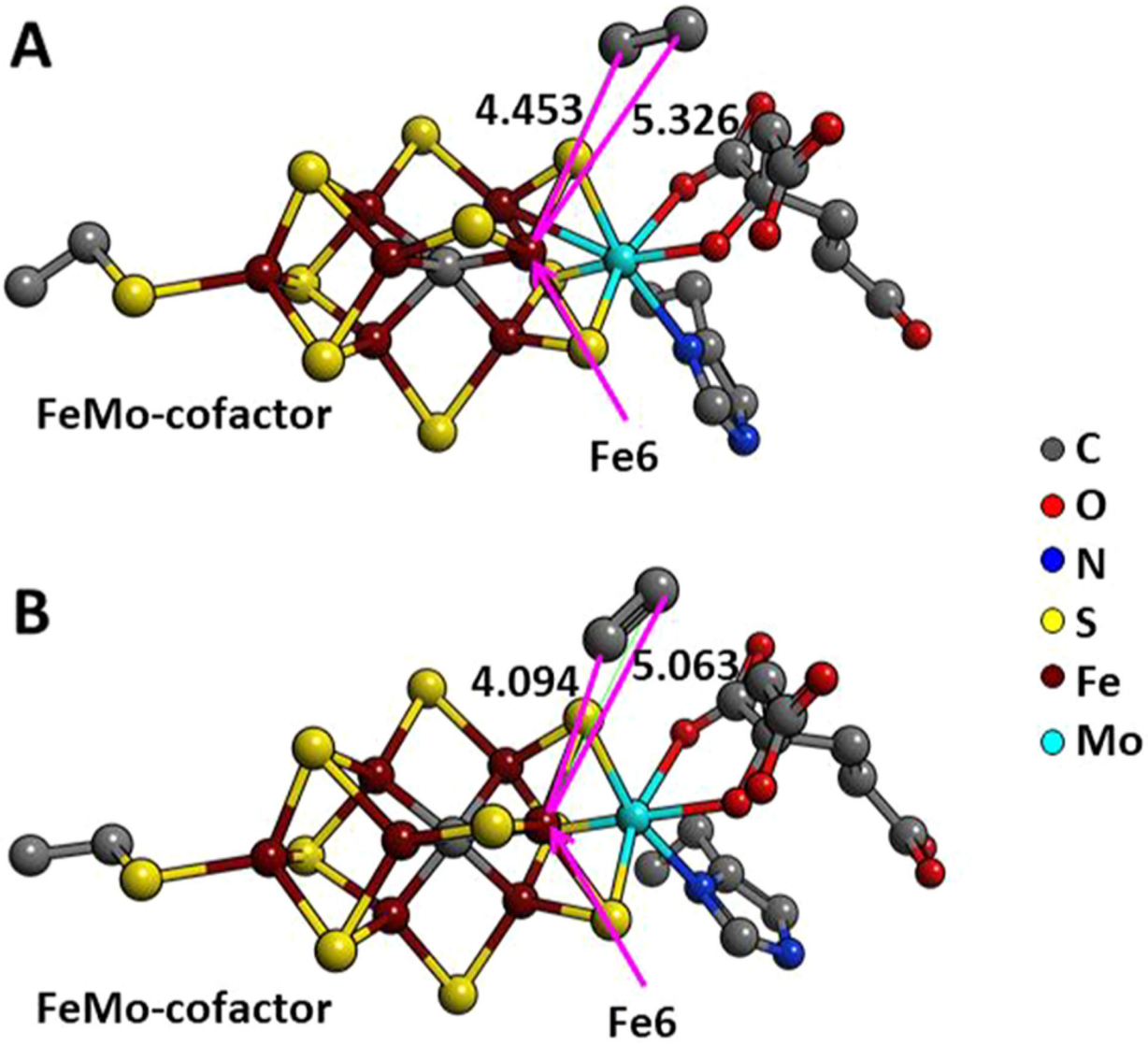

Figure 22.

Comparison of the acetylene location at the FeMo-cofactor. The acetylene location at the FeMo-cofactor is compared between X-ray (A) and DFT optimized structures (B). The interatomic distances are shown with red lines. Reproduced with permission 215. Copyright 2017 Elsevier, Ltd.

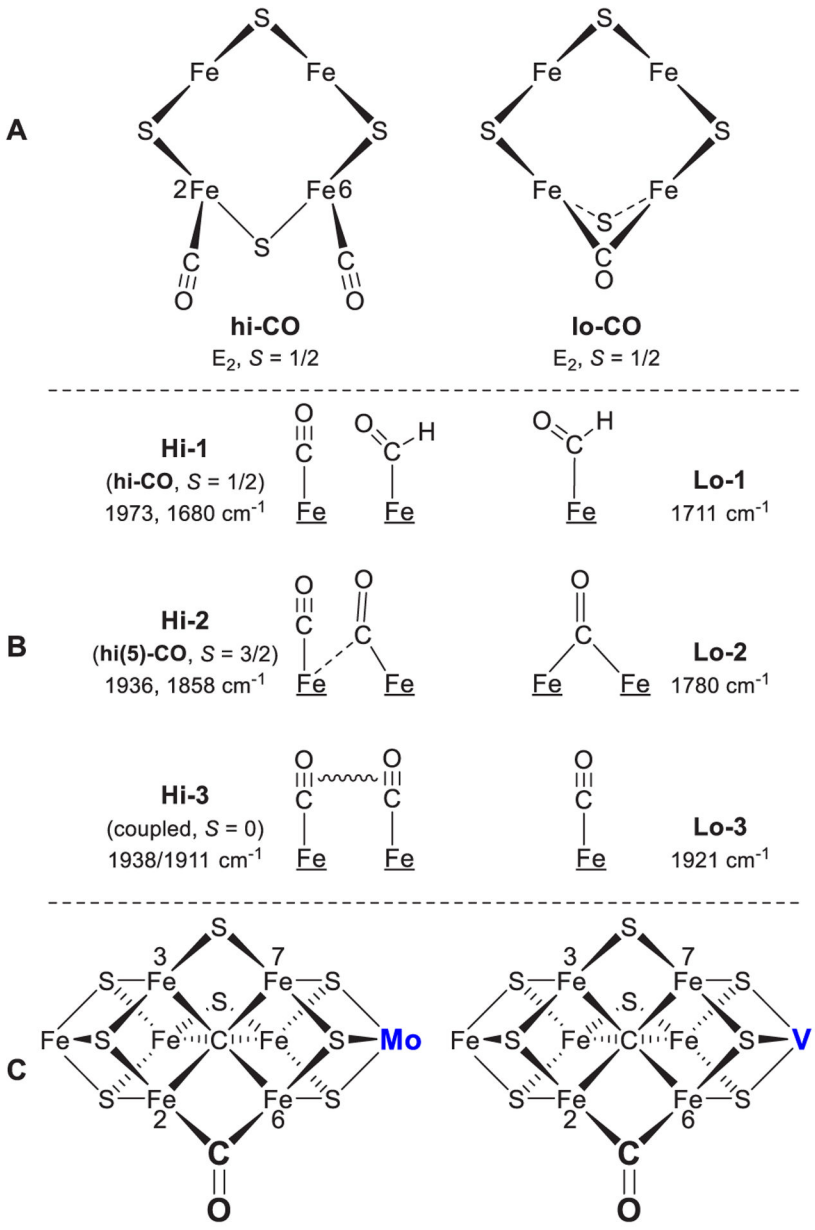

Figure 23.

Schematic structures of CO complexes as proposed based on (A) EPR/ENDOR,[202,230,235–238] (B) IR-monitored photolysis,[240–242] and (C) X-ray crystallography of Mo-nitrogenase[143] and EPR comparison of Mo- and V-nitrogenases.[243] The presence of a bound carbonate in the VFe-co was revealed later by X-ray crystallography.

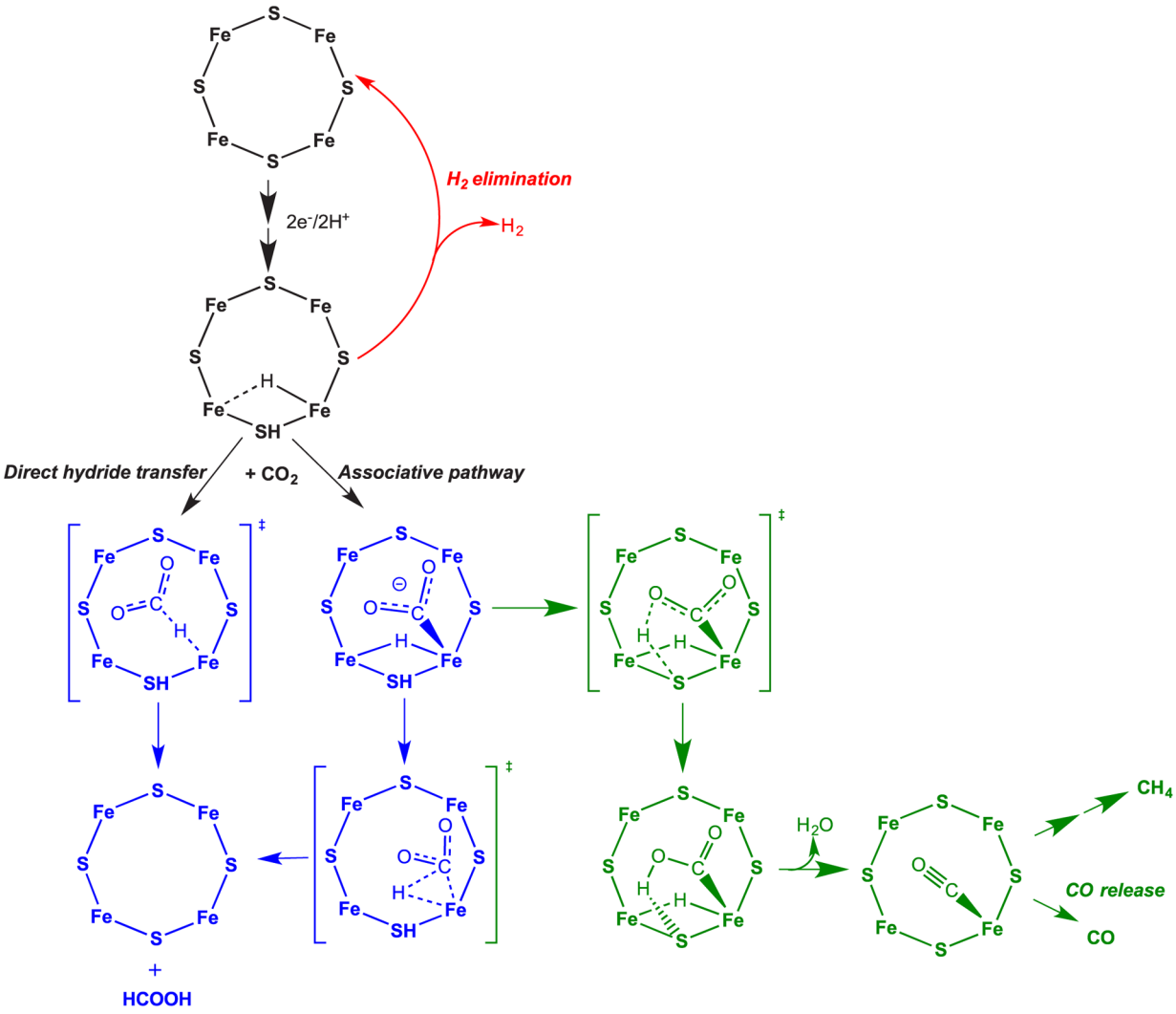

Figure 24.

Possible CO_2 reduction pathways. CO_2 activation at one FeS face of the E_2 state of FeMo-co is shown. The E_2 state is proposed to contain a single Fe-hydride and a proton bound to a sulfide shown bound to one face of FeMo-co. Reduction to formate (blue pathways) can go by either direct hydride transfer or an associative pathway. A pathway to formation of CO and CH_4 is shown in the green. Adapted with permission from ref 253. Copyright 2016 American Chemical Society.

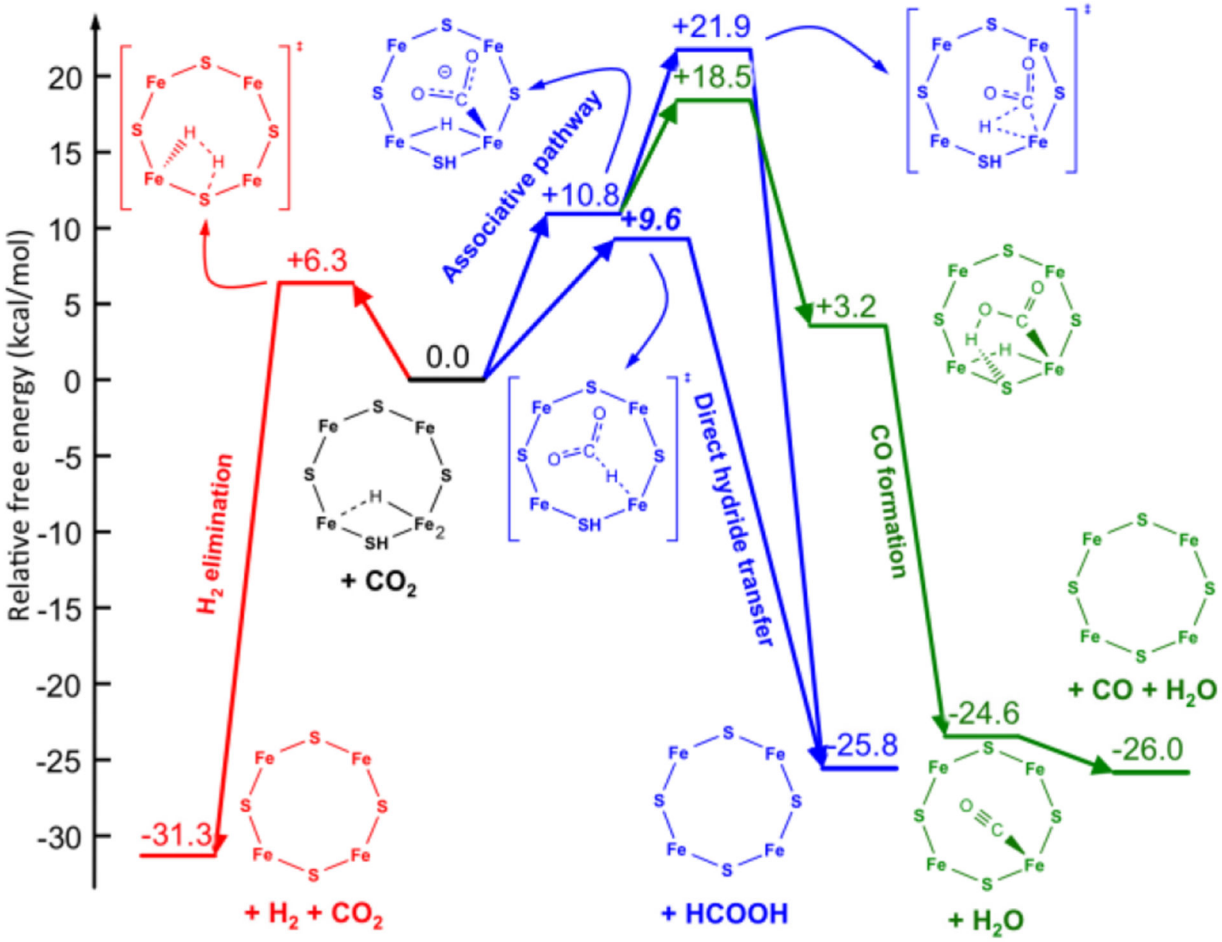

Figure 25.

Computed free energy diagram for CO_2 reduction and H_2 formation occurring at the E_2 state of FeMo-cofactor. Reproduced with permission 253. Copyright 2016 American Chemical Society.

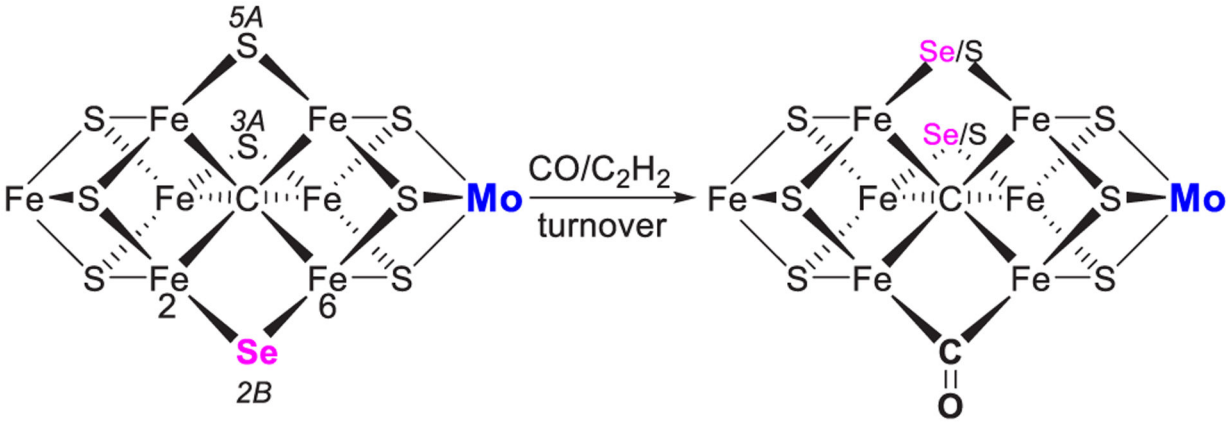

Figure 26.

Simplified schematic representation of conversion of Se-modified FeMo-cofactor by CO, highlighting the migration of Se^{2-} to S3A and S5A position from the Se2B position.[144]

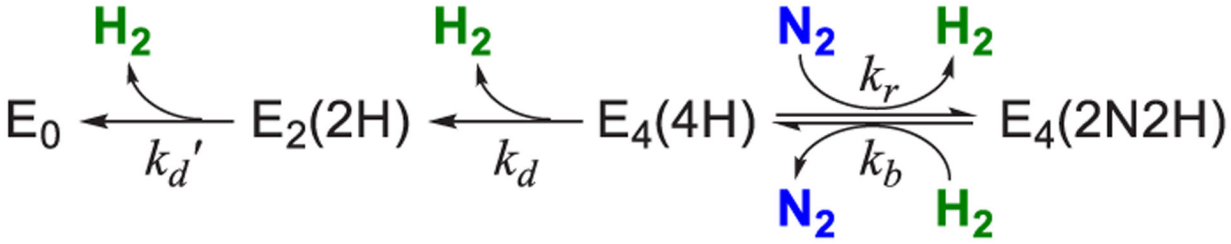

Scheme 1. Kinetic Scheme for the Decay of Freeze-Trapped E_4(2N2H) Derived from Figure 3[a]

Reproduced with permission from ref 124. Copyright 2015 American Chemical Society. [a]k_r and k_b are the second-order rate constants for *re* and its reverse; k_d and $k_{d'}$ are the rate constants for the irreversible decay of E_4(4H) and E_2(2H), respectively.

D_2 or T_2 only react during N_2 Turnover, during which:

(a) 2HD form stoichiometrically:

$$\mathbf{M}\text{-}N_2 + D_2 + 2H^+ + 2e^- \Longrightarrow 2HD + \mathbf{M} + N_2$$

(b) No Scrambling with solvent:

No T^+ released to solvent under T_2

(c) Reduction Level of this reaction:

D_2/T_2 reacts at $E_4(2N2H)$ level

Chart 1.
Key Constraints on the Nitrogenase Mechanism[20]